Applying Omics Techniques to Uncover Polyhydroxyalkanoate (PHA) Feast-Famine
Metabolisms by Mixed Microbial Consortia Cultured on Fermented Dairy Manure

A Thesis

Presented in Partial Fulfilment of the Requirements for the

Degree of Master of Science

with a

Major in Environmental Sciences

in the

College of Graduate Studies

University of Idaho

by

Glenda Maribel Alfaro Salmerón

Major Professor: Erik R. Coats, P.E., Ph.D.

Committee Members: Michael Strickland, Ph.D.; Inna Popova, Ph.D.

Department Administrator: Alistair Smith, Ph.D.

August 2021

Authorization to Submit Thesis

This thesis of Glenda Maribel Alfaro Salmerón, submitted for the degree of Master of Science with a Major in Environmental Science and titled "Applying Omics Techniques to Uncover Polyhydroxyalkanoate (PHA) Feast-Famine Metabolisms by Mixed Microbial Consortia Cultured on Fermented Dairy Manure," has been reviewed in final form. Permission, as indicated by the signatures and dates below, is now granted to submit final copies to the College of Graduate Studies for approval.

Major Professor: _____ Date: _____

Erik R. Coats, P.E., Ph.D.

Committee Members: _____ Date: July 19, 2021

Michael Strickland, Ph.D.

_____ Date: July 20, 2021

Inna Popova, Ph.D.

Department

Administrator: _____ Date: July 22, 2021

Lee Vierling, Ph.D.

Acknowledgements

Thank you to my supervisor, Dr. Erik R. Coats, P. E., for his patience, guidance, and support. I have benefited greatly from his wealth of knowledge and meticulous editing. I am extremely grateful that he took me on as a student and continued to have faith in me over these years.

Thank you to my committee members, Dr. Michael Strickland, and Dr. Inna Popova for their guidance and support.

Thank you to Cindi Brinkman for offering advice and encouragement with a perfect blend of insight and humor. I am proud of, and grateful for, my time working with her.

I would also like to thank all graduate and undergraduate students in the Coats Lab for all their support and assistance in my research work.

Dedication

This thesis work is dedicated to my husband, Landon Sutherland, who has been a constant source of support and encouragement during the challenges of graduate school and life. I am truly thankful for having you in my life.

Acronyms and abbreviations

ADF	Aerobic Dynamic Feeding
ATP	Adenosine Triphosphate
CoASH	Coenzyme-A
DFL	Dairy Fermenter Liquor
BPR	Biological Phosphorus Removal
FAD	Flavin Adenine Dinucleotide
F-F	Feast-Famine PHA synthesis
H	Hydrogen
HA	Hydroxyalkanoic Acids
MMC	Mixed Microbial Consortium
N	Nitrogen
NAD	Nicotinamide Adenine Dinucleotide
P	Phosphorus
PAOs	Phosphorus Accumulating Organisms
PHA	Polyhydroxyalkanoates
PHB	Poly-3-hydroxybutryate
PHBV	Hydroxybutyrate-co-3-hydroxyvalerate
PHV	Poly-3-hydroxyvalerate
RQ	Research Question
TCA	Tricarboxylic Acid
VFA	Volatile Fatty Acid

Table of Content

List of Tables

Table of Figures

Chapter 1:   Introduction

1.1   **Research motivation and significance**

Meeting basic human needs while preserving planet earth's resources and the greater environment is the core of sustainability; this concept has continued to evolve as the human population grows and impacts natural systems. More critically, research suggests that a fundamental shift from knowledge into action is needed immediately if society wishes to address critical sustainability problems [1]. This 'need into action' is particularly critical as agricultural and industrial sectors expand; as the human population grows, these sectors generate byproducts that can and do negatively impact the environment and society. Two unexpectedly aligned areas of impact are in dairy manure management and plastic pollution, both of which present significant social and environmental sustainability challenges. While human needs for dairy products and plastic packaging will continue to grow, as consumers and users it is our responsibility to find sustainable solutions that will benefit both society and the environment.

1.2   **Dairy manure management challenges**

The U.S. dairy industry continues to grow and intensify operations; as a result, large amounts of dairy cow manure is produced; U.S. dairies produce over a billion tons of animal manure (wet weight) every year [2]. Consequently, the dairy sector can potentially create significant impacts on the environment. Carbon emissions are one primary concern. Methane (CH_4) emissions from manure management have increased by 78.3% since 1990, and manure is the fourth largest anthropogenic source of CH_4 emissions in the United States [3]. Most of this increase was from dairy cow manure. In 2015 manure management also placed third in the direct and indirect emission sources of nitrous oxide (N_2O), another potent greenhouse gas, in the United States [3]. Finally, dairy manure contains quantities of nutrients that can also present environmental management challenges. The percent of nutrients in manure differ based on cow type and age. In particular, one lactating cow of 1,400 lbs. produces 155 lbs of

wet manure (as excreted) per day. On average, dairy manure contains 1.01 lbs of Nitrogen, 0.52 lbs of Phosphorus, and 0.57 lbs of Potassium [4]. Phosphorus and nitrogen contamination of surface waters is a real concern in dairy regions.

Geographically, one area of potential concern for nutrients and the environment is the state of Idaho, which ranks 3rd nationally in milk production. According to the Idaho Dairymen's Association (IDA - 2014), there are 541,587 lactating cows in Idaho; more critically, the average herd size is approximately 1,500 cows, and the majority of dairies are concentrated in the Magic Valley of SE Idaho. As a result, an estimated 42,000 tons of manure (as excreted, wet basis) are produced per day, or 15,500,000 tons of manure per year in Idaho; such production is generated in relative high density, considering the average dairy size, and on an equivalency basis would be a human population of over 5 million (almost 3X the population of Idaho). This magnitude of manure production equates to roughly 100,000 tons of Nitrogen, 52,000 tons of Phosphorus, and 57,000 tons of Potassium that could potentially be released annually into the environment.

Because of manure's high nutrient properties, the perspective about manure has changed over the years, from being seen as a waste to nowadays being considered a resource [5] – in particular as a fertilizer. But there remain issues associated with utilizing manure as fertilizer; when applied at excess rates, nutrients accumulate and drain from land into waterways. Discharge of nutrients into waterways can cause accelerated eutrophication and can potentially pollute drinking water, disturb soil microbial ecology, and affect grazing animals, while also creating conflicts with federal and state environmental regulations [6] .

Achieving an equilibrium between the amounts of manure produced on a dairy farm and the utilization of manure is a significant challenge [5]. When manure is not directly applied to land, farms use storage structures and lagoons to keep manure under anaerobic conditions, because anaerobic bacteria can decompose larger amounts of volatile solids per unit volume than aerobic bacteria with less energy input *[7].* In this sense, manure can be treated anaerobically, but gases (CH_4, N_2O) and other compounds are released during this process. When bacteria present in manure are not controlled, it can also increase the amount of odor generated [7]. Manure managed as liquid systems also tends to produce greater CH_4 emissions [3].

1.3   **Plastic pollution**

Plastic waste contamination in the environment has been receiving significant global attention, in particular because macro-plastics and micro-plastics have polluted shorelines, oceans, and freshwater bodies [8]. Annual plastic production increased substantially from 1.5 million tons in the 1950s to 348 million tons in 2017 [9]; plastic waste in the environment has increased at a commensurate rate, if not more rapid. Petroleum-based plastics are composed of multiple polymers that are resistant to degradation [10]. Because of their makeup, most plastic debris will persist for decades to centuries in the environment and can be transported over long distances throughout the environment, including quite problematically the oceans [8]. Industrial, commercial, and fishing activities are large contributors to plastic pollution, putting organisms at risk in the environment. Organisms can ingest or become entangled in the plastic; therefore, plastic waste is dangerous to the entire ecosystem [8].

Remedying excess environmental plastic pollution has been covered by multiple national and international regulations such as the United Nations, the Environmental Protection Agency, and the European Commission. But besides regulating plastic utilization and making plastic industries take responsibility for the end-of-life of their products, which is arguably a reactive strategy, it is critical to proactively develop advanced techniques to create renewable plastic substitutes. It is no longer possible to ignore the increasing amount of plastic waste in the environment, and its threat to ecosystems, and human health [11]. Therefore, it is time to focus on serious solutions such as creating bioplastics from waste-based materials.

1.4   **Convergence of Manure + plastics: A renewable plastic - Polyhydroxyalkanoates (PHAs)**

Policymakers, stakeholders, and researchers must collectively advance and promote sustainable manure reuse, resource recovery, and management strategies on dairy farms through technologies that will improve nutrient use and reduce pollution in the environment. In this regard, there is an interesting convergence of dairy manure management and environmental plastics remediation – producing bioplastics (polyhydroxyalkanoates, or

PHAs) from fermented dairy manure. PHAs are promising bioplastics that have the potential to be synthesized from renewable substrate sources while concurrently reducing landfill waste and environmental pollution associated with petro-plastics [12]. In addition to addressing carbon pollution, PHA production from dairy manure can also generate useful revenue to help deploy nutrient removal technologies such as phosphorus removal.

In 1920, the French researcher Maurice Lemoigne reported the first form of PHA as poly(3- hydroxybutyrate (PHB) inside bacteria [13]. Numerous, diverse forms of PHA have since been discovered. Bacteria store carbon intracellularly as granules, creating a source of energy and carbon reserves inside the cell [12, 13]. These granules consist of polymerized chains of hydroxyalkanoic acids (i.e., PHA). Complementing the central metabolic function for bacteria, in a desiccated state PHA exhibits thermoplastic properties. Importantly, PHA granules can be extracted from the bacteria cell, processed, and molded into a diverse form of products [14]. The PHAs can also be retained in the biomass to produce composite products [15].

PHA characteristics make them suitable for a variety of industrial applications [12]. Presently, PHAs have been produced using synthetic substrate (e.g., refined corn sugar) and pure microbial cultures; however, coupled with necessary bioreactor operating conditions (axenic), current commercial PHA production practices exhibit high capital and environmental costs [16]. Studies on waste-based PHA production utilizing mixed microbial consortia (MMC) have been previously explored, however insufficient PHA yield and process stability has been obtained, which makes it difficult for PHAs bioplastics to compete economically with synthetic plastics. Substrate is one of the highest costs in producing PHAs [17]; the use of agricultural waste such as dairy manure can significantly reduce production costs [13].

MMC have the potential to be utilized in PHA production because they have the capability to adapt to non-pure substrates such as those present in organic-rich waste streams. However, MMC selected for bioplastics synthesis must exhibit high PHA yield and storage, with sufficiently high cell concentrations for industrial PHA production, to be economically feasible. This has become a challenge, since MMC are composed of variable bacterial populations [13], and their metabolic pathways or biochemical conditions required to synthesize PHAs have remained unknown. Additionally, carbon sources play an important

role for bacteria to synthesize PHAs. Properties of PHAs depend substantially on the type of carbon substrate that the MMC are fed; a more diverse array of PHAs yields a better quality, more versatile bioplastic.

It is in the use of MMC cultured on diverse carbon sources where remedying the impacts of dairy manure management and plastic pollution fully align. Specifically, research has demonstrated that fermented dairy manure can serve as a carbon source for PHA accumulating MMC [13]. Once manure is fermented, its organic material has been converted into abundant volatile fatty acids (VFAs), which are a critical substrate for PHA synthesis. When MMC are fed with VFA-rich fermented dairy manure and then exposed to aerobic dynamic feeding (ADF) conditions in a sequencing batch reactor (SBR), the MMC become enriched with bacteria that are capable of a Feast–Famine (F-F) PHA metabolic response [18]. Figure 1 illustrates a typical F-F metabolic response. To induce the feast response, the MMC is rapidly provided with VFAs under aerobic conditions; the MMC convert VFAs into PHAs. These PHAs are then used as carbon and energy sources in the subsequent famine period, when VFAs have been fully utilized. ADF and the resultant F-F metabolic response is necessary for PHA production by MMC on waste substrate. The F-F metabolic response has been shown to be capable of generating significant quantities of PHA [19]. However, F-F PHA synthesis is a complex metabolic process that has remained unclear in previous studies; an enhanced understanding of this metabolic response is crucial to the improvement of the PHA production and accumulation in MMC, if process commercialization is to be realized.

1.5 **Research questions, hypothesis, and objectives**

Research presented and discussed in this thesis was driven by the following research questions, hypotheses, and objectives, with the focus on better elucidating key metabolic aspects of F-F PHA synthesis.

RQ 1: Under Feast conditions, MMC need ATP to uptake and catabolize VFAs to initiate PHA synthesis. ATP production aerobically principally occurs via oxidative phosphorylate, which requires electrons via NADH. The TCA pathway is the primary source of NADH for aerobic heterotrophs; acetyl-CoA, which is a byproduct of catabolized VFAs, is oxidized to

produce NADH. A confounding question arises regarding NADH and ATP: considering the need for acetyl-CoA for NADH, the need for NADH for ATP synthesis, and the need for ATP for VFA uptake and catabolism to acetyl-CoA, how are MMC producing ATP during the feast stage? And why does a rapid uptake of VFAs always occur?

Hypothesis 1: Glycolysis provides ATP to activate VFA uptake and initiate Feast PHA synthesis. Details on this metabolism can be demonstrated via metabolomic analysis.

Objective 1: Illustrate the carbon consumption and energy production metabolic routes of feast metabolisms. Monitor VFA transport and describe metabolites related to ATP synthesis during the feast phase. Evaluate PHA productivity in contrast to metabolic activity in both, feast and famine phases. Identify a type of biomarker to monitor the feast metabolic activity in real time, illustrating what metabolic pathways are active at the different time points in the feast phase.

RQ 2: PHA production initiates with VFA uptake, but once the cell is fully functional to consume VFAs and generate ATP via oxidation phosphorylation, the parameters that control the flux of acetyl-CoA to the TCA cycle versus to PHA synthesis remain unknown. Furthermore, PHA synthesis stops when MMC are fed with excess of VFAs in SBR and ADF conditions. Understanding the flux of carbon to PHA, and associated metabolic controls, is key in advancing efficient PHA production. Considering these potential metabolic-level controls, why and how does PHA synthesis occur contrary to just cell growth?

Hypothesis 2: There are features that negatively affect the TCA cycle and re-direct acetyl-CoA to PHA synthesis: NADH can repress citrate synthase and dehydrogenase in the TCA cycle. This prevents acetyl-CoA from entering the TCA cycle, and instead acetyl-CoA is converted to Acetoacetyl-CoA by 3-ketothiolase (*phaA*). As a result, PHA synthesis occurs, and a declined flux of carbon through the TCA cycle will also occur.

Objectives 2:

- Evaluate Feast PHA synthesis using chemical inhibitors (e.g., Valinomycin, CCCP, DCCD) that will stop key metabolisms, including the TCA cycle, and glycolysis pathway.

- Evaluate the effect of NADH addition on the TCA cycle.

- Utilize the inhibitor data to map out critical metabolisms associated with the acetyl-CoA to better understand its flux to the TCA cycle and the flux of carbon to PHA synthesis.

- Conduct targeted metabolomic studies to further refine a metabolic-level understanding of Feast PHA synthesis. Purchase comprehensive list of metabolites that should be detected in PHA metabolisms. Test unknown metabolites against library metabolites, and monitor the concentration of metabolites in PHA systems.

RQ 3: Do MMC enriched on fermented dairy manure under ADF operational conditions have an enough abundance of key PHA genes to synthesize PHAs in a production level?

Hypothesis 3: Class II *phaC* genes detected in MMC are not actively transcribed. Optimization of *phaC* genes classes will demonstrate that MMC contains at least 2 of the 4 *phaC* gene classes (*phaC* classes I and II). MMC in bench and pilot-scale systems have the potential to synthesize both, short-chain-length PHAs and medium-chain-length PHAs.

Objective 3: Calculate the diversity and relative abundance of PHA synthase genes (*phaC*) in the MMC and valuate the potential presence of all four *phaC* gene classes in the MMC through gel electrophoresis of PCR-amplified genomic DNA.

Chapter 2:   Literature Review

2.1   **Polyhydroxyalkanoates (PHAs)**

Bacteria can store carbon intracellularly as granules, creating a source of energy and carbon reserves inside the cell [12, 13]. These granules consist of polymerized chains of hydroxyalkanoic acids (i.e., PHA). As described in Chapter 1, PHA was discovered by the French researcher Maurice Lemoigne in 1920. He reported the first form of PHA as poly(3-hydroxybutyrate (PHB) inside bacteria [13]. Numerous, diverse forms of PHA have since been discovered. Complementing the central metabolic function for bacteria, in a desiccated state PHA exhibits thermoplastic properties. Importantly, PHA granules can be extracted from the bacteria cell, processed, and molded into a diverse form of products [14]. The PHAs can also be retained in the biomass to produce composite products [15]. PHAs are the only polymers that are 100% biodegradable and have properties such as polypropylene or polyethylene that are comparable to different synthetic plastics [20]. In addition, PHAs can be generated from renewable carbon sources, enabling these biopolymers to take place in an eco-friendly process.

To date, more than 100 different types of monomer units have been identified in PHA polymers [21]. Based on the monomer composition of the polymers, PHAs are classified as short chain length PHAs (SCL-PHA) and medium chain length PHAs (MCL-PHAs). The SCL-PHAs are composed of 3-hydroxy fatty acid subunits that contain four to five carbons, and MCL-PHA are composed of 3-hydroxy fatty acid subunits that contain six to sixteen carbons [21].

Since polyhydroxybutyrate (PHB) was the first PHA discovered, it is the PHA that has been most commonly studied and best characterized [20]. This has caused a special marketable interest in this class of polymer. However, PHB is distinctly crystalline (>50%), which makes it brittle and stiff, with a low elongation to break ratio [21]. A strategy that has been implemented by numerous investigations is to produce PHA containing 3-hydroxyvalerate (3HV) and 4-hydroxybutyrate (4HB) monomers. The combination of HV monomers into PHB polymers produces poly(3-hydroxybutyrate-co-3-hydroxyvalerate) [P(3HB/3HV)], a PHA-type polymer that is less stiff and brittle and has much higher

flexibility than pure P(3HB)[21]. These characteristics make P(HB-co-HV) suitable for different commercial applications. Figure 2.1 shows the chemical structures of PHB, PHV, and P(HB-co-HV).
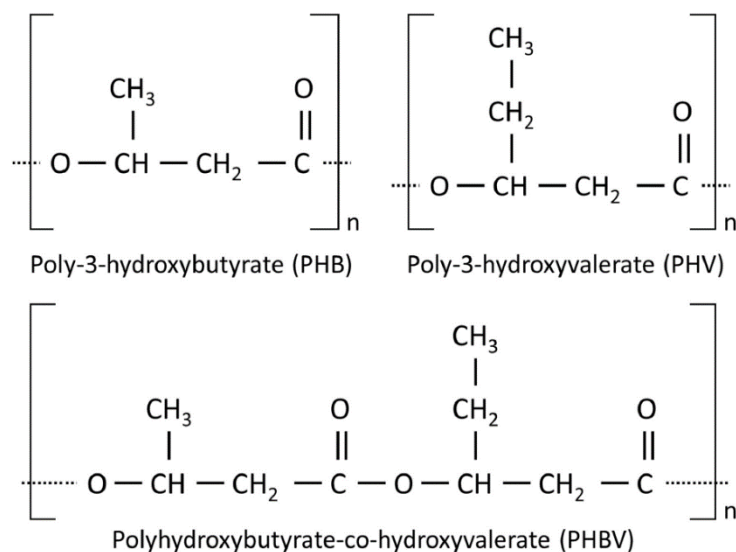
Figure 2.1: Polydroxyalkanoate monomers.

[22] Reproduced with permission

2.1.1   *PHA and Biodegradability*

Because of their unique characteristics to biodegrade naturally in the environment, PHAs are promising bioplastics that can serve a variety of applications. PHAs are part of the group of bioplastics that meet the biodegradation requirements suggested by international standards, where bioplastics must have the capabilities to be degraded in both controlled and uncontrolled environments [23]. Indeed, investigations have found that PHAs are able to degrade in soil, lakes, marine water, and sewage sludge [24]. The efficiency of biodegradation of PHA is related to the polymer's physical and chemical characteristics, and the presence of additives. Complex medium to long chain polymers are harder to biodegrade by

microorganisms. Consequently, the bio-assimilation of less complex PHAs is easier, but they are limited because of their high crystallinity [25]. Combining polymers and/or adding composites could improve the thermomechanical properties of PHAs, but it has to be taken into account that this could also affect their biodegradation capacity [23].

PHA biodegradation requires microorganisms that degrade PHAs, and microorganisms that feed from the by-products of the degradation such as acetic acid and butyric acid [25]. PHA biodegradation pathways are comparable to that of starch; microorganisms that degrade starch can also degrade short chain PHAs. Under aerobic conditions, PHA are degraded to water and carbon dioxide; under anaerobic conditions, PHA are degraded to methane by microorganisms in soil, sea, water, and sewage[20]. Composting studies from Meereboer et al. [25] have shown that in mature compost, PHBV can be 100% degraded in up to 60 days. Figure 2.2 shows PHA degradation in an aerobic sewage sludge environment. However, different aspects can affect the biodegradation of PHAs outside the lab such as temperature, nutrients, UV light exposure, salinity, and dissolved oxygen [25]. Understanding the degradation process of these biobased and biodegradable polyesters is important to develop the appropriate materials for industrial needs.
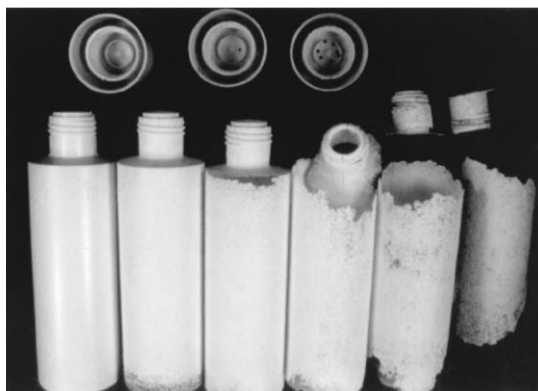
Figure 2.2: P(3HB-3HV) bottles degradation in 20°C aerobic sewage sludge. Treatment for 0, 2, 4, 6, 8, and 10 weeks, from left to right [26].

2.2   **Aerobic Dynamic Feeding and the Feast -Famine Metabolism**

Presently, PHAs have been produced using synthetic substrate (e.g., refined corn sugar) and pure microbial cultures; however, coupled with necessary bioreactor operating conditions (axenic) and the use of synthetic substrate (refined corn sugar), current commercial PHA production practices exhibit high capital and environmental costs [16]. Low-cost PHA production is necessary for these bioplastics to compete with petroleum-based plastics and to establish PHA industrial processes. In this regard, previous investigations have discovered that MMC are eligible candidates for this mission since they have adaptive capacities, do not need sterilization, and can be fed with waste-based substrates [27]. Moreover, as has been previously reported in the literature, some waste substrate (e.g., dairy manure) can serve as a carbon source for PHA-accumulating microorganisms [13, 28-33]. However, some of these waste substrates, including dairy manure, need to undergo a fermentation process first to produce necessary PHA precursors [34]. Fermentation of organic-rich substrate yields acetic acid and volatile fatty acids (VFAs) such as butyric, acetic, propionic, and valeric acid. These carboxylic acids are critical substrate for PHA synthesis, and most importantly, the molecular structure of PHA depends on the composition used as a source of carbon [35]. For example, acetate and butyrate yield 3HB monomers because the carboxylic acids each have even number of carbons, while propionate and valerate with odd number of carbons yield 3HV monomers.

Enriching a MMC culture with PHA-accumulating microorganisms utilizing critical precursor substrates such as carboxylic acids requires operating a bioreactor under aerobic dynamic feeding (ADF) conditions; the ADF conditions induce a metabolic feast-famine (F-F) response where the MMC store carboxylic acids as PHA and then subsequently consume the PHA for growth [27]. When MMC are fed with carboxylic acids and then they are exposed to ADF conditions in a sequencing batch reactor (SBR), the MMC become enriched with bacteria that are capable of feast and famine. Figure 2.3 shows a simple representation of the feast-famine (F-F) metabolic response in MMC, while Figure 2.4 illustrates the typical coupled response of carboxylic acid consumption and PHBV synthesis in a sequencing batch reactor. To induce feast, the MMC is rapidly provided with carboxylic acids under aerobic conditions; in this step, MMC convert carboxylic acids into PHAs. These PHAs are then

utilized as carbon and energy sources in the famine metabolic phase. PHA-accumulating bacteria have growth advantage over non-storing microorganisms because they store PHA fast in the feast phase [27]. This makes the regulation of the feast and famine ratio and times important in MMC systems.
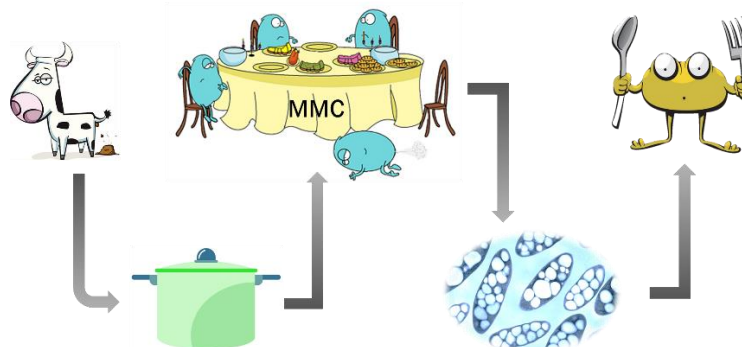
Figure 2.3: Pictogram of the Feast and Famine metabolic response. To induce feast, MMC is rapidly provided with VFAs under aerobic conditions; bacteria convert VFAs into PHAs. PHAs are then used as carbon and energy sources in the famine period.
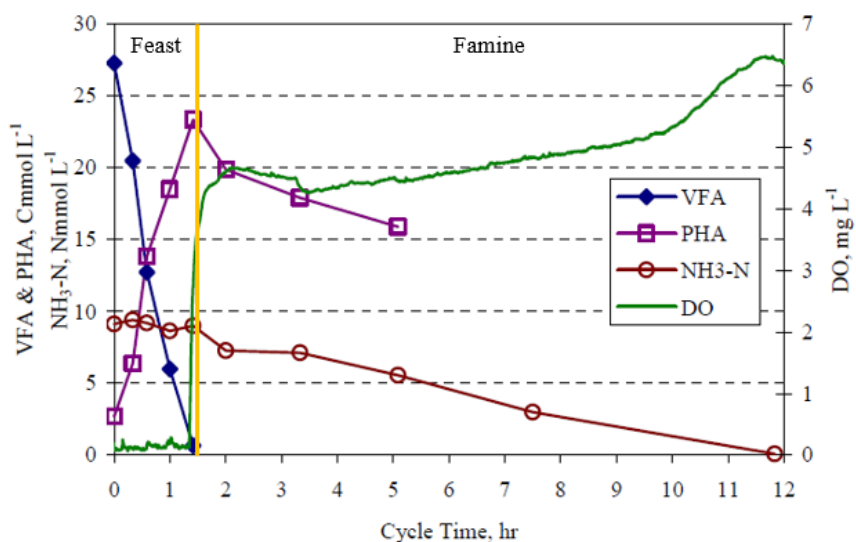
Figure 2.4: Typical Feast-Famine Response in a Sequencing Batch Reactor [36]

Reproduced with permission.

For PHA production, ADF conditions selects for microorganisms capable of storing excess of substrate, allowing them to survive in the famine stage. This enriched MMC is then utilized in the PHA production stage. When operating the production stage at a higher organic loading rate (OLR), higher intracellular PHA concentrations are achieved, thus exceeding

those of the enrichment stage [37]. Figure 2.5 illustrates the typical three stage process – fermentation, enrichment, production.
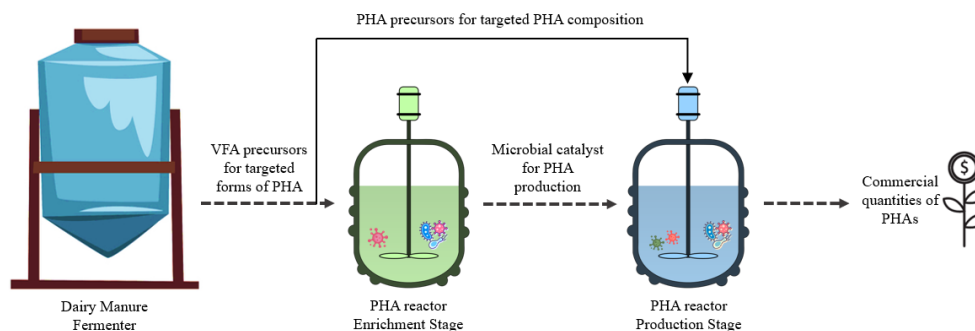
Figure 2.5: Three-Stage PHA Production Process Using Dairy Manure Feed

ADF and the F-F metabolic response are necessary for PHA production by MMC using waste substrate, and it has been proven that this metabolic response is capable to produce significant quantities of PHAs [27]. Thus, in considering process commercialization, characterizing the feast and famine metabolisms in MMC is crucial to better understand what factors inhibit and/or enhance the efficient conversion of VFAS into PHAs. To further enhance the potential of this novel process, molecular analysis of PHA biosynthesis such as genomics and metabolomics have been implemented in this thesis.

2.3 **PHA synthase (*phaC*):**

Studying the regulatory mechanisms of PHA synthesis pathways can elucidate important characteristics of the key genes involved in the polymerization of PHA precursors. Moreover, the MMC composition influences the quality, quantity, and the type of PHAs that a system produces. By characterizing the MMC, the PHA production process and performance in feast-famine systems can be improved.

The main enzymes of the short-chain-length PHA biosynthesis pathway are 3-ketothiolase (*phaA*), acetoacetyl-CoA reductase (*phaB*), and PHA synthase (*phaC*). Figure 2.6 illustrates these key genes involved in PHA synthesis. Organisms such as *Ralstonia eutropha* (*Cupriavidus Necator*), *Aeromonas hydrophila* or *Pseudomonas stutzeri* have been shown to contain this pathway [38]. Ultimately PHA synthase (*phaC*) is the most critical gene

associated with PHA synthesis because it polymerizes 3-hydroxyalkyl-CoAs to form PHAs
[39]. To date, four distinct classes of *phaC* have been identified: classes I, III, and IV
polymerize short-chain-length (SCL; C3-C5) monomers, while class II is believe to only
polymerize medium-chain-length (MCL; C6-C14) monomers [40, 41].
Medium-chain-length PHAs can be accumulated by *Pseudomonas* species. There are a few
pathways associated with medium-chain-length PHA synthesis, but only the β-oxidation
biosynthesis pathway utilizes fatty acids as carbon source. Presumably, with the help of the
enzyme (R)-specific enoyl-CoA hydratase (*PhaJ*), the metabolized fatty acid produces 3-
hydroxyacyl-CoA, a precursor for PHA synthesis [38]. Whether or not medium-chain-length
PHAs synthesis involve *phaA*, *phaB*, and *phaC*, in addition to other pathways to metabolize
longer chain fatty acids, is still unknown.

2.4   **PHA metabolism and Regulation of PHA biosynthesis**

Optimal ADF operations for commercial PHA production seek to maximize
enrichment of bacteria capable of PHA feast-famine PHA synthesis. Moreover, ideal
operations desire maximum conversion of VFAs to PHA during the "feast" period – optimally
100% conversion. For efficient PHA systems, the goal is to reduce bacterial growth during the
'feast' phase, with most/all electrons and associated ATP used to support VFA uptake and
PHA synthesis. To accomplish this goal, it is key to understand what conditions can affect
biomass growth and PHA accumulation during the feast phase of SBR operations.

Figure 2.6 illustrates potential pathways that MMC could utilize to synthesize PHA utilizing
glucose, acetic acid, butyric acid, propionic acid, and valeric acid as substrates; note that CoA
molecules are the critical precursors to the PHA cycle. Acyl-CoAs are involved in many
metabolic pathways, such as TCA cycle, fatty acid β-oxidation, and PHA synthesis. For
example, acetyl-CoA is a key metabolite in primary metabolisms; it is biochemically formed
from pyruvate connecting glycolysis with the TCA cycle, and is also involved in fatty acid
metabolisms [42]. For fatty acids to enter into cellular processes, they need to bind to a
coenzyme A to form Acyl-CoAs. Depending on the chain length, the fatty acid will be
catalyzed by one of the acyl-CoA synthetase isoforms. Fatty acids of less than 6 carbons will

be activated by short-chain acyl-coa synthetases; fatty acids of 6-10 carbons will activated by medium-chain acyl-coa synthetases [43]. This thesis work aims to identify and quantitate specifically short-chain acyl-coAs involved in PHA synthesis such as acetyl-CoA, propionyl-CoA, valeryl-CoA, and butyryl-CoA.

As shown in Figure 2.6, glucose is converted to pyruvate via the Enter-Doudoroff pathway; pyruvate is then converted to acetyl-CoA by a process called pyruvate decarboxylation. For PHB synthesis, β-ketothiolase (*phaA*) condenses two acetyl-CoA molecules to form acetoacetyl-CoA reductase encoded by *phaB*, to produce (R)3-hydroxybutyrl-CoA which is then polymerized by PHA synthase (*phaC*) to become a high molecular weight PHB. For the PHV synthesis, *phaA* condenses one molecule of acetyl-CoA and one molecule of propionyl-CoA to form 3-ketovaleryl-CoA to produce (R)3-hydroxyvaleryl-CoA which is then polymerized by pha*C* to become PHV.

Similarly, acetic acid is activated directly to acetyl-CoA; *phaA* catalyzes a Claisen condensation of two molecules of acetyl-CoA to form acetoacetyl-CoA, which is then reduced in an NADPH-dependent reaction to produce d-(−)-3-hydroxybutyryl-CoA (3HB-CoA). 3HB-CoA is the substrate for the PHB synthase, which catalyzes the polymerization reaction of 3HB-CoA to form PHB [44]. From propionate, two molecules of propionyl-CoA condense to form 3-hydroxy-2-methylvaleryl-CoA, the precursor for poly-3- hydroxy-2-methylvalerate (P(3H2MV)) [45]. However, if acetyl-CoA is present, together with propionyl-CoA will form P(3HV) or P(3H2MB)[46]. Butyrate can be used directly to produce P(3HB) and valerate to P(3HV), as well as through β-oxidation [46].

In regard to the regulation of PHA biosynthesis, specifically during the feast phase, the key intermediate is acetyl-CoA because it will be principally oxidized under aerobic conditions through the tricarboxylic acid (TCA) cycle to generate NADH for ATP synthesis via oxidative phosphorylation. However, depending on environmental conditions (e.g., oxygen limitation, which limits oxidation of NADH produced through the TCA cycle), acetyl-CoA is also utilized as substrate for PHA synthesis. As noted in Figure 2.6, α-Ketoglutarate is also a key intermediate in the TCA cycle, coming after isocitrate and before succinyl CoA. Studying the presence of these metabolites during PHA production can help interrogate whether Acetyl-CoA is mostly being used in the TCA cycle to carry out cellular respiration or for PHA synthesis. In the TCA cycle, citrate synthase and isocitrate dehydrogenase can be

repressed by excess NADH; this prevents acetyl-CoA from entering the TCA cycle, and instead acetyl-CoA is routed to PHA through conversion to acetoacetyl-CoA by 3-ketothiolase (*phaA*). As a result, PHA synthesis occurs, and a decreased flux of carbon through the TCA cycle also occurs. However, if the CoA concentration is high and sufficient oxygen is available for NADH oxidation, CoA is released as acetyl-CoA which enters the TCA cycle and the *phaA* is inhibited, thus restricting PHA synthesis [47]. Consequently, the two metabolisms are essentially competing for acetyl-CoA. Ultimately bacteria would preferably employ the TCA cycle for ATP production to support bacterial growth. PHA synthesis is just a "stress response" that is induced with the TCA cycle is impaired. Detecting the concentration of these key metabolites during the different stages of PHA synthesis, and elucidating MCC metabolic pathways has remained to be addressed in the previous literature.

As RQ1 and RQ2 describe, PHA synthesis requires ATP for carboxylic acid activation and the reducing equivalent NADPH for the conversion to the hydroxyacyl-CoA. ATP production aerobically principally occurs via oxidative phosphorylate, which requires electrons via NADH. The TCA pathway is the primary source of NADH for aerobic heterotrophs; acetyl-CoA, which is a byproduct of catabolized VFAs, is oxidized to produce NADH. Low dissolved oxygen concentrations limit ATP synthesis, thereby potentially inhibiting carboxylic acid transport into the cell and catabolism to acetyl-CoA, which is a critical precursor to PHA synthesis; however, lower oxygen concentrations can also limit use of carboxylic acid for growth, which is favorable to the PHA synthesis process. Conversely, high dissolved oxygen concentrations can allow bacteria to produce ATP at maximum efficiency, allowing for higher growth rates and commensurate catabolic use of carboxylic acids, with concurrent reduced PHA accumulation. PHA biosynthesis requires acetyl-CoA and NADPH (source of electrons, as PHA is both a carbon and electron sink), while biomass biosynthesis requires acetyl-CoA and ATP. Therefore, both metabolisms require acetyl-CoA, and its distribution highly depends on the NADH/NADPH and ATP availability [48].

Under ADF conditions ATP and reducing equivalents are obtained from partial respiration of the substrate [35]. There are different hypotheses that explain the source of reducing equivalents necessary for PHA synthesis, but they are characteristically for the BPR phenomenon, which is controlled by anaerobic conditions; much less is known about aerobic

'feast' PHA metabolism control. One BPR theory indicates that the TCA cycle is partially active or split under anaerobic conditions. The TCA cycle can generate very few reducing equivalents for a lower demand for reducing power carbon source [49]. Other literature suggests that glycolysis generates the major part of the reducing power anaerobically, especially in acetate and propionate metabolisms [49]. Glycogen degradation to pyruvate (through glycolysis) could also serve as a source of ATP for PHA synthesis from acetate. Pyruvate can be oxidized to acetyl-CoA or reduced to propionyl-CoA by a reducing pathway. Then, the acetyl-CoA and propionyl-CoA produced can be synthesized into PHA [50]. So, both TCA cycle and glycolysis are involved in the production of reducing equivalents in BPR systems under anaerobic conditions. This could lead to the assumption that for aerobic conditions, some PHAs can be depleted and used for glycogen synthesis through reversed glycolysis [50]. For ADF PHA synthesis, glycogen degradation could provide NADH and ATP to 'initiate' feast PHA synthesis, however, there is not enough literature to back up this thought. For this reason, and to answer research question 1, Chapter 3 presents a series of batch experiments with VFA chemical inhibitors to compare and assess VFA uptake by MMC under conditions wherein mechanisms associated with VFA uptake were potentially inhibited. A specific focus was to examine the performance of ATP synthase during the 'feast' period of PHA production. To complement findings, D-fructose 1,6-bisphosphate, an important glycolysis metabolite has been targeted in metabolomics studies as well.
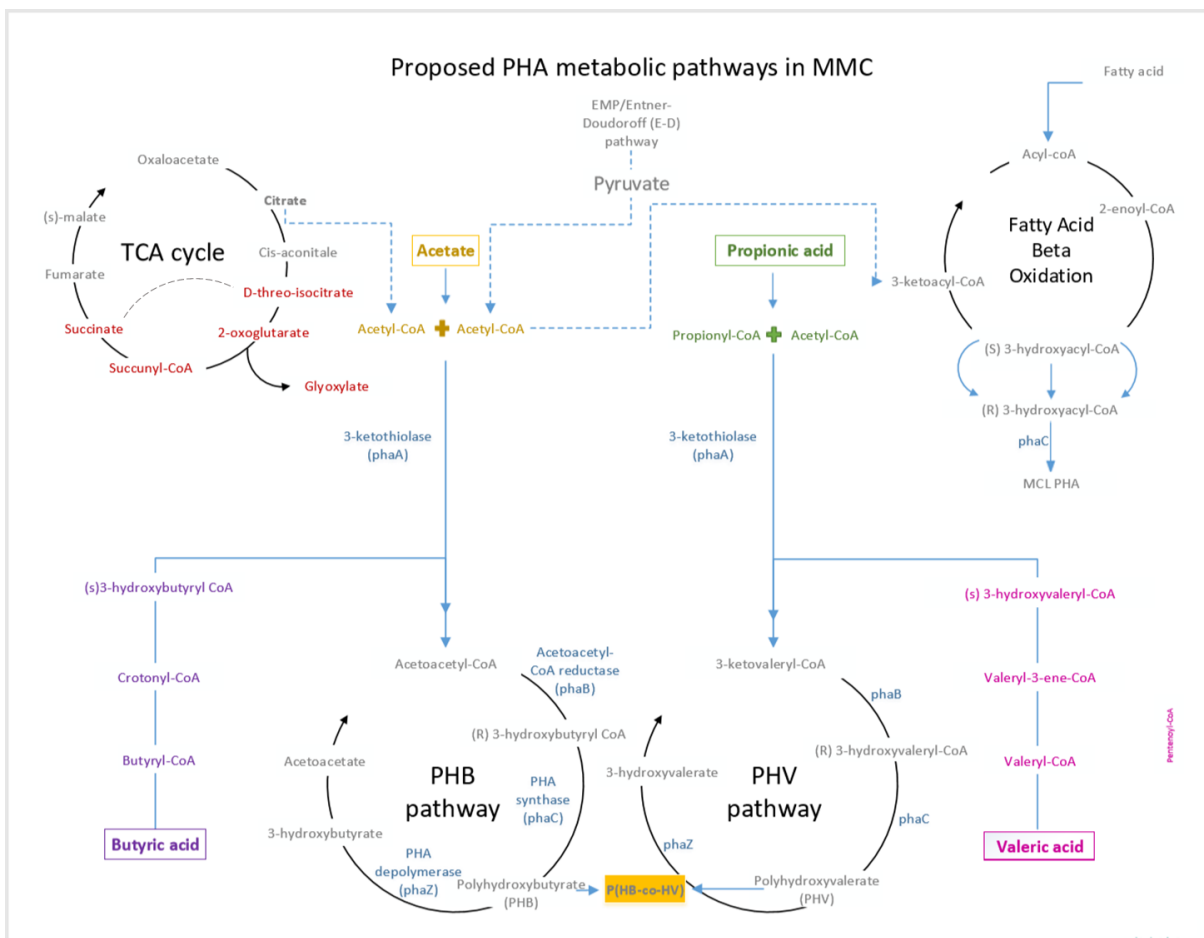
Figure 2.6: Integrated metabolisms in MMC cultured in fermented dairy manure utilizing different substrates.

2.5 **Microbial Metabolomics**

Studying PHA biosynthesis at a molecular level, coupled with analytical chemistry investigations (i.e., PHA and carboxylic acid quantitation), can elucidate potentially important structure-function relationships that will inform the feast-famine metabolic response by MMC cultured on fermented dairy manure and facilitate future process scale-up [18]. The genome, transcriptome, and proteome are mediums that can be studied to understand gene expression, and the metabolome represents the final -omic level in a biological system that can reflect changes in phenotypes and functions [19]. Metabolomics techniques are capable of explaining complex genotypes, phenotypes, and metabolisms in diverse biological systems, such as MMC cultured on fermented dairy manure. For instance, metabolomics analysis can provide

experimental data for quantitatively predicting important pathways that MMC utilize to synthesize PHA and elucidate important molecular mechanisms of PHA-producing bacteria. A multi-omic approach will help analyse cell activities, potentially show changes at different environmental conditions in the PHA reactors and obtain a comparison of the metabolite levels and PHA genes transcripts during feast and famine responses. The metabolome analysis of MMC performing PHA synthesis will also be very valuable for the development of methods to study other PHA producing microorganisms in the future.

2.5.1 Liquid chromatographic mass spectrometry (LC-MS)-based metabolomics

The principal goal of metabolomics analysis is to describe function at a molecular level, based on detected metabolites, for targeted processes. In addition, metabolomics aims to accurately and efficiently identify the metabolites detected in a biological sample and explain changes in response to experimental conditions [51], such as the ones MMC are exposed to when synthesizing PHAs.

There are different analytical methods and instruments used to accomplish identification and quantification of metabolites. The metabolomics method chosen should depend on the goals of the study that is being conducted. Examples of methods include Nuclear Magnetic Resonance (NMR) and Mass Spectrometry (MS) technologies [52]. NMR-based metabolomics provides advantages for data acquisition and sometimes does not even require sample preparation [53]. NMR is specifically popular for research in cell extracts biofluids, cell cultures, and tissues in vitro or in vivo. NMR's multinuclear potential allows it to observe different chemicals [53]. The NMR technique requires energy absorption and re-emission of the atom nuclei. Molecules are positioned in a strong magnetic field and the nuclei of certain atoms become magnetic. This allows the resonant frequencies of the nuclei to be measured and transformed into an NMR spectrum [52]. The main limitations of this technique include less spectral resolution and sensitivity [53]. MS-based metabolomics focuses on measuring the mass-to-charge ratio (m/z) and fragment ions of a molecule after it has been ionized. Mass separation depends on the movement of charged ions under the control of magnetic and/or electric fields [52]. Ion separation by m/z can be evaluated in a

field-free region (no specific magnetic or electric field), but to avoid ions collisions, high vacuum conditions are recommended [52]. Contrary to NMR, mass spectrometry requires sample preparation with the objectives of extracting substances from a complex biological matrix and to enhance the analytes in order to improve detection limits [52]. MS is a highly sensitive method for detection, accuracy, quantitation, and structure explanation of hundred metabolites in a single measurement [54].

Ionization is a key step in MS-based metabolite studies because it determines the ability to identify and quantify a metabolite [54]. Examples of ionization methods include electrospray ionization (ESI), atmospheric pressure chemical ionization (APCI), atmospheric pressure photoionization (APPI), and fast atom bombardment (FAB). Presently, many instruments include dual ionization capabilities because this allows them to increase the coverage of metabolites in samples. A common ionization method is ESI because it provides soft ionization which is helpful when dealing with biological molecules of large molecular mass. Soft ionization also yields more ions through charge exchange in solution and can form intact molecular ions which helps with early identification [55]. ESI can universally ionize metabolites of <1,000 amu and larger molecules such as peptides and proteins [54]. To ensure the metabolites coverage in a sample, it is recommended to analyze the samples in both positive and negative ionization (under scan range of m/z 50–1000) [55]. Although ionization techniques have improved through the years, chromatographic separation has become more widespread utilized, especially for complex biological samples. Different metabolomics techniques have been developed where MS and chromatography are combined.

Chromatography involves taking a mixture of chemicals and using either liquid or solid to separate it out into its different components. Chromatography relies on a mobile phase, and a stationary phase. The mobile phase passes through the stationary phase in which the substances to be examined are collected [56]. Separation of metabolites through chromatography offers advantages such as increased quantification, decreased matrix effects, and isomer separation, and provides supplementary data to enhance metabolite characterization [52]. Some of the bioanalytical techniques utilized in MS-based metabolomics coupled with chromatography analysis include gas chromatographic mass

spectrometry (GC-MS), liquid chromatographic mass spectrometry (LC-MS), capillary electrophoresis mass spectrometry (CE-MS), and spectroscopy [57].

GC-MS is known for accomplishing good metabolite separation. An advantage of this technique is that it generally avoids ion suppression due to its use of the gaseous phase and the quality of its MS ionization. Ion suppression is important because it can negatively affect several key analytical figures, such as detection capability, accuracy, and precision. However, application of GC-MS also requires chemical derivatization of the metabolic species before the GC-MS analysis, such that the target is volatilized [54].

LC-MS-based metabolomics is capable of separating metabolites independently of their volatility or polarity. In this sense, LC is more multipurpose than GC. The mobile phase in LC is a liquid that flows through a column to form the stationary phase [52]. LC-MS and related techniques such as ultra-performance LC (UPLC) and high-performance LC (HPLC) have become widely utilized because of their high throughput and soft ionization techniques. Such techniques also have good compatibility of reverse-phase (RP) separations with biological samples, sensitivity, and good coverage of metabolites without the need for chemical modification [54, 55, 58].

LC-MS systems for metabolite identification and quantitation include a mass analyzer, an ion source, and a detector. Mass analyzers are paired with LC and ionization to achieve metabolite detection with high resolution and sensitivity. Currently, there are two types of mass analyzers: single (MS) and tandem (MS/MS) mass analyzers. Single-configuration mass analyzers include the quadrupole (Q), linear ion trap (LIT), quadrupole ion trap (QIT), time of flight (TOF), Fourier transform ion cyclotron resonance (FTICR), and Orbitrap. Quadrupole and ion trap analyzers provide limited resolution but high sensitivity. Conversely, TOF, FTICR, and Orbitrap provide high mass resolution. Tandem configuration mass analyzers are a combination of two or more analyzers. These include triple-quadrupole ion trap (QTrap), triple quadrupole (TQ), quadrupole-TOF (Q-TOF), and linear-quadrupole ion trap-Orbitrap (LTQ-Orbitrap). TQ and Qtrap analyzers are most commonly used in targeted metabolic studies because of their high sensitivity and selectivity [54]. Moreover, Q-TOF, LTQ-Orbitrap, and FTICR analyzers are a better fit for global profiling and metabolite identification because of their higher mass-resolving power [54].

LC analyses also use separation methods prior to MS acquisition due to the complexity of biological matrices [54]. A popular separation method is high-performance liquid chromatography (HPLC). This method is coupled with mass spectrometry and is capable of separating compounds of a wide range of polarity through either isocratic elution or a gradient elution. Isocratic elution maintains a constant concentration in the mobile phase, while gradient elution keeps a variable concentration in the mobile phase. Gradient elution runs a faster analysis and produces narrower peaks compared to isocratic elution. Some common organic solvents are acetonitrile, methanol, and tetrahydrofuran (THF) [55].

Analysis of LC-MS metabolomic data involves a series of steps to transform, identify, and quantitate. After samples are collected, their names are typed and saved in individual files in the instrument computer. Utilizing software such as FreeStyle (Thermo Fisher Scientific, Waltham, MA, USA), the sample raw data are integrated into ion peaks organized by mass, retention time (RT), and peak area. Peaks are integrated, aligned by time, and normalized by intensity. Samples must be analyzed individually for metabolite identification, usually utilizing standard reference libraries or targeted metabolites to compare them with the standards known spectra [51]. LC-MS-based metabolomic studies frequently depend on experimental, analytical, and computational steps and methods to be successful. LC-MS data analysis is also dependent on whether the method chosen is targeted or untargeted metabolomics. The targeted metabolomics approach aims to detect and quantify selected metabolites whose chemical characteristics are known. This approach is typically hypothesis-driven, while untargeted metabolomics is capable of generating new hypotheses by screening all metabolites within a biological system [55] which can lead to further tests and studies since none of those metabolites are known. Both targeted and untargeted metabolomics usually follow up with metabolic functional interpretations, quantitation, and pathway analysis.

To understand the metabolic pathways and regulatory networks of feast PHA synthesis, high throughput targeted, or untargeted metabolomics studies are necessary. To accomplish an adequate and dedicated targeted approach, it is important to choose the metabolites of potential interest. The constructed metabolite library must contain key metabolites involved in the different PHA pathways, aiming to identify them and quantitate them.

Chapter 3:   Materials and Methods

3.1   Experimental Setup

3.1.1   *Substrate*

Dairy manure was obtained from the University of Idaho dairy farm every two weeks and stored at 4°C until used. Collection took place in the loafing barns in order to avoid contaminating the manure with rocks and bedding material. For every new batch collected, Total Solids (TS) and Volatile Solids (VS) was measured in triplicate, with average values (n=36) of 16.3% ± 1.6% and 80.8% ± 4.7%, respectively.

3.1.2   *Bench-Scale Fermenter*

Dairy manure fermenter operations employed in this research were a legacy from and a continuation of previous related investigations [59-61]. The bench-scale fermenter was operated as an SBR, with an operational volume of 16 L and an SRT/HRT of 4 days; hence, 4 L was decanted and 4 L of diluted dairy manure was added on a 24-hour cycle. Manure was added to maintain an organic loading rate of 11.0 gVSS/L*day. The fermenter was equipped with a 3.75-inch diameter helical impeller powered by an Oriental Motor (San Jose, CA, USA) USM315- 401W 15W AC speed-control motor connected to a 3GN35SA reduction gearbox. Mixing speed was set to suspend material and ensure uniform reactor properties. The substrate for the enrichment and production reactors (i.e., DFL) was obtained from the fermenter effluent, which was centrifuged at 9000 rpm for 60 min. VFAs were measured tri-weekly with average values (n=172) of 1553 ± 434 mg/L (acetate), 858 ± 202 mg/L (propionate), 231 ± 164 mg/L (butyrate), 87 ± 58 mg/L (iso-butyrate), 112 ± 59 mg/L (valerate), 92 ± 43 mg/L (iso-valerate), and 24 ± 19 mg/L (caproate). Total carboxylates were on average 4006 ± 790 as mg-COD/L and 112 ± 22 as Cmmol/L.

3.1.3   *Microorganisms*

The inocula for the PHA enrichment reactors used in this investigation was obtained from an existing fermented dairy manure fed ADF processes' enrichment reactor that had been in operation since August 2011 [62, 63].

3.1.4   *Enrichment Reactors*

During the *phaC* genes evaluation phase of this thesis, three different enrichment reactors were tested: E.2.10, E.3.10, and E.4.10. The three reactors were operated as SBRs by a former graduate student in Civil Engineering, Alex Crozes [64]. Identification of enrichment reactors was based on Solids Retention Time (SRT, days) and Organic Loading Rate (OLR, Cmmol/L-d) as follows: E.SRT.OLR. The volume of each reactor was 2L, with different SRT (2, 3, and 4 days) and 10 Cmmol/L-d OLR. The total cycle length for all SBRs was 1 day. The wasting and feeding was accomplished using two Watson Marlow model 323 peristaltic pumps operating on digital timers. The wasting time was set for 10 min and the feed time was set at 5 min; the feed time was delayed until decanting was completed. The volume of substrate used to feed each SBR was fixed at a regular basis in order to keep the desired OLR which depended on the VFAs analysis in each DFL bottle. Aeration in the SBR was accomplished utilizing stainless steel diffusers at roughly 1-1.5 LPM (Key Instruments rotometer (0-2.5 LPM range), Hatfield,

Figure 3.1: Enrichment reactors: E.2.10, E.3.10, and E.4.10.

PA, USA) depending on reactor SRT and OLR. Dissolved oxygen (DO) was controlled at 3 mg/L using a Hach (Loveland, CO, USA) sc100™ Controller equipped with a Hach LDO™ Dissolved Oxygen Sensor. The reactors were mixed with Teflon™-coated stir bars and magnetic stir plates. The reactors are covered but are vented to the atmosphere.

3.1.5   *Enrichment reactor "E.2.20"*

For the inhibitors testing phase and the untargeted-targeted metabolomics studies conducted in this thesis, the reactor E2.10 was utilized due to its optimum performance [64]. Figure 3.2 shows the E.2.20 enrichment reactor which was operated as an SBR with a working volume of 8 L. The SRT and HRT were maintained at 2 days, with a total cycle length of 1 day. The reactor was decanted and fed (4 L) every day following the same method as described herein. The target OLR was set at 20 Cmmol L-1 d^{-1}. Aeration was achieved using a 9-inch diameter Sanitaire Silver Series II membrane fine bubble disc diffuser at approximately 8 LPM (Xylem, Rye Brook, NY, USA). A three-bladed, 6 inch diameter impeller was used for mixing, powered by an Oriental Motor Co., LTD. (Tokyo, Japan) (1500 rpm max at 60 Hz), model 5GN3.6SA. The "optimum" reactor has been operating from 7/12/19 to this date.
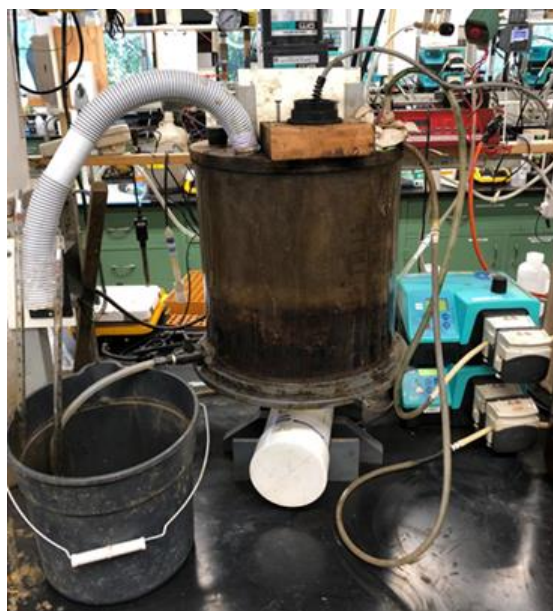
Figure 3.2: E.2.20 Enrichment Reactor.

3.2   **Analytical Techniques**

Samples were collected to monitor pH, DO, VFAs, and PHA. Prior to analyzing soluble constituents, samples were centrifuged to remove biomass, from which the

supernatant was filtered through a 0.22 µm syringe filter (Millipore Corp., Billerica, MA, USA). For the analysis of PHA, 10 mL samples were taken from the reactor and centrifuged at 5,000 rpm for 4 min. The resulting supernatant was then decanted before the samples were dried at 100ºC for at least 24 hours. Measurement of pH was accomplished using a Hach (Loveland, CO, USA) Intellical pHC101 pH Electrode. DO concentrations were measured using a Hach HQ40d Meter configured with a LDO101 DO probe [65].

3.2.1   *Carboxylic Acid Analysis*

Carboxylic acids (acetic, propionic, butyric, isobutyric, valeric, isovaleric, and caproic acids) were quantified using a Hewlett-Packard 6890 series gas chromatograph (GC) equipped with a flame-ionization detector (FID) and a 7679 series injector (Agilent Technologies, Inc., Santa Clara, CA, USA). The system was interfaced with the Hewlett-Packard GC ChemStation software (version A.06.01; Agilent Technologies, Inc.). Carboxylic acid separation was achieved using a capillary column (Zebron ZB-Waxplus, 30 m, 0.25 mm ID; Phenomenex Inc., Torrance, CA, USA) subjected to the following temperature program: (i) hold at 50 ◦C for 2 min, (ii) increase to 95 ◦C at 30 ◦C/min, (iii) increase to 150 ◦C at 10 ◦C/min, (iv) hold at 150 ◦C for 3 min, (v) increase to 200 ◦C at 25 ◦C/min, and (vi) hold at 200 ◦C for 12 min. Helium was used for the carrier gas (1.2 mL/ min). The injector and detector were operated isothermally at 210 ◦C and 300 ◦C, respectively. Prior to analysis, samples were acidified to a pH of 2 using nitric acid. 0.5 µL of each sample was injected in 20:1 split mode. Carboxylic acid concentrations were determined through retention time matching with known standards (Sigma-Aldrich Co., St. Louis, MO, USA; Thermo Fisher Scientific Inc., Waltham, MA, USA) and linear standard curves ($R2 > 0.99$).

3.2.2   Intracellular PHA analysis

The PHBV content of biomass samples was determined by gas chromatography/mass spectrometry (GC-MS). Enrichment assessment biomass samples (10 mL) were preserved with 100 µL bleach, stored on ice, centrifuged (5 min at 2400g), drained, rinsed with deionized water, and dried at 105 ◦C. After massing, biomass samples (20 to 40 mg) were

digested for 4 h at 100 ∘C in 4 mL of a 1:1 (v/ v) mixture of acidified methanol ($3\%H_2SO_4$; v/v) and chloroform (with 0.25 to 0.5 mg/mL benzoic acid; an internal standard). After digestion and cooling, the solution was separated into organic and aqueous phases with the addition of 1 to 2 mL of deionized water followed by vortex mixing. The organic phase was then extracted and filtered through a small column of anhydrous Na_2SO_4 (to remove excess moisture and particulates) into a GC vial. GC–MS was performed on an ISQ7000- Trace1300 GC–MS system (Thermo Fisher Scientific Inc.). Separation was achieved on a capillary column (ZB1, 30 m, 0.25 mm ID; Phenomenex Inc.) with helium as the carrier gas (1.2 mL/min) and an initial temperature of 40 ∘C (held for 2 min) ramped to 200 ∘C at 5 ∘C/min. 3HB and 3HV were quantified relative to the internal standard from known standards (0.12 to 0.21 mol3HV/molPHBV; Sigma-Aldrich Co.; TianAn Biologic Materials Co., Ltd., Ningbo, People's Republic of China), as confirmed by retention time and mass spectral matching; the optimal ion for quantification was determined to be $m/z = 103$ for both monomers. Additionally, two degradation products generated during the methanolysis of PHBV were similarly quantified and included in the final 3HB and 3HV quantities: methyl-2-butenoic acid (from 3HB, quantified by ion $m/z = 100$) and methyl-2-pentenoic acid (from 3HV, quantified by ion $m/z = 114$), both prepared from known standards (Alfa Aesar, Haverhill, MA, USA; Acros Organics, Geel, Belgium). The Xcalibur software program (v4.1.31.9; Thermo Fisher Scientific Inc.), MSFileReader (v3.0 sp1; Thermo Fisher Scientific Inc.), and the Thermo Raw File Reader (Pacific Northwest National Laboratory, https://omics. pnl.gov/software/thermo-raw-file-reader) were used for PHBV quantification.

3.2.3 *Phosphorus Analysis*

Testing for soluble PO_4-P was performed in accordance with Hach method 8048 (equivalent method to Standard Methods 4500-PE [65]). Absorbance for each reacted sample was measured using a Thermo-Fisher Scientific Corp (Waltham, MA, USA) Spectronic® 20 Genesys ™ spectrophotometer at a wavelength of 890 nm. Concentrations were calculated using linear standard curves ($R^2 > 0.99$).

3.3 **PHA synthase (*phaC*) studies**

3.3.1 *Quantitative polymerase chain reaction (qPCR)*

qPCR was performed on genomic DNA to calculate the abundance of class I, II, III, and IV *phaC* genes relative to the total eubacterial population. The DNA was obtained from the bench enrichment reactors E2.10, E3.10 and E4.10; additional biomass was obtained from a pilot PHA enrichment reactor on operational days 58, 61, 67, 71, 78, and 84 of summer 2019 [cite Guho's pub here]. Genomic DNA was extracted using the MO BIO PowerSoil DNA Isolation Kit (Qiagen, Hilden, Germany). Genomic DNA yield and purity was quantified using a NanoDrop ND-1000 Spectrophotometer (Thermo Fisher Scientific Inc.). Table 1 summarizes the primer sets utilized to quantify the total bacteria and *phaC* gene classes I, II, III, and IV abundances.

Quantification and amplification were accomplished with an Applied Biosystems Step-one-plus qPCR system (Thermo Fisher Scientific Inc.); qPCR settings and estimation of phaC gene relative abundance in the bacterial population were in accordance with Winkler et al. [66]. Replicate qPCR was achieved for all samples on a 96 well plate. qPCR melting curves were evaluated to confirm a single melting peak; agarose gel analysis confirmed a single band for each primer set. Amplification efficiencies were calculated for each primer set using baseline-corrected fluorescence data (StepOne software v2.3, Thermo Fisher Scientific Inc.) and the LinRegPCR program [67]. The cycle threshold was set at a constant value of 0.2 within the log-linear region across all samples for determination of quantification cycle values.

Table 1: PCR primers used in this thesis.

Name	Nucleotide sequence	Amplicon/PCR product length	Reference
phaC class I phaCF1 phaCR4	ATC AAC AAR TWC TAC RTC YTS GAC CT AGG TAG TTG TYG ACS MMR TAG KTC CA	*phaC* class I - 406 bp	Ciesielski et al. [68]
phaC class II I-179L I-179R	ACA GAT CAA CAA GTT CTA CAT CTT CGA C GGT GTT GTC GTT GTT CCA GTA GAG GAT GTC	*phaC* class II - 540 bp	
phaC class III P1 P2	ATN GAY TGG GGN TAY CCN RAA DAT CCA YTT YTC CAT	*phaC* class III - 500 bp	
phaC class IV B1F B1R	AAC TCC TGG GCT TGA AGA CA TCG CAA TAT GAT CAC GGC TA	*phaC* class IV - 590 bp	
eubacteria 341F 534R	CCT ACG GGA GGC AGC AG ATT ACC GCG GCT GCT GG		Muyzer et al. [69]

3.4 **Targeted metabolomics**

3.4.1 *Chemicals:*

LC-MS grade water, LC-MS grade acetonitrile, and ammonium acetate
(TraceSELECT®) were purchased from Sigma-Aldrich (Vienna, Austria) and used for
chromatography. LC-MS grade methanol was purchased from Fisher Scientific
(Loughborough, UK).

Table 2: The following standards were purchased from Sigma-Aldrich.

Glyoxylate sodium monohydrate	Isovaleryl coenzyme A lithium salt	NADPH
Sodium citrate tribasic dihydrate	Acetyl-CoA	A-ketoglutaric acid
Sodium pyruvate	NADH	(-)-Methyl (r)-3-hydroxyvalerate
N-propionyl coenzyme A lithium	Succinate	D-fructose 1,6-bisphosphate trisodium.

3.4.2 *LC-MS/MS method for Acyl-CoA thioesters*

Metabolomics analyses were completed using a TS Vanquish LC system and Thermo Scientific TSQ Endura ESI-MS/MS as described in Neubauer et al. [70]. Separation was achieved on an Atlantis T3® analytical column (150×2.1 mm, 3μmparticlesize, 100 Å pore size) from Waters (Milford, MA, USA). Eluent A was composed of water, 50 mmol L−1NH$_4$OAc, and with a pH of 6.9. Eluent B included just acetonitrile. The optimized gradient program resulted in a total run time of 15 min.

TSQ Endura tandem mass spectrometer from Thermo Scientific was used for MS detection, featuring a heated electrospray ionization (ESI) interface. The positive mode of the ion source parameters are vaporizer temperature, 300 °C; ion transfer tube temperature, 350 °C; aux gas pressure, 10 arbitrary units; sheath gas pressure, 35 arbitrary units; ion sweep gas pressure, 0 arbitrary units; declustering voltage, 0 V; and spray voltage values, 3000 V; collision gas pressure for multiple reaction monitoring (MRM) was set to 1.5 mTorr. Table 4 lists the precursor ions, product ions, and energy values.

Table 3: Chromatographic conditions used for CoA separation.

Time/min	Gradient program (no isomer separation)	
	Fraction B (%)	**Flow rate (µLmin−1)**
0	0	250
1	0	250
1.1	5	250
7	25	250
8	40	250
11	40	250
11.1	0	250
15	0	250

Table 4: MRM settings of the LC-MS/MS instrument.

Abbreviation	Name of compound	Precursor ion	Precursor ion (m/z)	Quantifier (m/z)	CE Quantifier(V)	IS compound for quantification
AcCoA	Acetyl-coenzyme A	[M+H] +	810.1	303	27	$U^{13}C_{23}AcCoA$
HBCoA	Hydroxybutyryl-coenzyme A	[M+H] +	854.1	347	30	$U^{13}C_{23}AcCoA$
PrCoA	Propionyl-coenzyme A	[M+H] +	824.1	317	30	$U^{13}C_{24}PrCoA$

3.5 **Untargeted metabolomics method**

Untargeted metabolomics evaluations were conducted by Montana State University. Samples were prepared in the Coats Environmental Engineering laboratory at the University of Idaho, then shipped to MSU for analysis.

3.5.1 *Reverse Phase Chromatography*

For reverse phase analysis, a Kinetex 1.7 um C18 150 mm x 2.1 mm.column (Phenomenex, Torrance, CA) kept at 50 °C was used for LC separation with a flow rate of 600 uL min-1. Solvent A consisted of 0,1% formic acid in water, while solvent B was 0.1% formic acid in acetonitrile. The elution gradient consisted of 2% solvent B for 2 minutes (with the first two minutes going to waste to avoid contaminating the source with excess salt), to 95% solvent B over 24 minutes, held at 95% for 2 minutes, and then returned to 2% for 2 minutes, with a total run time of 30 minutes using an Agilent 1290 UPLC (Agilent, Santa Clara, CA) system connected to an Agilent 6538 Q-TOF Mass Spectrometer (Agilent, Santa Clara, CA).

3.5.2 *Hydrophilic interaction liquid chromatography (HILIC)*

Aqueous Normal phase analysis used a Cogent Diamond Hydride HILIC 150 mm x 2.1 mm column (MicroSolv, Eatontown, NJ) was used for LC separation with a flow rate of 600 pL min-1. Solvent A consisted of 0.1% formic acid in water, while solvent B consisted of 0.1% formic acid in acetonitrile. The elution gradient consisted of 95% solvent B for 2 minutes (with the first minute going to waste to avoid contaminating the source with excess salt), to 50% solvent B over 24 minutes, held at 50% for 2 minutes, and then returned to 95% for 2 minutes, with a total run time of 30 minutes using an Agilent 1290 UPLC (Agilent, Santa Clara, CA) system connected to an Agilent 6538 Q-TOF Mass Spectrometer (Agilent, Santa Clara, CA).

3.5.3 *Mass spectrometry (MS) parameters*

Mass spectrometry analysis was conducted in positive ion mode, with a cone voltage of 3500V and a fragmentor voltage of 120V. Drying gas temperature was 350 °C with a flow of 12 L min-1 and the nebulizer was set to 60 psig. Spectra were collected at a rate of 2.52 per second with a mass range of 50 to 1000 m/z. The mass analyzer resolution was 18,000 and post calibration tests had a mass accuracy of approximately one ppm.

3.5.4   *Data Analysis*

Data files from the LC-MS were converted to *.MZxml format using the Masshunter Qualitative software provided with Agilent instruments (Agilent, Santa Clara, CA). Analysis of LC-MS data was done using the software package MZmine (version 2.14). Procedures, together with parameters used for the alignment of features and identification in MZmine, were as follows: LC-MS files were imported into MZmine, followed by data set filtering to remove the first minute of elution data for HILIC analysis, and the first two minutes of elution data for RP analysis. A minimum intensity cutoff of 5000 and a minimum elution time window of 0.1 minutes were used to create molecular feature lists. Lists included retention time (R/T) adjusted with a tolerance of approximately 0.2 minutes. These R/T-adjusted lists were then aligned into one mass list, and then gap-filled to add missing peaks not detected in all runs with an m/z tolerance of 15.0 ppm. The m/z peak intensities were normalized by normalizing the total ion intensity of each run to the most intense total ion intensity. Significance was determined using a two-tailed T-test.

3.5.5   *Metabolomics software:*

The following software was utilized for data analysis and interpretation:
MetaboAnalyst 5.0: Web-based interface that supports raw MS spectra processing, comprehensive data normalization, statistical analysis, functional analysis, and omics integration data.
XCMS Online: Cloud software that facilitates statistical assessment of the detected peaks across LCMS and GCMS datasets.
MZmine 2: Open-source software program for mass-spectrometry data processing; it focusses on LC-MS data analysis workflows.

3.6 **Experimental Design: Triggering PHA Mechanisms**

Several batch tests were performed on waste biomass from reactor E.2.10 in order to evaluate the PHA feast metabolome.

3.6.1 *Metabolic inhibitors and VFA research*

Chemicals selected for the inhibitor investigations were Carbonyl Cyanide 3-Chlorophenylhydrazone (CCCP), Valinomycin, and N, N′-Dicyclohexylcarbodiimide (DCCD). DCCD inhibits oxidative phosphorylation [71], and CCCP reduces ATP production [72]. Valinomycin slows ATP synthesis without blocking electron transfer to O_2 [73]. These inhibitors were utilized by Burow et al. [71] to study carboxylic acid uptake in enhanced biological phosphorus removal systems; however, in this research they have been used to study carboxylic acid uptake in MMC for aerobic dynamic feeding PHA production. Carboxylic acid, PHA, and phosphorus removal analysis were performed in each sample to evaluate the metabolic functions that each chemical inhibited.

For the batch tests reactors, 600 ml of WAS from the PHA E.2.10 reactor, and 600 ml of feed (200 DFL and 400 water) were added to a 2 L beaker, yielding a reactor volume of 1.2 L. All metabolic inhibitors utilized in these experiments required solubilization in ethanol, with a final concentration of 0.25% (v/v). Valinomycin was the only inhibitor that included the addition of KCl at a final concentration of 200 mM [71]. Table 5 is an example of the experimental design utilized for every experiment, and lists the number of samples collected in every batch test. Table 6 describes the concentration of every chemical that were necessary to achieve inhibition as per Burow et al. [71].

Table 5: Experiment design for studying VFA uptake in MMC.

Metabolic phase	Time (minutes)	Reactor 1	Reactor 2	Parent PHA reactor
		Inhibitor 1	Inhibitor 2	
Famine	0	✓	✓	✓
	5	✓	✓	✓
Feast	15	✓	✓	✓
	30	✓	✓	✓
	45	✓	✓	✓
	60	✓	✓	✓
	75	✓	✓	✓
	90	✓	✓	✓
Famine	105	✓	✓	✓
	120	✓	✓	✓
	135	✓	✓	✓
	150	✓	✓	✓

Table 6: Concentrations of chemicals necessary to achieve inhibition.

	Valinomycin	DCCD	CCCP
Molecular weight (g/mol)	1111.32	206.33	204.64
Required concentration as per Burow et al. [71].	5 μM	150 μM	100 μM
Calculated amount of respective inhibitor for 1.2 L reactor	3.34 mg	37.14 mg	24.5 mg

3.6.2 *Effects of NADH as potential inhibitor of the TCA cycle:*

The purpose of this experiment was to evaluate potential metabolic features that negatively affect the TCA cycle and re-direct acetyl-CoA to PHA synthesis. Adding NADH could potentially inhibit the TCA cycle and induce greater PHA synthesis. NADH was purchased from Sigma-Aldrich (Vienna, Austria). For this batch test, 600 ml of WAS from the PHA reactor was added to the mini reactor or reactor 1. For the feed, 200 ml DFL and 400 water ml were added to complete a 600 ml feed. The water and DFL ratios were calculated according to the targeted OLR which was 20 Cmmol/L-d, and 2 days SRT/HRT. The total mini reactor volume was 1.2 L. Table 7

Figure 3.3: Example of mini reactor utilized to run batch tests.

details the experiment design utilized in this investigation. Carboxylic acid, PHA, and metabolomics analysis were performed in each sample to evaluate and compare the metabolic effects the NADH had on the PHA system.

Table 7: NADH experiment design for studying TCA cycle inhibition.

Metabolic phase	Time (minutes)	Reactor 1 NADH	Parent PHA reactor
Famine	0	✓	✓
	5	✓	✓
Feast	15	✓	✓
	30	✓	✓
	45	✓	✓
	60	✓	✓
	75	✓	✓
	90	✓	✓
Famine	105	✓	✓
	120	✓	✓
	135	✓	✓
	150	✓	✓

Table 8: Concentrations of NADH necessary to achieve inhibition.

	NADH
Molecular weight (g/mol)	663.43
Required conc as per Liu et al. [74].	100 μM
Calculated amount of respective inhibitor for 1.2 L reactor	79.61 mg

3.6.3 *Acetate and Propionate as sole carbon sources*

The purpose of these batch experiments was to investigate PHA formation from individual acids to examine how feast-famine driven PHA-accumulating bacteria react, and what PHA composition is obtained from these substrates. The main objective of these experiments was to compare and contrast metabolomics data to understand the activity of different metabolites during the accumulation of PHAs. For these batch tests, 600 ml of WAS from the PHA reactor were added to each mini reactor. For the synthetic feed, calculations on concentrations of each carbon source were made to match the concentration of DFL in the parent PHA reactor. Table 9 details the experiment design utilized in this investigation. Table 10 describes the synthetic feed recipe utilized [35]. VFA, PHA, and metabolomics analysis were performed in each sample to evaluate and compare the metabolic changes in each time point of feast and famine phases.

Table 9: Experiment design for studying PHA synthesis from sole carbon sources.

Metabolic phase	Time (minutes)	Reactor 1 Propionic acid	Reactor 2 Acetic acid	Parent PHA reactor
Famine	0	✓	✓	✓
	5	✓	✓	✓
Feast	15	✓	✓	✓
	30	✓	✓	✓
	45	✓	✓	✓
	60	✓	✓	✓
	75	✓	✓	✓
	90	✓	✓	✓
Famine	105	✓	✓	✓
	120	✓	✓	✓
	135	✓	✓	✓
	150	✓	✓	✓

Table 10: Synthetic feed recipe.

Acetic Acid		Propionic Acid	
10X macronutrients	100 ml	10X macronutrients	100 ml
10X trace nutrients	0.2 ml	10X trace nutrients	0.2 ml
Acetic Acid	4 g	Propionic Acid	0.91 ml
Fill to 1 L of DDI		Fill to 1 L of DDI	

Chapter 4:   Results and Discussion

4.1   Assessing phaC gene presence in MMC

As mentioned in the literature review, PHA synthase (*phaC*) is the most critical gene associated with PHA synthesis because it polymerizes 3-hydroxyalkyl-CoAs to form PHA [39]. To date, four distinct classes of phaC have been identified: classes I, III, and IV polymerize short-chain-length (SCL; C3-C5) monomers, while class II is believe to only polymerize medium-chain-length (MCL; C6-C14) monomers [40, 41].

Molecular studies in this thesis focused on evaluating the potential presence, diversity, and relative abundance of PHA synthase genes (*phaC*) in the MMC. In particular, research aimed to answer RQ3: Do MMC enriched on fermented dairy manure under ADF operational conditions have an enough abundance of key PHA genes to synthesize PHAs in a production level?

4.1.1   *phaC in Bench-scale PHA Enrichment Reactors:*

Research was first conducted to examine the potential presence of all four *phaC* gene classes in the three respective bench-scale MMC performing ADF PHA synthesis [75]. Gel electrophoresis of the PCR-amplified genomic DNA revealed that the MMC only contained phaC class II, and not classes I, III or IV (Figures 4.1-4.4). The relative abundance of the *phaC* genes in MMC was completed through qPCR. Results revealed that **E.2.10** reactor has a *phaC* class II gene presence of 13.6%, E.3.10 has a *phaC* class II gene presence of 17.3%, and finally, the E.4.10 reactor has a *phaC* class II gene presence of 14.9%. The presence of phaC class II was surprising, given that research on both bench and pilot-scale reactors shows that the PHA synthesized by MMC fed fermented dairy manure is limited to SCL monomers (3HB and 3HV) [13, 32, 75]. The lack of MCL monomers in each system suggests that the class II *phaC* genes detected were either not actively transcribed, or were responsible for synthesizing SCL PHA. This result highlights how little is known about the potential of MMC to synthesize a diversity of polymers.

To improve the *phaC* primer sets amplification efficiency, bovine serum albumin (BSA) was added prior to amplification. BSA, or Betaine, is the most common PCR additive used to enhance amplification because of its capability to dissolve secondary structure that blocks polymerase action [76]. Figure 4.7 shows the results from betaine addition to *phaC* genes classes I and II primer sets. However, even with this additive, other *phaC* gene classes were not detected.

To further understand PHA synthase in MMC, the primer "*phb*" was tested in this work. According to Yang, et al. [77], the *phbC* gene is the PHA synthase version for PHB synthesis. Gel electrophoresis results from this particular experiment revealed that the MMC contained only short (amplicon/PCR product length of 602 bp) *phbC* genes in all three reactors (Figures 4.8-4.9). This primer was also optimized with different annealing temperatures (58-63 °C).

The "phaC BO" gene – a combination of *phaC* gene classes I and II – was also tested as an effort to corroborate the presence of *phaC* diversity in MCC. However, the results from this gel electrophoreses did not show any interesting signal of the *phaC* genes classes I and II in any of the bench-scale reactors (Figure 4.5).

Figure 4.6 shows the image of the agarose gel electrophoresis of qPCR products obtained from DNA extracted from *Cupriavidus necator* and *Meganema perideroedes*. These pure cultures were grown with the purpose to compare and contrast the presence of *phaC* gene classes in a popular PHA producer such a *Cupriavidus necator*; *Meganema* was selected because it is a PHA producing microbe that dominates in our MMC [18, 78]. As noted in Figure 4.6, *C. Necator* (which is current name for *Ralstonia eutropha*) showed a bright signal on the gel for *phaC* class I, with strong positive Ct value (17.69). Conversely, *Meganema* did not show any signal for *phaC* classes. The *phaC* gene (from Ralstonia Eutropha sequence) was not detected in Meganema. Research showed that there is no whole genome for *Meganema*, and no literature related to the *phaC* gene in Meganema was found. More testing using this pure culture is recommended in future research.
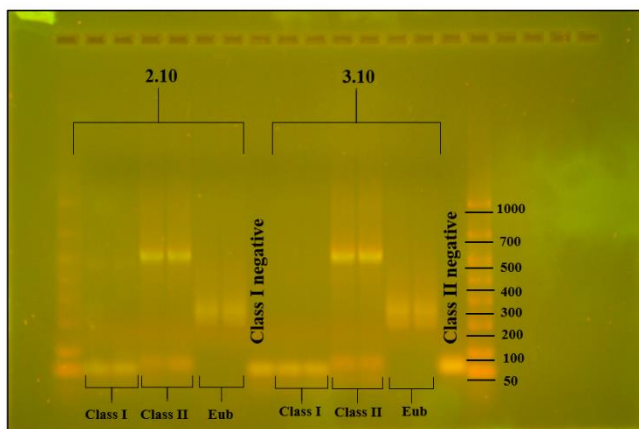
Figure 4.1: Image of the agarose gel electrophoresis of qPCR products obtained from DNA extracted from enrichment reactors **E.2.10 and E.3.10** biomass samples amplified with the **phaC** genes classes **I and II** primer sets.

Amplicon/PCR products lengths:
phaC gene class I: 496 bp
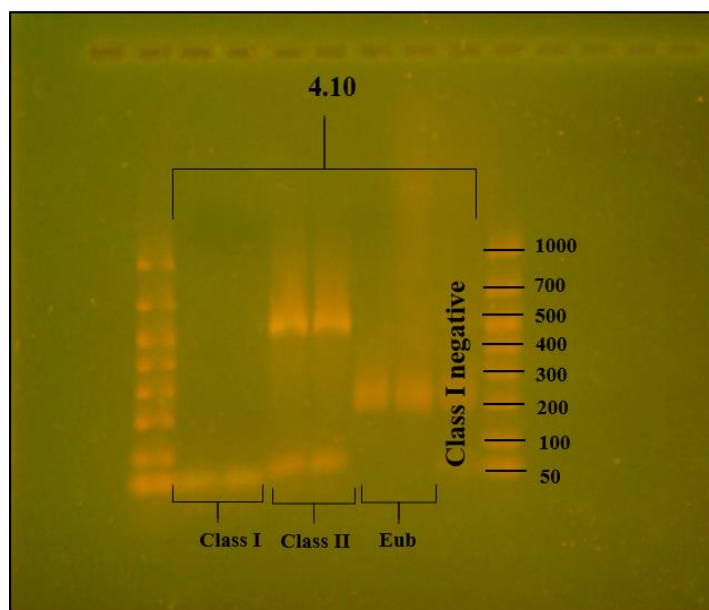phaC gene class II: 540 bp
Eubacteria: 195 bp
Date:07/12/2019

Figure 4.2: Image of the agarose gel electrophoresis of qPCR products obtained from DNA extracted from enrichment reactor **E.4.10** biomass samples amplified with the **phaC** genes classes **I and II** primer sets.

Amplicon/PCR products lengths:
phaC gene class I: 496 bp
phaC gene class II: 540 bp
Eubacteria: 195 bp
Date:07/12/2019

Figure 4.3: Image of the agarose gel electrophoresis of qPCR products obtained from DNA extracted from enrichment reactors E.2.10, E.3.10, and E.4.10 biomass samples amplified with the phaC genes classes I and II primer sets.

Amplicon/PCR products lengths:
phaC gene class I: 496 bp
phaC gene class II: 540 bp
Date:07/17/2019

Figure 4.4: Image of the agarose gel electrophoresis of qPCR products obtained from DNA extracted from enrichment reactors **E.2.10, E.3.10, and E.4.10** biomass samples amplified with the **phaC** genes classes **III and IV** primer sets.

Amplicon/PCR products lengths:
phaC gene class III: 500 bp
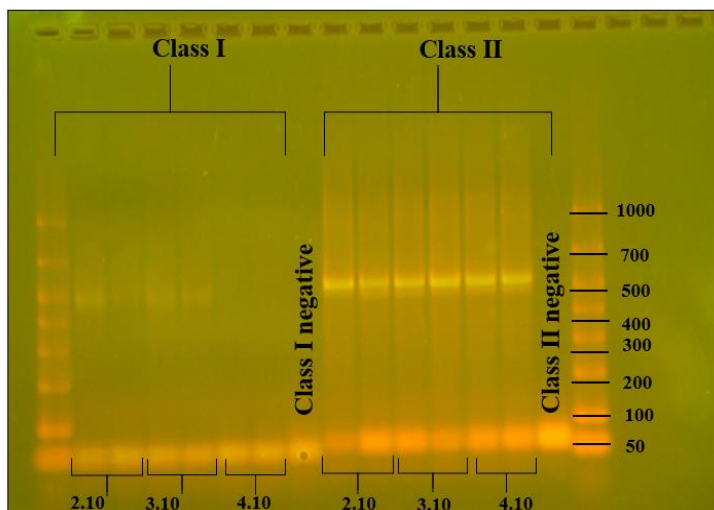phaC gene class IV: 590 bp

Date:07/17/2019

Figure 4.5: Image of the agarose gel electrophoresis of qPCR products obtained from DNA extracted from enrichment reactors **E.2.10, E.3.10, and E.4.10** biomass samples amplified with the **phaC BO gene** primer set.

Amplicon/PCR products lengths:
phaC gene BO: 246 bp
Eubacteria: 195 bp
Date:07/17/2019
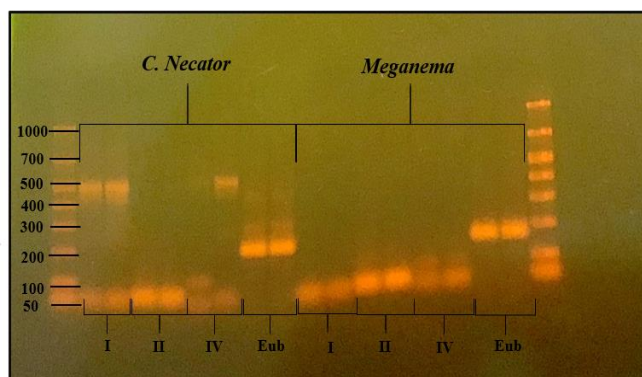
Figure 4.6: Image of the agarose gel electrophoresis of qPCR products obtained from DNA
extracted from *C. Necator* and *Meganema* amplified with the **phaC** genes *classes I, II and IV* primer sets.
Amplicon/PCR products lengths:
phaC gene class I: 496 bp
phaC gene class II: 540 bp
phaC gene class IV: 590 bp
Eubacteria: 195 bp
Date: 01/03/2020

2.10   **3.10**   **4.10**

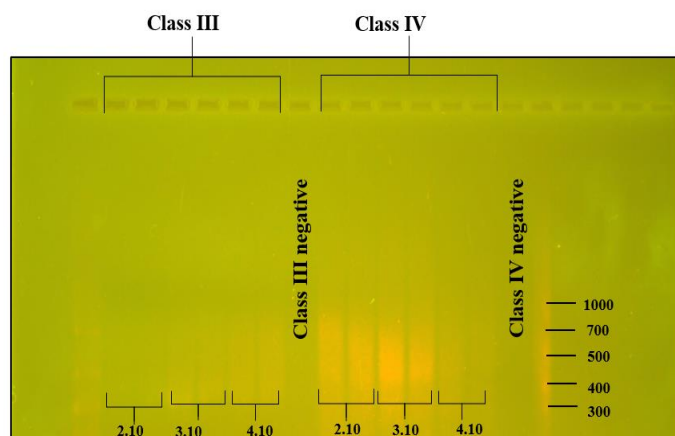Short   Long   Short   Long   Short   Long

Figure 4.8: Image of the agarose gel electrophoresis of qPCR products obtained from DNA extracted from enrichment reactors **E.2.10, E.3.10, and E.4.10** biomass samples amplified with the *phbC* **gene** primer set.

Amplicon/PCR products lengths:
Short: 602 bp
Long: 1812 bp
Date: 06/28/19

phaC class I with Betaine
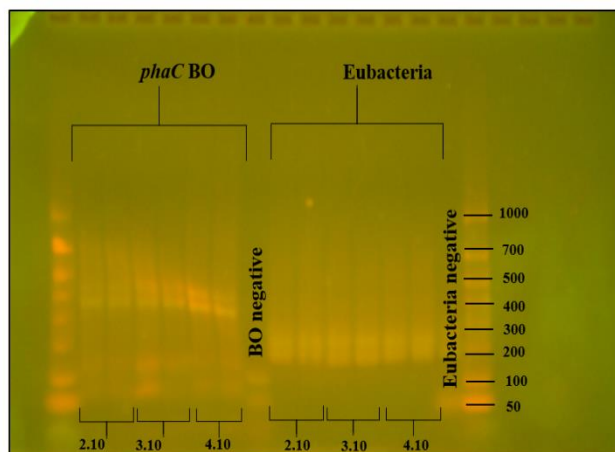

phaC class II with Betaine

2.10   3.10   4.10

Figure 4.7: Image of the agarose gel electrophoresis of qPCR products obtained from DNA extracted from enrichment reactors **E.2.10, E.3.10, and E.4.10** biomass samples amplified with the **phaC** genes classes **I and II** primer sets with **Betaine**.
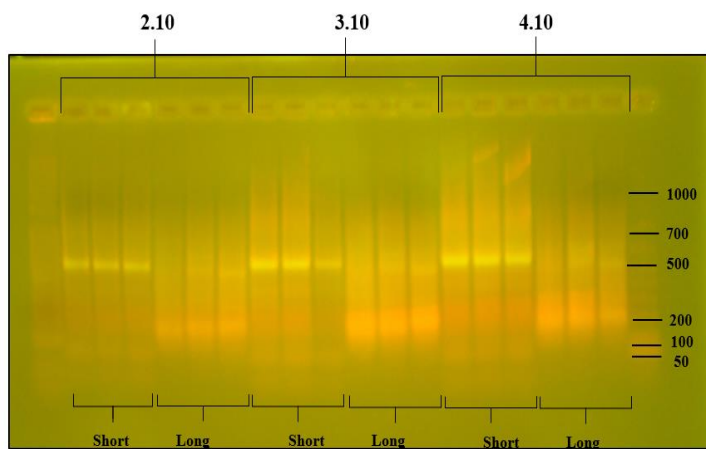Amplicon/PCR products lengths:
phaC gene class I: 496 bp
phaC gene class II: 540 bp
Date:08/05/2019

Figure 4.9: Image of the agarose gel electrophoresis of qPCR products obtained from DNA extracted from enrichment reactor **E.2.10** 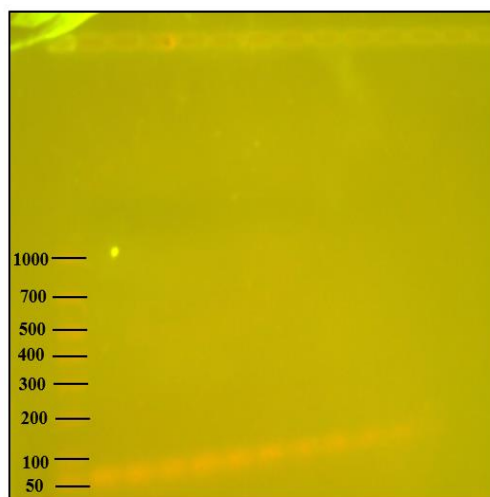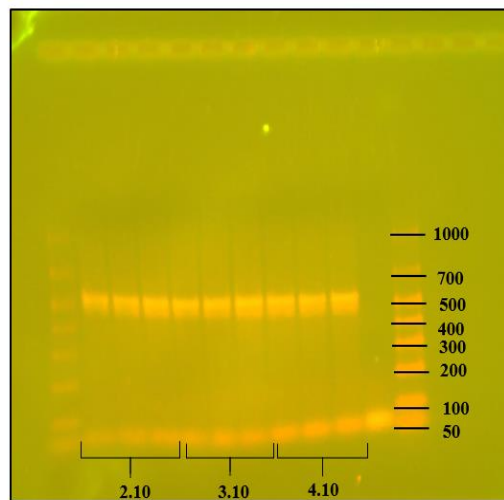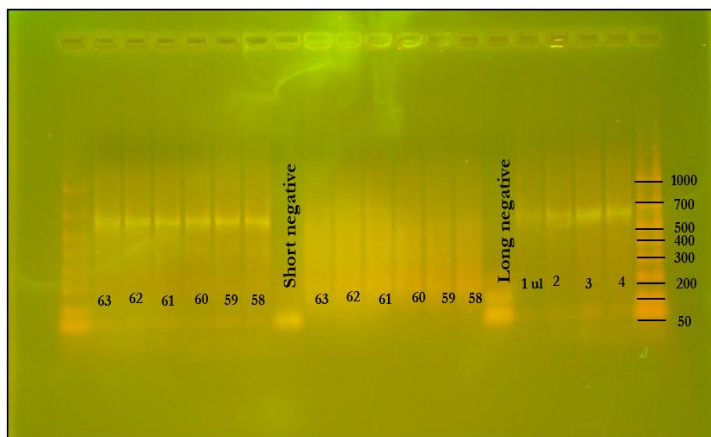biomass samples amplified with the **phbC gene** primer set. Amplification optimization conditions included different annealing temperatures (58-63 °C).

Amplicon/PCR products lengths:
Short: 602 bp
Long: 1812 bp
Date: 07/10/19

4.1.2   *phaC in a Pilot Scale PHA Model*

Investigations on PHA synthase in a pilot-scale system [32] gave even more surprising results, contrasted with the bench-scale PCR investigations. Gel electrophoresis of the PCR-amplified genomic DNA revealed that the MMC contained phaC classes I and II, but not classes III or IV (Figures 4.10-4.13). Relative abundance analysis of the *phaC* gene—completed through qPCR—revealed that *phaC* class II gene presence at 2.3% over six operational days. While *phaC* class I showed a bright signal on the gel for all operational days evaluated (Figure 4.10), amplification efficiency was less than 35%. Even though the bench-scale and the pilot scale systems were operated similarly and used the same manure, these results suggest that in a pilot-scale, MCC could have the potential to synthesize both short-chain-length and medium-chain-length polymers.

Considering that the pilot scale model is a real setting of a larger scale PHA production from dairy manure, it might be a safe assumption to say that 2.3% of *phaC* gene abundance is a fair number. This amount of phaC genes might be what MMC needs to provide a consistent production of PHBV. By comparing the abundance of phaC genes with the overall production of PHBV, we have acquired a hint about the ability of the MCC to accumulate PHBV.

MMCs enriched in bench-scale and pilot-scale systems have consistently produced SCL PHA, yet with MCL *phaC* class II genes detected. The detection of *phaC* class II genes in independent PHBV systems and across time further suggests that this potential was not limited to the MMC enriched in one operational run, indicating unrealized MCL PHA production potential worthy of future exploration, yet also suggesting that class II genes may be responsible for SCL PHA synthesis.

Figure 4.10: Image of the agarose gel electrophoresis of qPCR products obtained from DNA extracted from enrichment reactor biomass samples collected on operational days **58, 61, 67, 71, 78, and 84** amplified with the *phaC* **gene class II** primer set (amplicon/PCR product length: 540 bp).

Figure 4.11: Image of the agarose gel electrophoresis of qPCR products obtained from DNA extracted from enrichment reactor biomass samples collected on operational days **58, 61, 67, 71, 78, and 84** amplified with the *phaC* **gene class I** primer set (amplicon/PCR product length: 496 bp).

Figure 4.12: Image of the agarose gel electrophoresis of qPCR products obtained from DNA extracted from enrichment reactor biomass samples collected on operational days **58, 61, 67, 71, 78, and 84** amplified with the *phaC* **gene class III** primer set (amplicon/PCR product length: 500 bp).
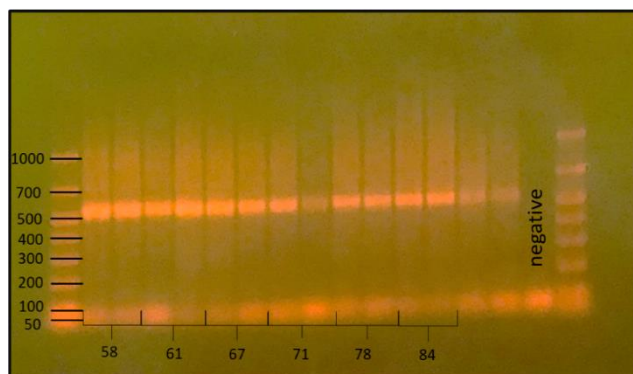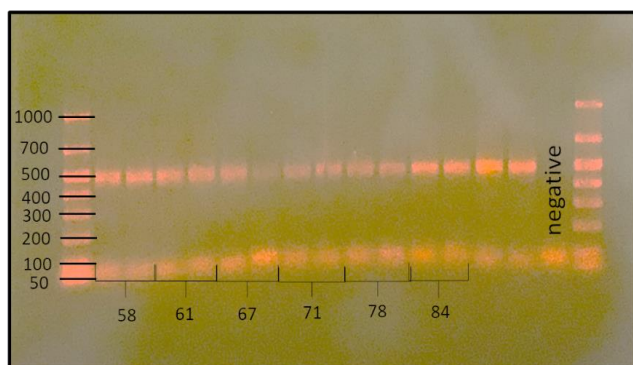
Figure 4.13: Image of the agarose gel electrophoresis of qPCR products obtained from DNA extracted from enrichment reactor biomass samples collected on operational days **58, 61, 67, 71, 78, and 84** amplified with the ***phaC gene class IV*** primer set (amplicon/PCR product length: 590 bp).

4.1.3   *phaC class I primer set optimization*

To potentially improve the phaC class I primer set amplification efficiency, Betaine was added prior to amplification. Additionally, the primer concentration and annealing temperature were further evaluated (Figure 4.14-4.15), with variable primer concentration (400 nM and 200 nM) as well as the initial DNA concentration. As shown, unfortunately none of the conditions evaluated improved the amplification efficiency enough to warrant quantification of the phaC class I gene.

Figure 4.14: Image of the agarose gel electrophoresis of qPCR products obtained from DNA (50 ng) extracted from enrichment reactor biomass samples collected on operational days **58, 61, 67, 71, 78, and 84** amplified with the phaC gene class I primer set (amplicon/PCR product length: 496 bp).
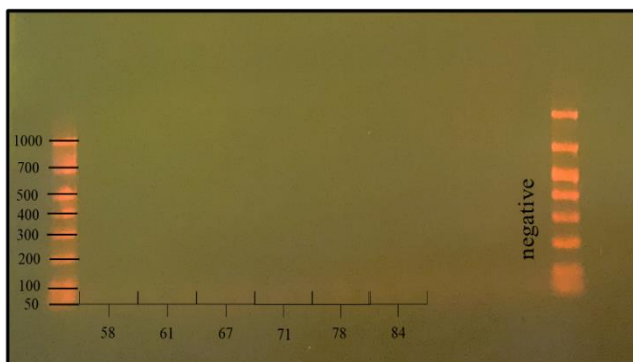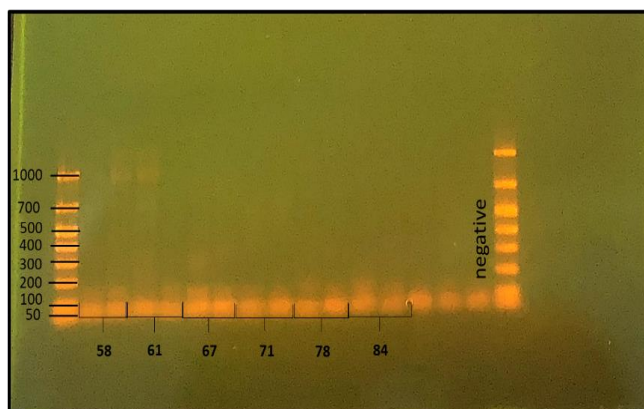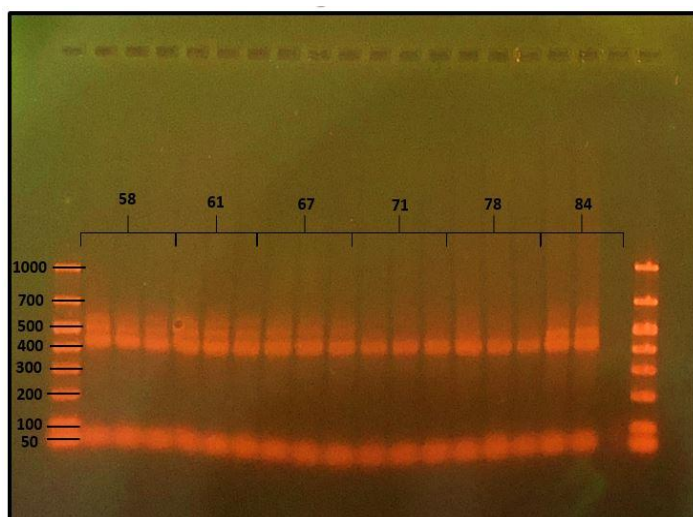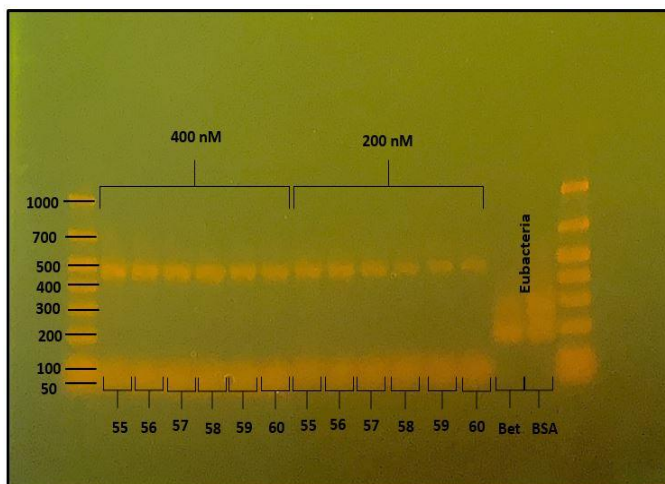
Figure 4.15: Image of the agarose gel electrophoresis of qPCR products obtained from DNA (50 ng) extracted from enrichment reactor biomass samples collected on operational day 84 amplified with the phaC gene class I primer set (amplicon/PCR product length: 496 bp). Optimization based on primer concentration 400 nM and 200 nM, and temperatures 55-60 C, utilizing BSA. Betaine was utilized only for Eubacteria primers.

4.2 **Assessment of VFA uptake in MMC**

The purpose of the experiments using VFA metabolic inhibitors was to compare and assess VFA uptake by MMC under conditions wherein mechanisms associated with VFA uptake were potentially inhibited. In particular, this research aimed to answer RQ1: **how are MMC producing ATP during the feast stage? And why does a rapid uptake of VFAs always occur?** The MMC were enriched under ADF conditions and were producing PHA via induced feast-famine metabolisms. A specific focus was to examine the performance of ATP synthase during the 'feast' period of PHA production.

The chemicals selected for this investigation were Carbonyl Cyanide 3-Chlorophenylhydrazone (CCCP), Valinomycin, and N, N′-Dicyclohexylcarbodiimide (DCCD). Depending on the concentration, some of these metabolic uncouplers can cause a decrease or loss in intracellular ATP. Uncouplers facilitate the influx of protons and this makes the activity of membrane bound ATPase to increase [79]. These inhibitors were utilized by Burow et al. [71] to study carboxylic acid uptake in BPR systems; however, in this research they have been used to study carboxylic acid uptake in MMC for aerobic dynamic feeding PHA production.

Carboxylic acid, PHA, and phosphorus removal analysis were performed to evaluate the potential metabolic functions that each chemical inhibited. These experiments were the premise to investigate how MMC are producing ATP during the feast stage and understand

why a rapid uptake of VFAs constantly occurs. Using such chemicals, it was predicted that the TCA cycle and oxidative phosphorylation would be inhibited; thus, if there was PHA production, ATP must come from different sources.

4.2.1   *Valinomycin and Potassium Chloride*

Valinomycin is an antibiotic that has a strong preference for potassium ions. It acts as a potassium-specific carrier and aids the flow of potassium ions through lipid membranes to the electrochemical potential gradient. Its molecular structure is more specific for cations than for anions and is held by hydrogen bonds. Valinomycin can interact with some anion-cation pairs and transport them through barriers of nonaqueous solvents [80]. Valinomycin also slows ATP synthesis without blocking electron transfer to O_2. Hamman et al. [73] showed that in the absence of valinomycin ATP levels decrease rapidly, while in the presence of valinomycin ATP utilization occurs at reduced amounts. The same study also reported that in the presence of valinomycin and K^+ concentration, ADP can be phosphorylated rapidly, but when valinomycin and ADP are added together, K+ uptakes are chosen over ATP synthesis by the cells.

In experiments conducted in this thesis, valinomycin was only inhibitory in the presence of potassium, suggesting a genuine effect on the membrane potential. Valinomycin in the presence of K^+ did not inhibited carboxylic acid uptake, but partially inhibited phosphorus removal (Figures 4.16-4.17). These results suggest that either there was not a high enough dose of V+KCl or that membrane potential does not drive VFA uptake.

PHA results show that under the presence of valinomycin and KCl, the MCC produced up to a 25% of intracellular PHA weight (Figures 4.18-4.19). The PHA production steadily increased, while PHA synthesis in the parent reactor exhibited substantially less productivity (Figs. 4.18 vs. 4.19). Moreover, on a yield basis the V+KCl batch reactor exhibited greater diversion of carbon to PHA. This finding is particularly interesting because both reactors had very similar carboxylic acid uptake, but more PHA synthesis occurred with V+KCl in the batch reactor. These results suggest that there was less $NADH_2$ oxidized for ATP synthesis when subjected to the V+KCl inhibitor, with more of the electrons diverted to PHA synthesis.

Figure 4.19: Parent PHA reactor - VFA, DO, and P data. No inhibitor.

Figure 4.18: VFA and P removal analysis results in the presence of Valinomycin and KCl.
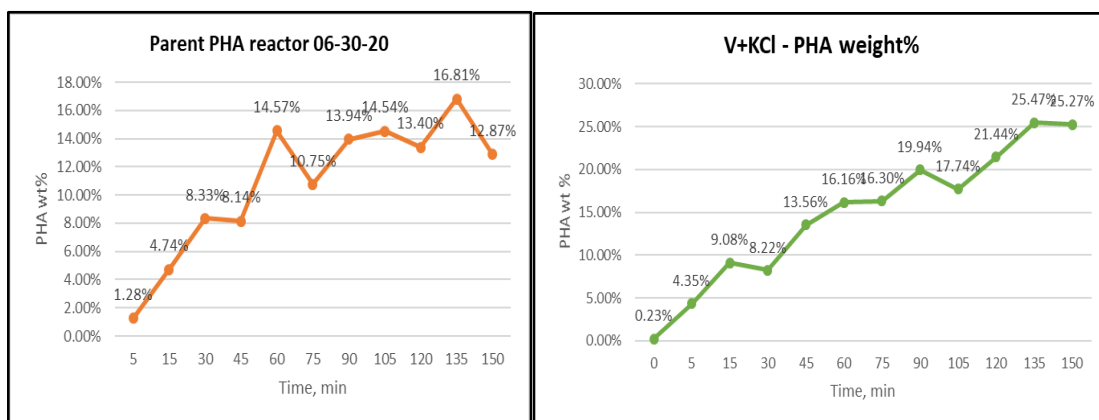
Figure 4.17: PHA % weight results - no inhibitor.

Figure 4.20: VFA and PHA Cmmol/L results in the presence of Valinomycin and KCl.
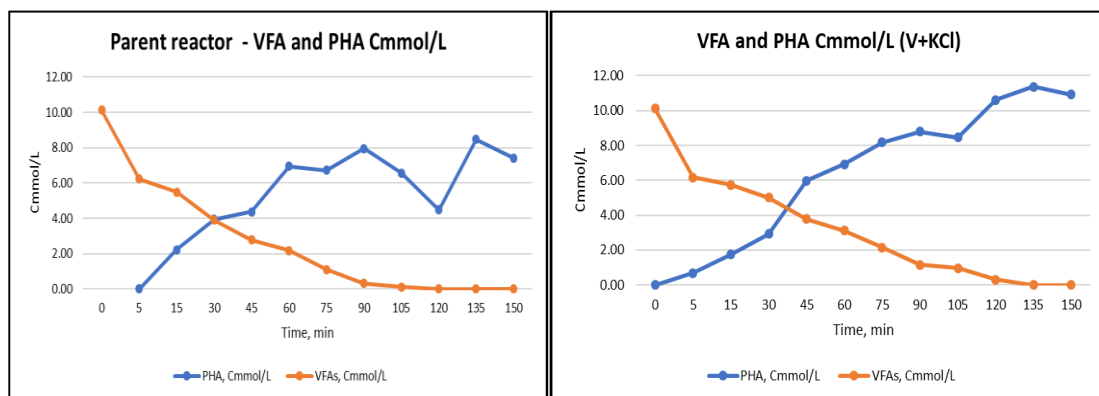
Figure 4.16: VFA and PHA Cmmol/L results - no inhibitor.

Figure 4.21: PHA % weight results in the presence of Valinomycin and KCl.
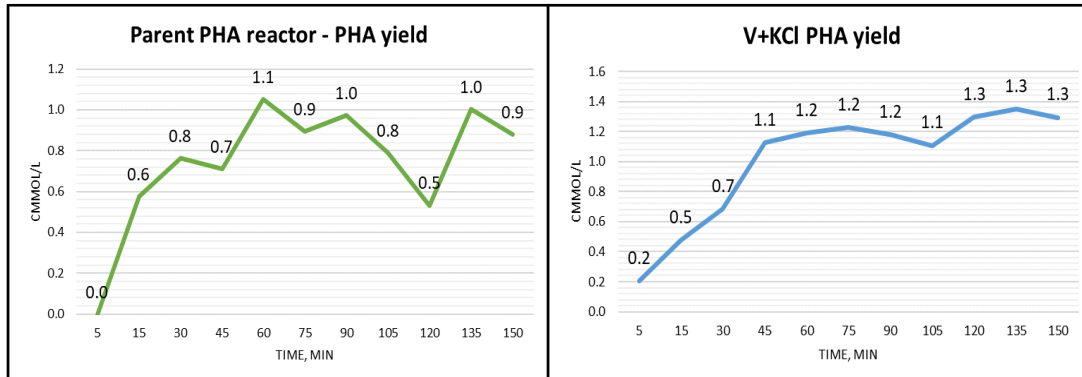
Figure 4.22: PHA yield results - no inhibitor.
Figure 4.23: PHA yield results in the presence of Valinomycin and KCl.

4.2.2   N, N'-Dicyclohexylcarbodiimide (DCCD)

DCCD is a carbodiimide compound that inhibits oxidative phosphorylation which is where ATP production occurs aerobically in PHA systems. DCCD reduces intracellular ATP levels via covalent modification of membrane bound ATPases [71]. Beechey et al. [81] showed that even at low concentrations DCCD can inhibit the synthesis of ATP in mitochondria and the ATP-driven partial reactions of oxidative phosphorylation. DCCD impacts oxidative phosphorylation by reacting at the level of a phosphorylated intermediate by the molecular carbodiimide moiety. DCCD has no effect on the substrate-linked ATP synthesis associated with -oxoglutarate oxidation. DCCD inhibits reactions that would involve synthesis or utilization of ATP, so it will inhibit the electron transport only when is linked with ATP synthesis.

Carboxylic acid analysis showed that under the presence of DCCD, ATP-dependent carboxylic acid uptake was significantly reduced; DCCD also affected phosphorus removal (Figures 4.24-4.25). Ultimately it appears the inhibited ATPase activity interfered with both phosphorus and carboxylic acid uptake by the cells. Interestingly, PHA was still produced, obtaining up to a 15.5% of intracellular PHA weight (Figure 4.26-4.27). However, PHA production was lower during the feast period in comparison to the parent reactor (Figure 4.26). In this experiment, the results suggest that the less ATP is produced, the less VFAs are consumed. Another interesting observation in these results was that the PHA yield (based on VFA consumption, which was the only PHA precursor quantified) was greater than 1 in the

DCCD-inhibited batch reactor; these results suggest that there is likely an alternate source of carbon utilized by the MMC for PHA production.
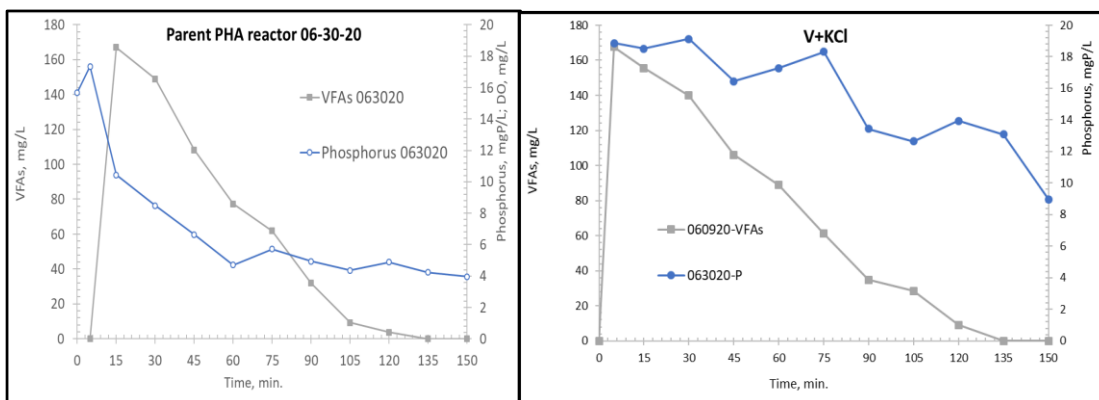

Figure 4.25: Parent PHA reactor - VFA, and P data. No inhibitor.
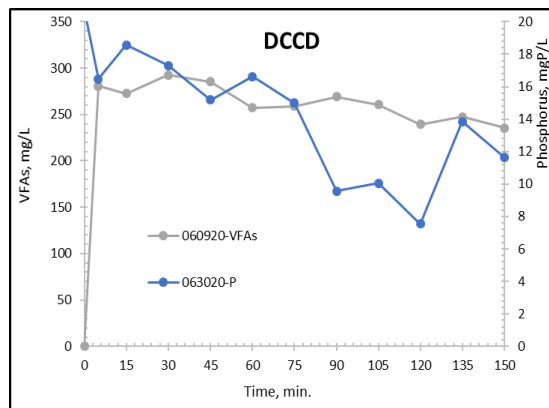
Figure 4.24: VFA and P removal analysis results in the presence of DCCD.

Figure 4.27: Parent PHA reactor – PHA wt% results. No inhibitor.
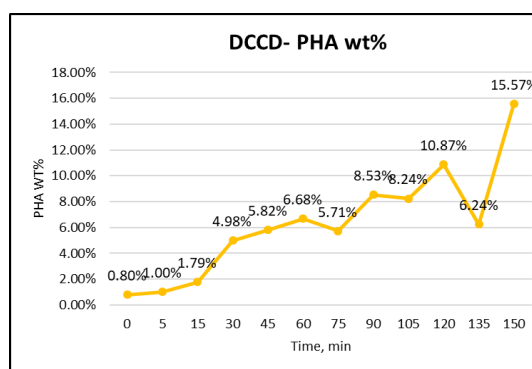
Figure 4.29: Parent PHA reactor – PHA wt% results in the presence of DCCD.
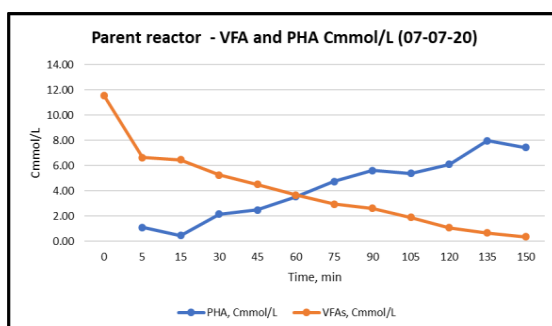
Figure 4.26: VFA and PHA Cmmol/L results - no inhibitor.
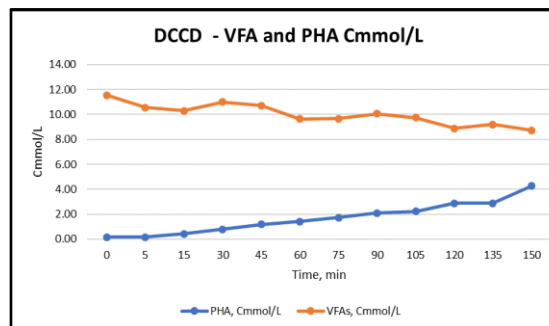
Figure 4.28: VFA and PHA Cmmol/L results - no inhibitor.
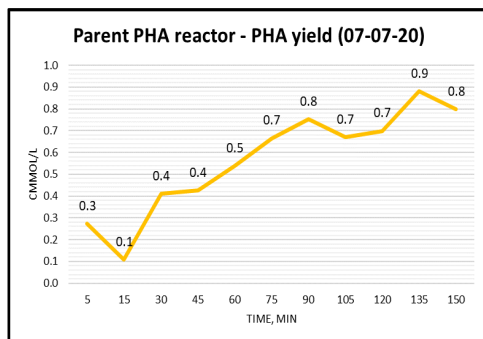
Figure 4.30: PHA yield results – no inhibitor
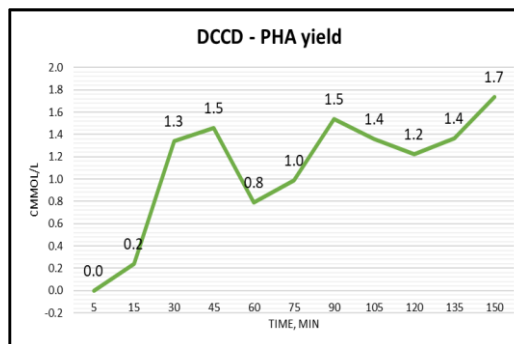
Figure 4.31: PHA yield results in the presence of DCCD.

4.2.3 *Carbonyl Cyanide 3 Chlorophenylhydrazone (CCCP)*

CCCP reduces ATP production and increases membrane permeability in bacteria by interfering with the transmembrane electrochemical gradient and proton motive force. This can indirectly affect the activity of proton pumps and cellular metabolism to cause cell death [72]. Diez-Gonzales et al. [79] documented that CCCP can cause a decline in intracellular pH, ATP, and potassium in *Escherichia coli* strains. CCCP is inhibitory at high concentrations and could trigger glucose consumption at low concentrations.

Similar to the effects of adding DCCD, Figure 4.33 shows that the inhibitor CCCP produced dramatic inhibition of carboxylic acid uptake. Also similar to the DCCD inhibition investigation, the MMC nonetheless accumulated PHA – up to 19.7% of intracellular PHA at the end of the feast period (120, 135 min), followed by a significant decline in PHA accumulation (5% at 150 minutes) (Figure 4.35). These results suggest that this inhibitor caused a decline in intracellular ATP and affected carboxylic acid uptake, but that again another carbon source was utilized for PHA production by the MMC.
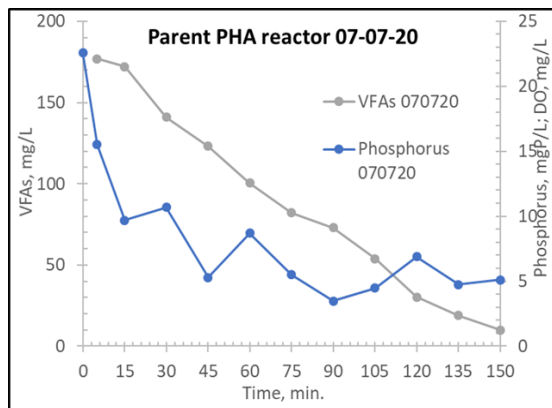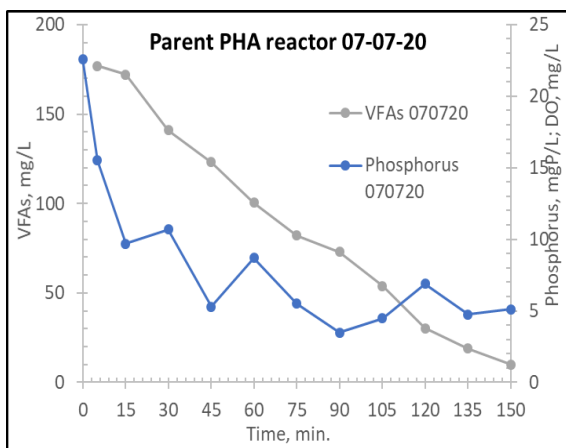
Figure 4.36: Parent PHA reactor - VFA, DO, and P data. No inhibitor.
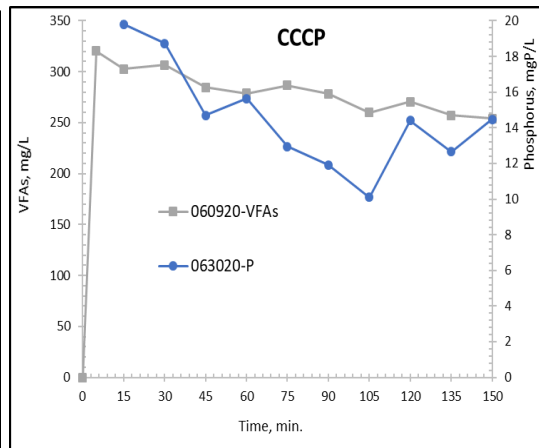
Figure 4.34: VFA and P removal analysis results in the presence of CCCP.
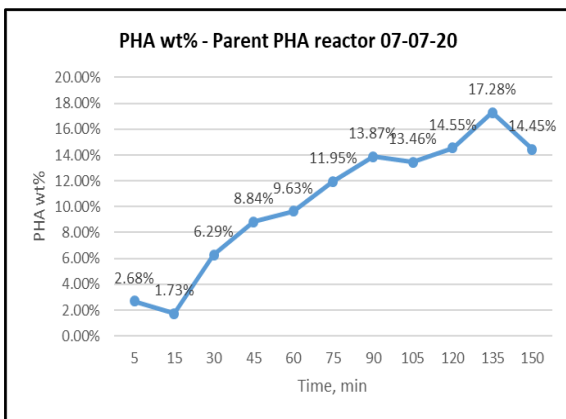
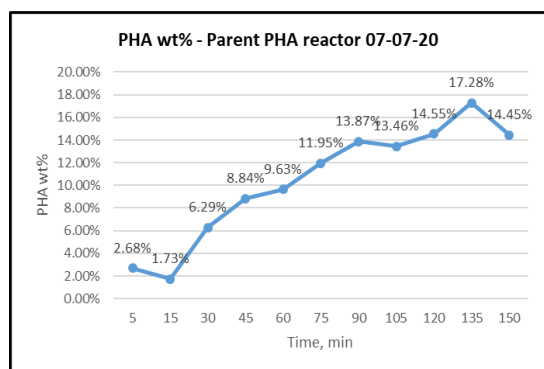**Figure 4.33:** PHA % weight results - no inhibitor.
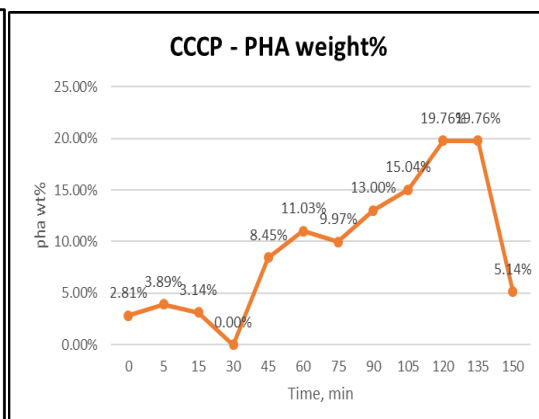
Figure 4.37: PHA % weight results in the presence of CCCP.
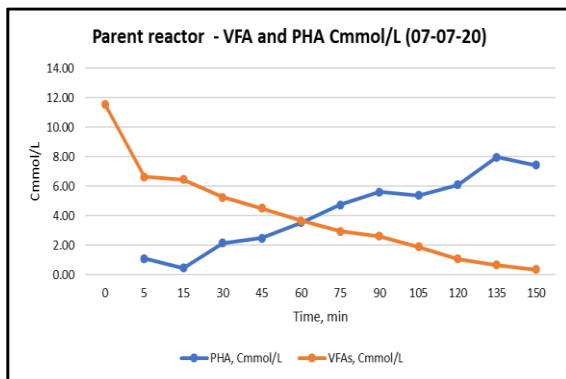
Figure 4.32: VFA and PHA Cmmol/L results - no inhibitor
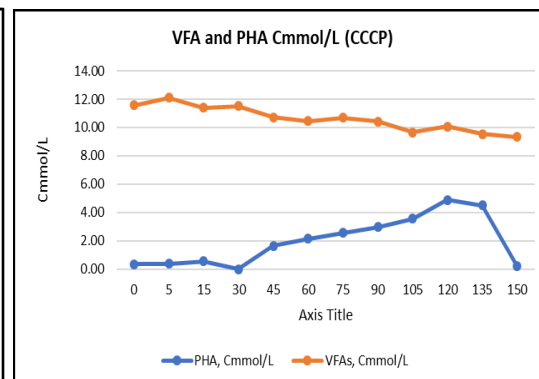

Figure 4.35: VFA and PHA Cmmol/L results under the presence of CCCP.
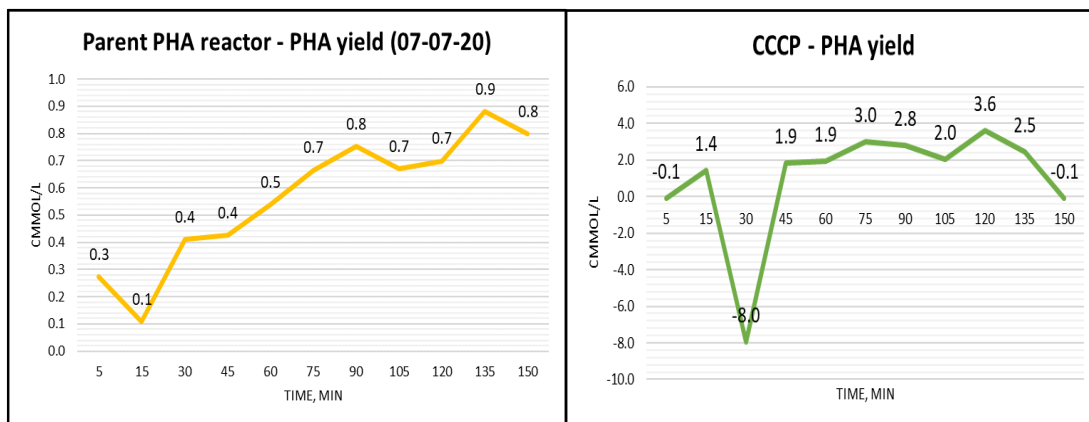
Figure 4.38: PHA yield results under the presence of CCCP.

Figure 4.39: PHA yield results – no inhibitor.

In summary, investigations on ADF PHA synthesis by MMC using DCCD and CCCP metabolic inhibitors appeared to have adversely effected mechanisms associated with carboxylic acid uptake, yet the MMC still accumulated significant PHA. These experimental results demonstrate that ATP could come from different sources, and that cells can still get carbon to produce PHA even when VFA uptake is impaired.

4.3 **Targeted Metabolomics Results**

MCC metabolomics analyses allowed this research to obtain information pertaining to the cellular metabolic potential of PHA production. This section highlights the results from the identification and quantification of intracellular metabolites that should, in theory, be detected in MMC performing ADF PHA synthesis. Unknown metabolites were tested against a library of metabolites generated for this research, and the concentration of metabolites in PHA systems over time within an SBR or batch reactor operational cycle was monitored.

LC-MS based targeted metabolomics was facilitated by the selected construction of a library with key metabolite standards. The identified metabolites were selected from the common metabolic pathways (see Figure 3.42) that MMC follow to synthesize PHA. By

integrating the data produced by the TOF-MS instrument, this research has identified and quantified 13 metabolites in 150 samples; the relative metabolite concentrations under different treatments for daughter reactors and the typical parent reactors were compared. The metabolic data was assessed in a point-by-point manner and the full data sets are available in supplemental information of this thesis.

The targeted metabolomic studies were conducted with the objective to further refine a metabolic-level understanding of Feast PHA synthesis. Investigations aimed to address part of research questions 1 and 2 of this thesis. **RQ1: how are MMC producing ATP during the feast stage? And why does a rapid uptake of VFAs always occur? RQ2: why and how does PHA synthesis occur contrary to just cell growth?** One specific focus of these experiments was to determine if glycolysis potentially provides ATP to activate carboxylic acid uptake and initiate 'feast' PHA synthesis. As described in Chapter 3, targeted metabolomics evaluations were performed on the parent vs. daughter reactors described in Table 11.

Table 11: Daughter Reactor Operational Perturbation vs. Parent Reactor for Targeted Metabolomics

(2X) NADH vs Parent Reactor
Acetic Acid vs Parent Reactor
Propionic Acid vs Parent Reactor
DCCD vs Parent Reactor

For these batch tests, the MMC were enriched in the parent reactor under ADF conditions and were producing PHA via induced feast-famine metabolisms. In addition to metabolomics analysis, PHA and VFA evaluations were performed for every sample collected.

4.3.1 Metabolic Effects of NADH Augmentation

Two NADH batch tests were performed. In the first batch test, the NADH-augmented daughter reactor produced more PHA and consumed more VFAs than the parent reactor. In the second batch test both reactors produced similar amounts of PHA, and the daughter reactor also consumed more VFAs with the NADH addition (Figure 4.40-4.43).

Metabolite levels varied in samples from both batch tests utilizing NADH, however a pattern was observed in ketoglutaric acid and propionyl-CoA, as both metabolites increased in concentration substantially in both batch tests. Conversely, citrate, D-fructose 1,6-bisphosphate, valeryl CoA, and NADPH decreased in both batch tests (Figure 4.44-4.46). Specific observations included:

- In the daughter reactor Acetyl-CoA, which is a critical PHB precursor, increased in concentration up to 120 minutes in the first batch test with NADH addition; PHA synthesis commensurately increased substantially after 120 minutes (best illustrated in Figure 4.40B for PHA and Figure 4.42A specifically for PHB). In contrast, acetyl-CoA concentrations remained relatively constant in the parent reactor, and intracellular PHA exhibited a similar pattern. Conversely, acetyl-CoA concentrations remained relatively constant in the second batch test with NADH addition (Figure 4.46A), while %PHB increased at a relatively constant rate (Figure 4.42B).

- Citrate, which is the first enzyme of the TCA cycle, substantially decreased under the addition of NADH, particularly in the first batch test over the first 75 minutes (Figure 4.44B); similar results were observed in the parent reactor for the first batch test. Related, the %PHB in both reactors increased relatively steadily until about 75-90 minutes. Collectively these results indicate the cells may have been preferentially using acetyl-CoA for PHB synthesis over the TCA cycle for the first 60-75 minutes of the operational cycle. The citrate concentration increased substantially at 105 minutes in the parent reactor, relative to the daughter reactor, and commensurately the %PHB remained relatively constant thereafter. Data from the 2nd batch test revealed a relatively constant citrate concentration over time in

the daughter reactor (Figure 4.46B), with a constant PHB synthesis (Figure 4.42B). For the parent reactor, the citrate concentration decreased at 90 minutes, increased significantly at 105 minutes, and decreased at 120 minutes (Figure 4.46BN); %PHB similarly increased at 75-90 minutes, stabilized in concentration till 120 minutes, and then increased at 135 minutes (Figure 4.42B). Backed by literature [47] it was hypothesized that in the TCA cycle, citrate synthase can be repressed by excess NADH; this would prevent acetyl-CoA from entering the TCA cycle, and instead acetyl-CoA would be routed to PHA synthesis.

- Related to the citrate concentration patterns over time, ketoglutaric acid, which is an intermediate in the TCA cycle downstream of citrate, revealed generally cyclical concentrations in both the daughter and parent reactors over time, which again indicates potential cyclical inhibition of the TCA cycle. As shown in Figures 4.44 B and E, and 4.46 B and E, an increase in ketoglutaric acid levels generally lagged the increase in citrate levels in both daughter reactors. The cyclical relationship between metabolites was not as clear in the parent reactor (Figures 3.44B, E and Figures 4.46B, E). These results further support that NADH addition inhibited the TCA cycle more strongly than in the uninhibited parent reactor.

- Propionyl-CoA is a necessary precursor for PHV synthesis. Excess NADH would inhibit the TCA cycle, and the MMC would accumulate more acetyl-CoA. To the best of our knowledge, acetyl-CoA cannot be readily converted to propionyl-CoA. As such, NADH addition would be expected to potentially increase the %PHB synthesized by the MMC. Indeed, examining Figure 4.42 shows that the daughter reactors synthesized a great fraction of PHB, vs. the parent reactors wherein NADH inhibition was not induced.

- A pathway related to the TCA cycle is the glyoxylate cycle, which involves the conversion of acetyl-CoA to succinate or glyoxylate (Figure 2.6). Levels of glyoxylate and succinate were a little controversial. Specifically, there were no detections of glyoxylate in the first daughter reactor, yet high levels were detected in the second daughter reactor (even higher that its respective parent reactor). Glyoxylate concentrations were relatively negligible in the parent reactor in batch test #1 (Figure 4.44F) yet high in batch test #2 (Figure 4.46F); similar results were

observed for succinate (Figures 4.44L, 4.46L). In the case of succinate, high levels were detected in the first daughter reactor, with lower, and more cyclical, levels of succinate detected in the second daughter reactor (Figures 4.44 F and L, 4.46 F and L). Collectively these results indicate that the MMC can, and does, employ the glyoxylate cycle to potentially mitigate the accumulation of NADH to sustain substrate oxidation.

- Regarding glycolysis metabolites, D-fructose 1,6-bisphosphate levels were very similar in daughter and parent reactors (in both batch tests). The concentration differences are very small. Pyruvate levels increased in the 'feast' period, in the daughter reactor from the first batch test. In contrast, pyruvate increased in the 'feast' period, in the parent reactor from the second batch test. Generally, the detections of both, D-fructose 1,6-bisphosphate and pyruvate could potentially indicate that glycolysis is functioning, which would provide additional carbon precursors for PHA synthesis that would not be counted in the calculated yield values. This can be corroborated with the results of the next batch tests performed and analysed in this thesis (specifically via the addition of DCCD, acetate and propionate as sole carbon sources).

- PHA catabolism during 'feast' is potentially indicated by the presence and concentration of 3-hydroxyvalerate. As shown in Figures 4.44H, NADH addition appeared to potentially induce PHA catabolism, cyclically, in batch test #1; however, the same results were not observed in batch test #2 (Figure 4.46H). Interestingly, PHA catabolism did not appear to occur in the parent reactor until the end of the feast period.

61
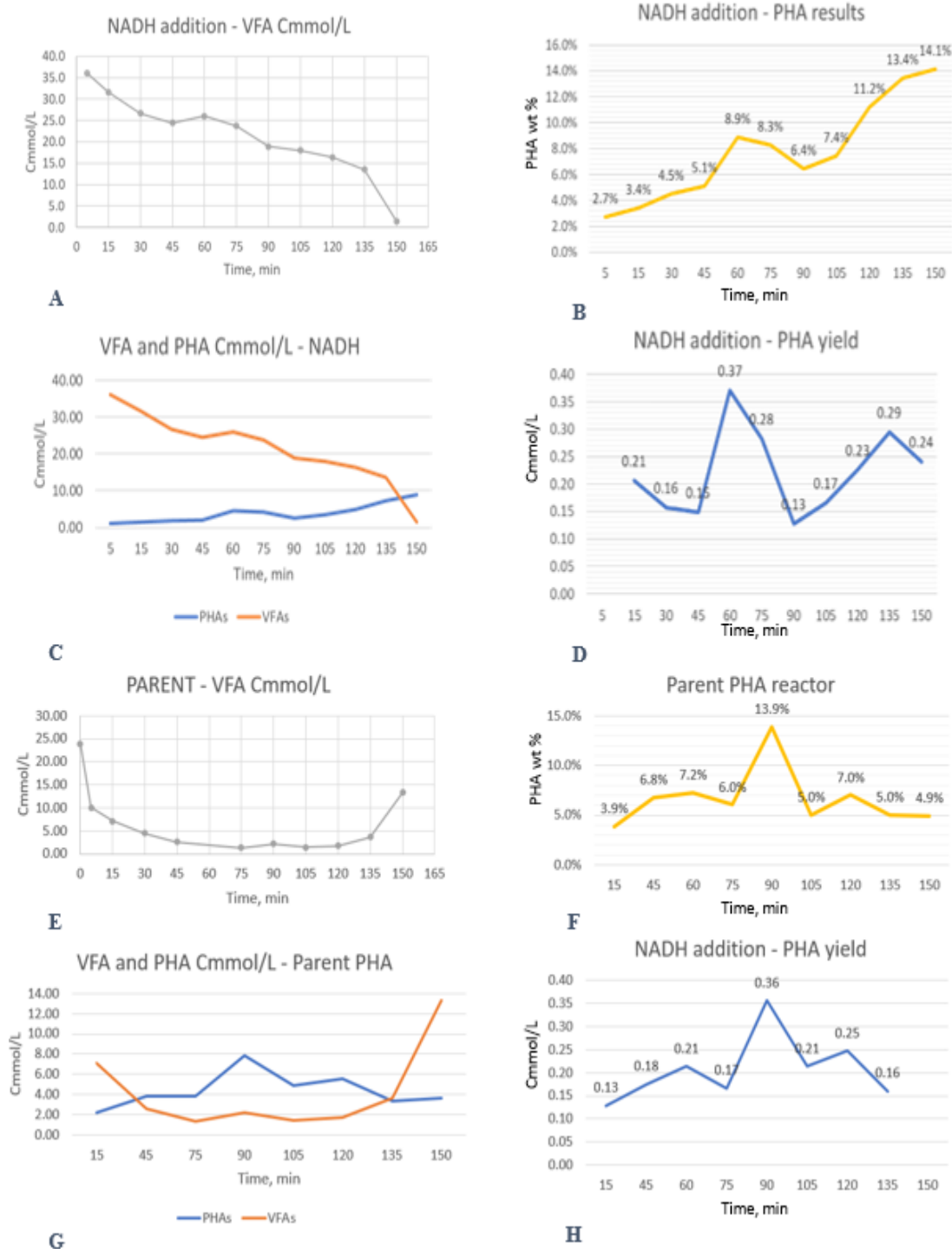
Figure 4.40: VFA and PHA results from NADH Batch Test #1 (1/26/2021). Figures A-D belong to the daughter batch reactor with NADH addition. Figures E-H belong to the parent reactor.
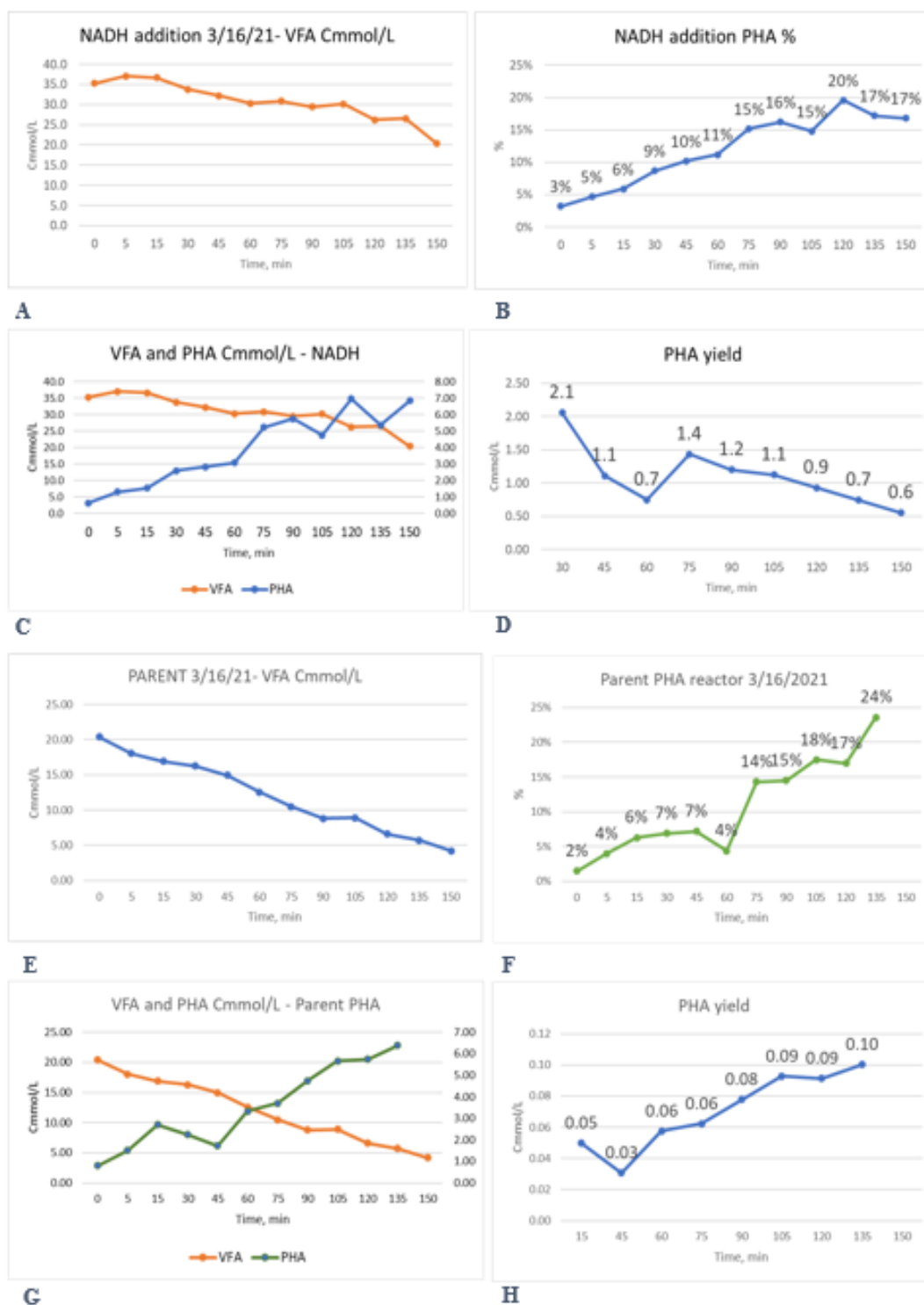
Figure 4.41: VFA and PHA results from NADH Batch Test #2 (3/16/2021). Figures A-D belong to the daughter batch reactor with NADH addition. Figures E-H belong to the parent reactor.
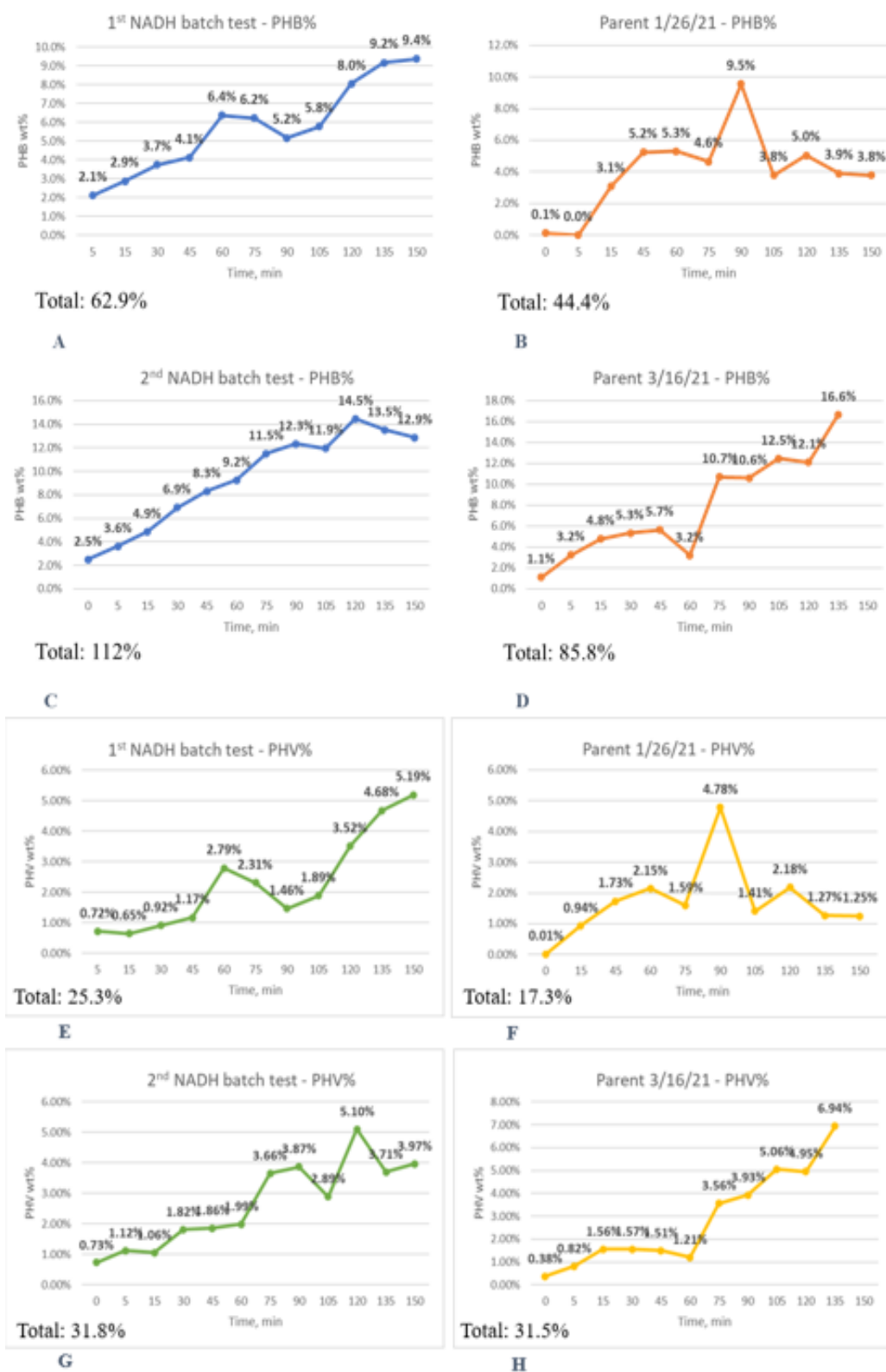
Figure 4.42: PHB wt% and PHV wt% in NADH batch tests. Plots A, C, E and G belong to daughter reactors. Plots B, D, F and H belong to parent reactors.
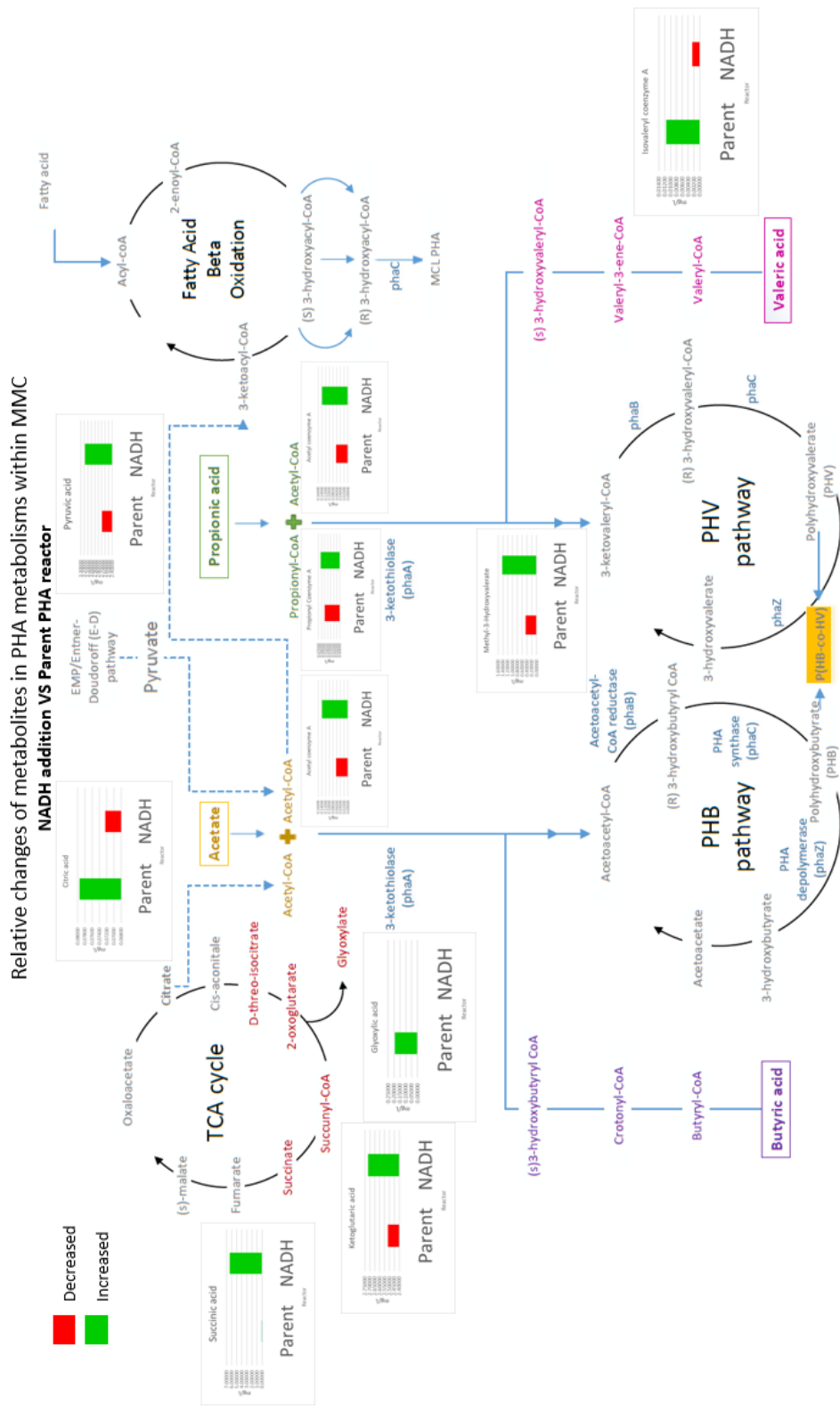
Figure 4.43: Changes of metabolites in PHA metabolisms within MMC. NADH addition VS PHA reactor. Batch Test #1.

1st NADH batch test
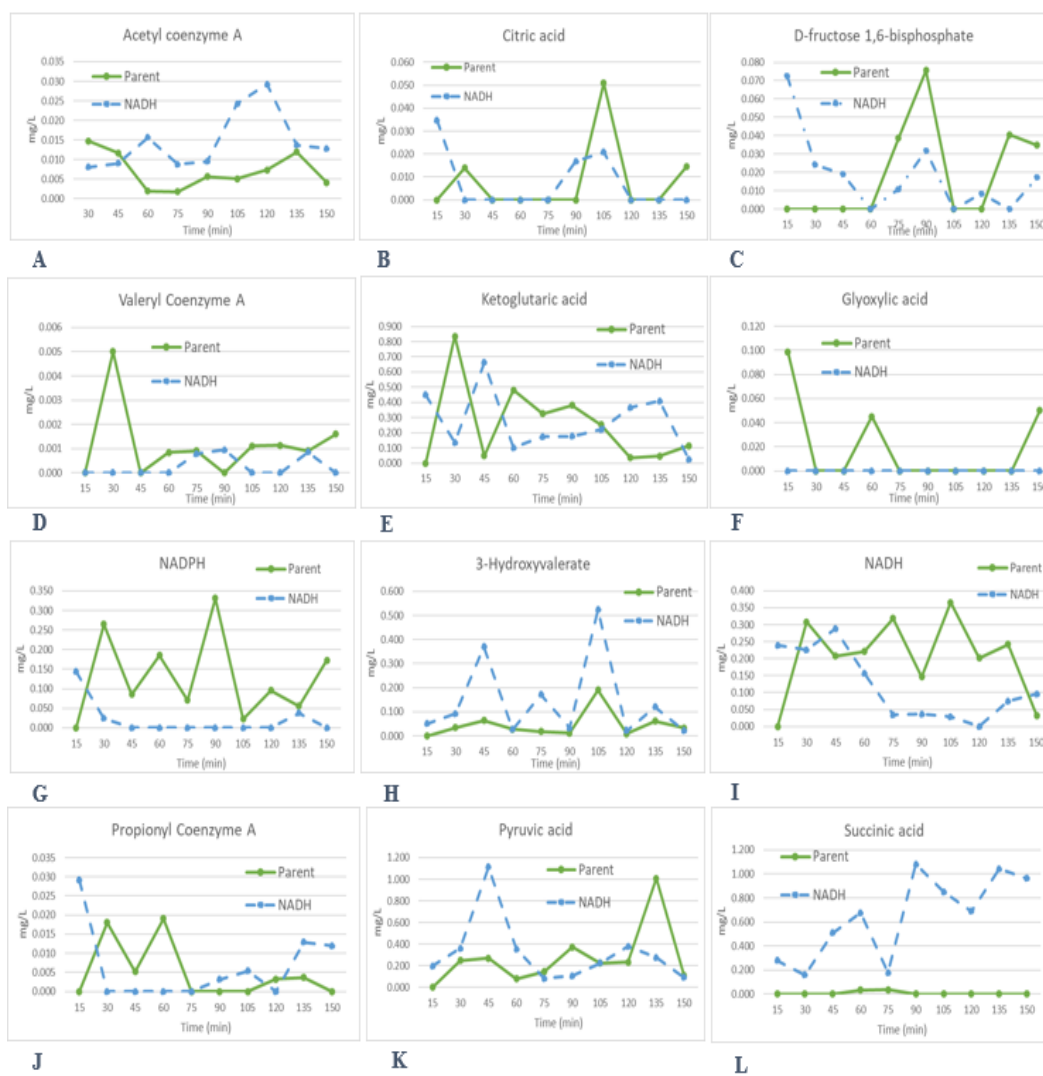
Figure 4.44: Levels of metabolites in each time point. NADH addition VS PHA reactor. Batch Test #1.
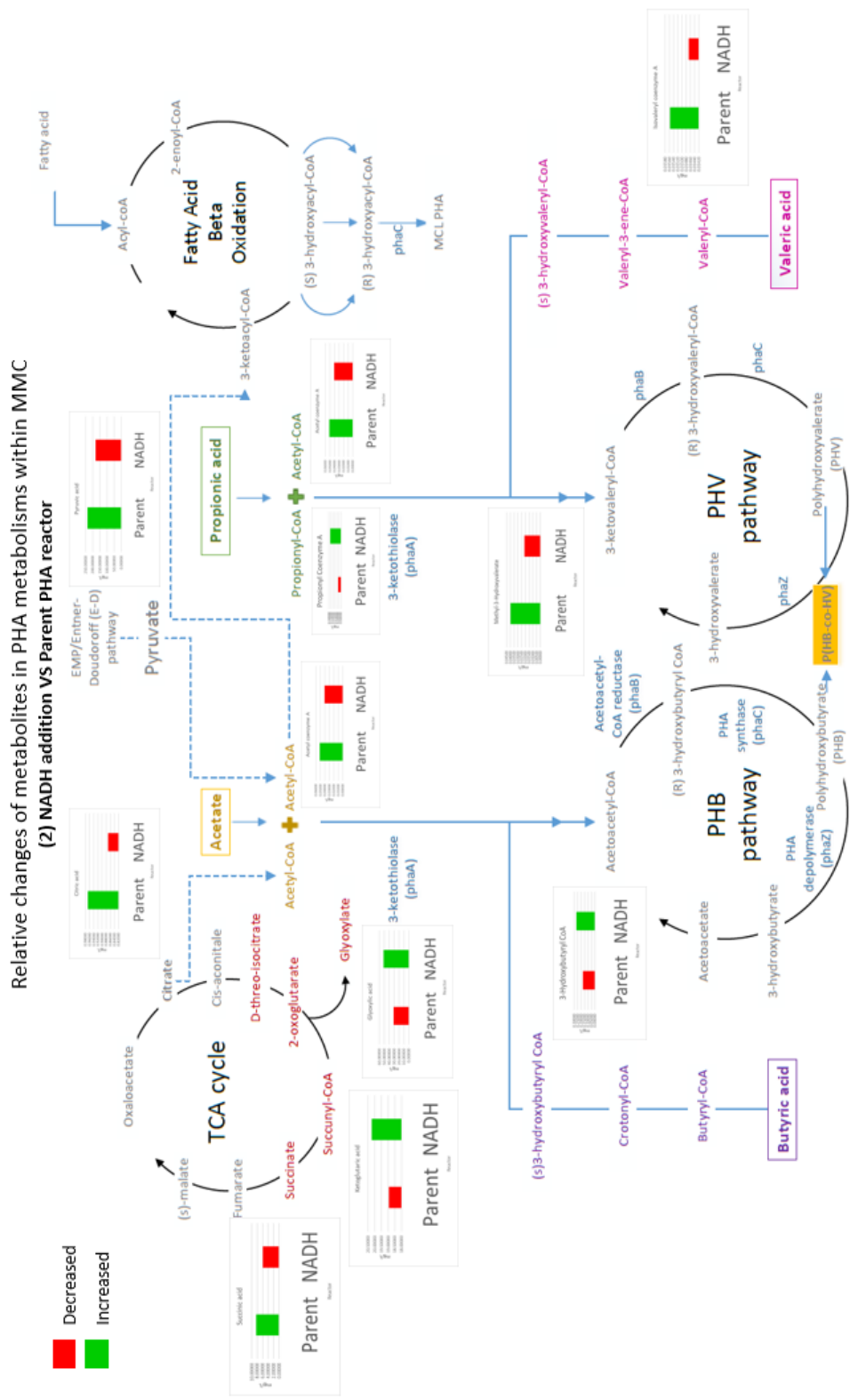
Figure 4.45: Changes of metabolites in PHA metabolisms within MMC. NADH addition VS PHA reactor. Batch Test #2.

2nd NADH batch test

Figure 4.46: Levels of metabolites in each time point. NADH addition VS PHA reactor. Batch Test #2.

4.3.2   Metabolic Effects with Acetic acid as Sole Carbon Source

PHA results show that the acetate-fed daughter reactor produced more PHA than the parent reactor (Figure 4.47 and Figure 4.48) and the daughter reactors only produced PHB since acetate cannot support PHV production. However, the acetate daughter reactor consumed four times more carboxylic acid than the parent reactor. Metabolomics results from utilizing acetic acid as sole carbon source showed that most of the key metabolites decreased in comparison to the parent reactor. The only metabolites that increased were valeryl coenzyme A, ketoglutaric acid, and pyruvate (Figure 4.49). Specific observations included:

- Acetyl-CoA levels remained consistently low when utilizing acetate as the sole carbon source. Conversely, acetyl-CoA levels were high at the beginning of the 'feast' phase in the parent reactor, then decreased to similar concentrations as the daughter reactor (Figure 4.49A). Related, citrate and ketoglutarate levels varied cyclically over time, presumably as acetyl-CoA was alternately diverted to the TCA cycle vs. PHA synthesis.

- Metabolite concentrations associated with glycolysis – specifically D-fructose 1,6-bisphosphate and pyruvate – again indicate activity of this pathway. Moreover, data indicates that the parent reactor had a potentially more actively glycolytic pathway, particularly with higher D-fructose 1,6 bisphosphate concentrations (Figure 4.49C).

- The glyoxylate pathway appeared to be partially active in both reactors, with negligible detection of glyoxylate but cyclical concentrations of succinate (Figures 4.49F, L).

- 3-Hydroxyvalerate was detected in both reactors, indicating some level of PHA catabolism over the feast period (Figure 4.49H). In particular, the metabolite concentration increased substantially at 75 minutes in the parent reactor and remained relatively high thereafter; commensurately the intracellular PHA concentration decreased substantially at 90 minutes, seemingly confirming PHA catabolism (Figure 4.47F).

- Interestingly, measurable NADH concentrations were primarily only detected in the parent reactor (Figure 4.49I). Only one hit was detected in the acetate reactor (minute 120). Similarly with NADPH, most hits were detected in the parent reactor. It appears that when acetate is utilized as sole carbon source, NADH and NADPH concentrations are maintained at near zero, indicating more efficient oxidation and PHA synthesis – seemingly confirmed by PHA data (Figure 4.47B).

- Propionyl-CoA levels were higher in the parent reactor, compared with the acetate reactor. Since acetate cannot be readily catabolized to propionyl-CoA, this result is not surprising.

Figure 4.47: Figures A-D are from the acetate batch-test. Figures E-H belong to the PHA parent reactor (2/2/21).

Figure 4.48: Acetate as sole carbon source VS PHA reactor. Changes of metabolites in PHA metabolisms within MMC.
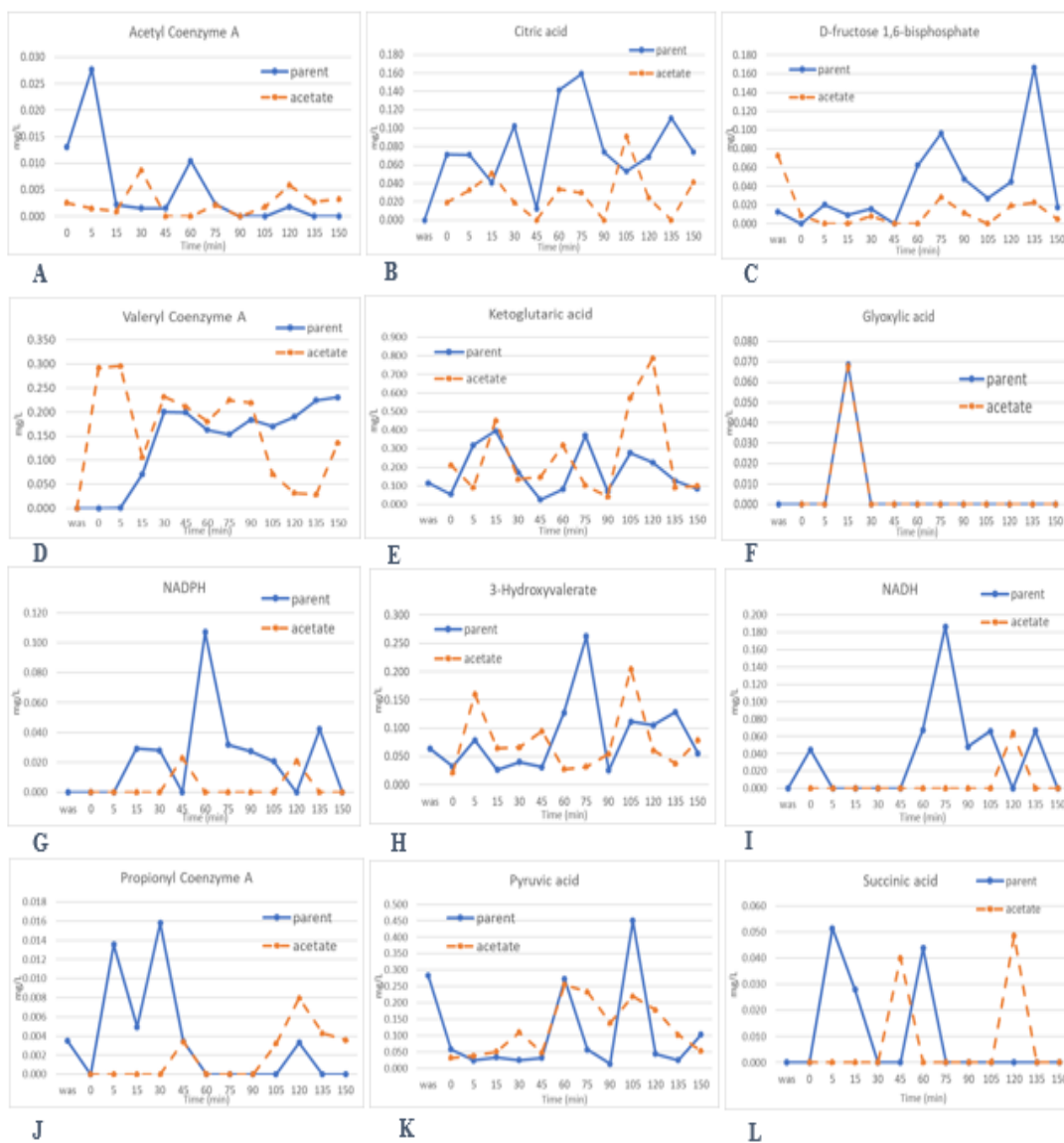
Figure 4.49: Levels of metabolites in each time point. Acetate as sole carbon source VS PHA reactor.

4.3.3 *Propionic acid as Sole Carbon Source*

PHA results show that the propionate daughter reactor produced less PHA than the parent reactor (Figure 4.49). Specifically, propionate fed MCC generated PHV, with low yields, since a two-carbon molecule is needed with the three carbons of propionate (Figure 2.6). The propionate daughter reactor also consumed eight times more VFAs than the parent reactor. Metabolomic results revealed that citrate, D-fructose 1,6-bisphosphate, valeryl-CoA, methyl-3-hydroxyvalerate, NADH, succinate, and 3-hydroxybutyryl CoA increased when propionate is utilized as sole carbon source. Conversely, acetyl-CoA, glyoxylate, ketoglutaric acid, NADPH, propionyl-CoA, and pyruvate decreased. Specific observations included:

- Acetyl-CoA levels remained consistently low when utilizing propionate as the sole carbon source; while propionate catabolism can generate acetyl-CoA (Figure 2.6), it is not necessarily the most favorable reaction. Conversely, acetyl-CoA levels were high at the beginning of the 'feast' phase in the parent reactor – which, again, received a blend of carboxylic acids – then decreased to similar concentrations as the daughter reactor (Figure 4.52A) but increased toward the end of the period evaluated. Related, citrate and ketoglutarate levels varied cyclically over time, presumably as acetyl-CoA was alternately diverted to the TCA cycle vs. PHA synthesis. Citrate levels were substantially higher in the propionate reactor, specifically in the 'feast' period.
- Metabolite concentrations associated with glycolysis – specifically D-fructose 1,6-bisphosphate and pyruvate – once again indicate activity of this pathway in both MMC. Moreover, data indicates that the daughter reactor had a potentially more actively glycolytic pathway, particularly with higher D-fructose 1,6 bisphosphate concentrations (Figure 4.52C). It is possible that the MMC in the daughter reactor was employing glycolysis to generate acetyl-CoA, thus allowing for some PHA synthesis with the propionyl-CoA.
- The glyoxylate pathway appeared to be active in both reactors, with high concentrations of both, glyoxylate and succinate (Figures 4.52F, L).
- 3-Hydroxyvalerate was detected in both reactors, indicating some level of PHA catabolism over the feast period (Figure 4.52H). In particular, the metabolite

concentration increased substantially at 105 minutes in the parent reactor and remained relatively high thereafter; commensurately the intracellular PHA concentration decreased substantially at 105 minutes, seemingly confirming PHA catabolism and the onset of 'feast' (Figure 4.50B, F).

- Home NADH concentrations were primarily detected in the daughter reactor (Figure 4.52I); in particular, the NADH concentration increased substantially at 75 minutes in the daughter reactor, with the peak at 120 minutes coinciding with peak concentration of 3-hydroxyvalerate. On the contrary with NADPH, higher concentrations were detected in the parent reactor. It appears that when propionate is utilized as sole carbon source, the MMC may utilize the VFA for energy production over PHA synthesis – seemingly confirmed by PHA data (Figure 4.50B, F).

- Propionyl-CoA levels were very similar in both reactors. Since propionate should be readily catabolized to propionyl-CoA, this result is not surprising (Figure 4.52 J).

Figure 4.50: Figures A-D belong to the results of the propionate batch-test. Figures E-H are from the parent PHA reactor results (3/17/2021).

75

Figure 4.51: Propionate as sole carbon source VS PHA reactor. Changes of metabolites in PHA metabolisms within MMC.
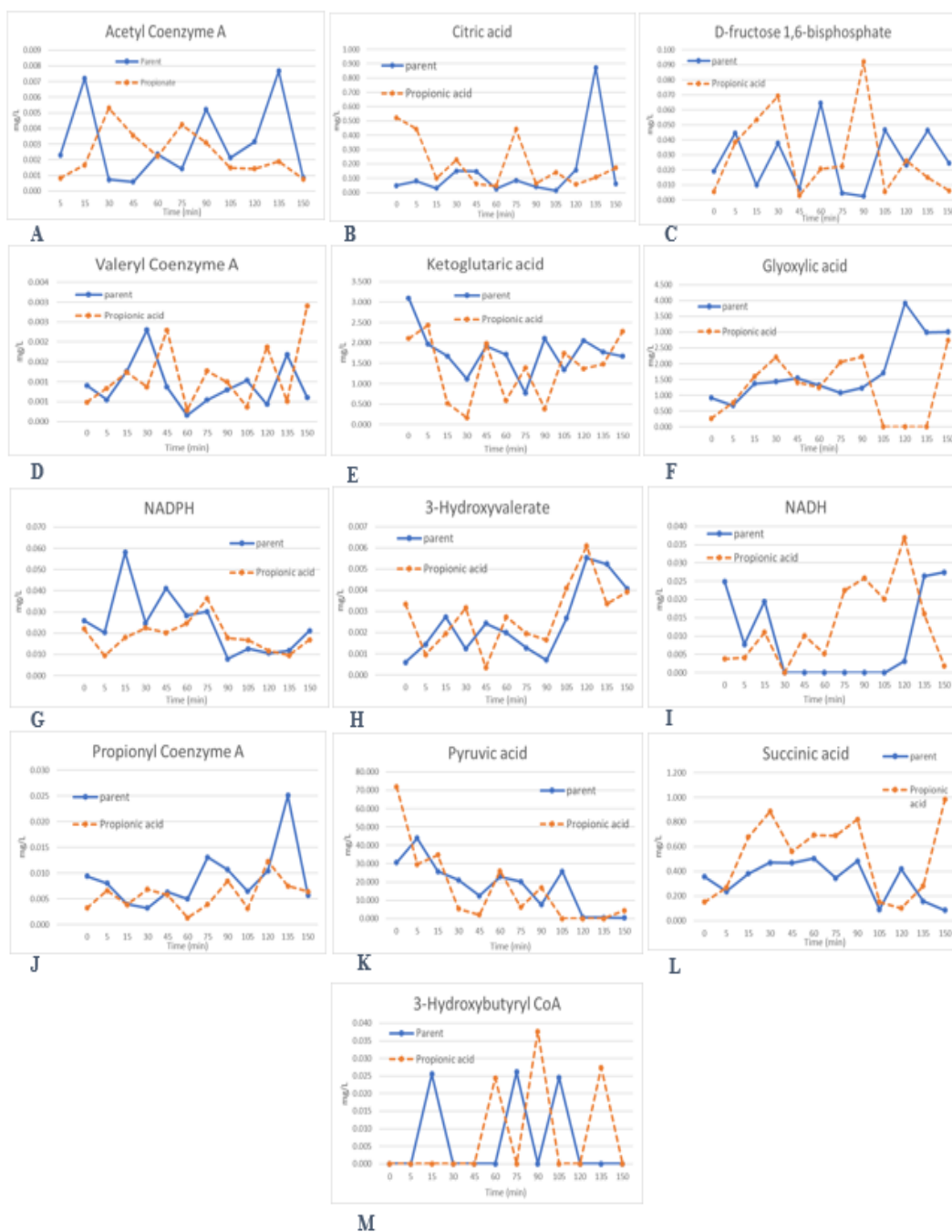
Figure 4.52: Levels of metabolites in each time point. Propionate as sole carbon source VS PHA reactor.

4.3.4. *DCCD as Inhibitor of Carboxylic Acid Uptake*

- Carboxylic acid analysis of the second DCCD batch test showed that under the presence of this inhibitor, ATP-dependent carboxylic acid uptake is significantly reduced (Figure 4.53A). Interestingly, like the first batch test, PHA was still produced, obtaining up to a 5% of intracellular PHA weight (Figure 4.53B). Metabolomics results revealed that citrate, glyoxylate, isovaleryl coenzyme A, ketoglutaric acid, 3-hydroxyvalerate, NADPH, propionyl CoA, succinate and 3-hydroxybutyryl CoA increased substantially under DCCD addition. In contrast, acetyl CoA, D-fructose 1,6-bisphosphate, NADH, and pyruvate decreased. Specific observations included:

- Acetyl-CoA levels remained slightly lower when adding DCCD. Conversely, acetyl-CoA levels were high at the onset of the 'famine' phase in the parent reactor (Figure 4.55A). Related, citrate and ketoglutarate levels varied cyclically over time, presumably as acetyl-CoA was alternately diverted to the TCA cycle vs. PHA synthesis. Citrate levels were substantially higher in the DCCD reactor, specifically in the 'famine' period – presumably as the MMC catabolized PHA.

- Metabolite concentrations associated with glycolysis – specifically D-fructose 1,6-bisphosphate and pyruvate – again indicate activity of this pathway. Moreover, data indicates that the parent reactor had a potentially more active glycolytic pathway (specifically in the 'feast' period), particularly with higher D-fructose 1,6 bisphosphate and pyruvate concentrations (Figure 4.55C, K). With carboxylic acid uptake inhibited, less ATP is required – which could explain less active glycolysis.

- The glyoxylate pathway appeared to be active in both reactors, with high concentrations of both, glyoxylate and succinate (Figures 4.55F, L).

- Surprisingly 3-hydroxyvalerate detections were relatively low in both reactors; the daughter reactor had the highest hit at minute 5, indicating some level of PHA catabolism early in the feast period (Figure 4.55H). The intracellular PHA concentration of the daughter reactor was substantially low at minute 5, seemingly confirming PHA catabolism (Figure 4.53B).

- Measurable NADH and NADPH concentrations were detected in both, the parent and daughter reactors (Figure 4.55G, I). In particular, the NADH concentration increased substantially at 30 minutes and NADPH levels increased at 90 minutes.

- Propionyl-CoA and valeryl-CoA levels were very similar in both, DCCD, and parent reactors. This indicates that DCCD does not affect the synthesis of these two important acyl-coenzyme A thioesters that lead to PHV (Figure 4.55 D, J).
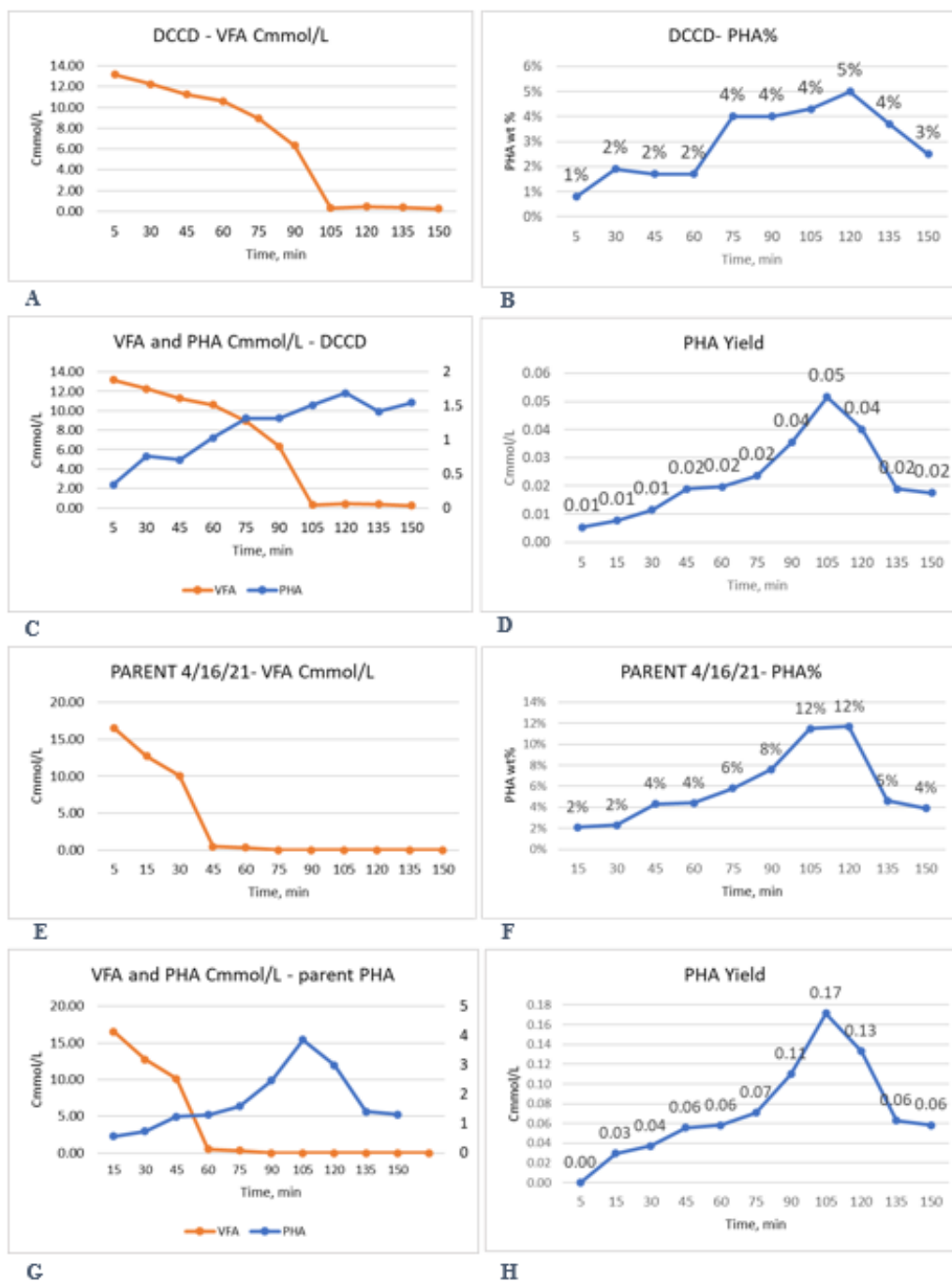
Figure 4.53: Figures A-D belong to the results of the DCCD batch-test. Figures E-H are from the parent PHA reactor results (4/16/2021).
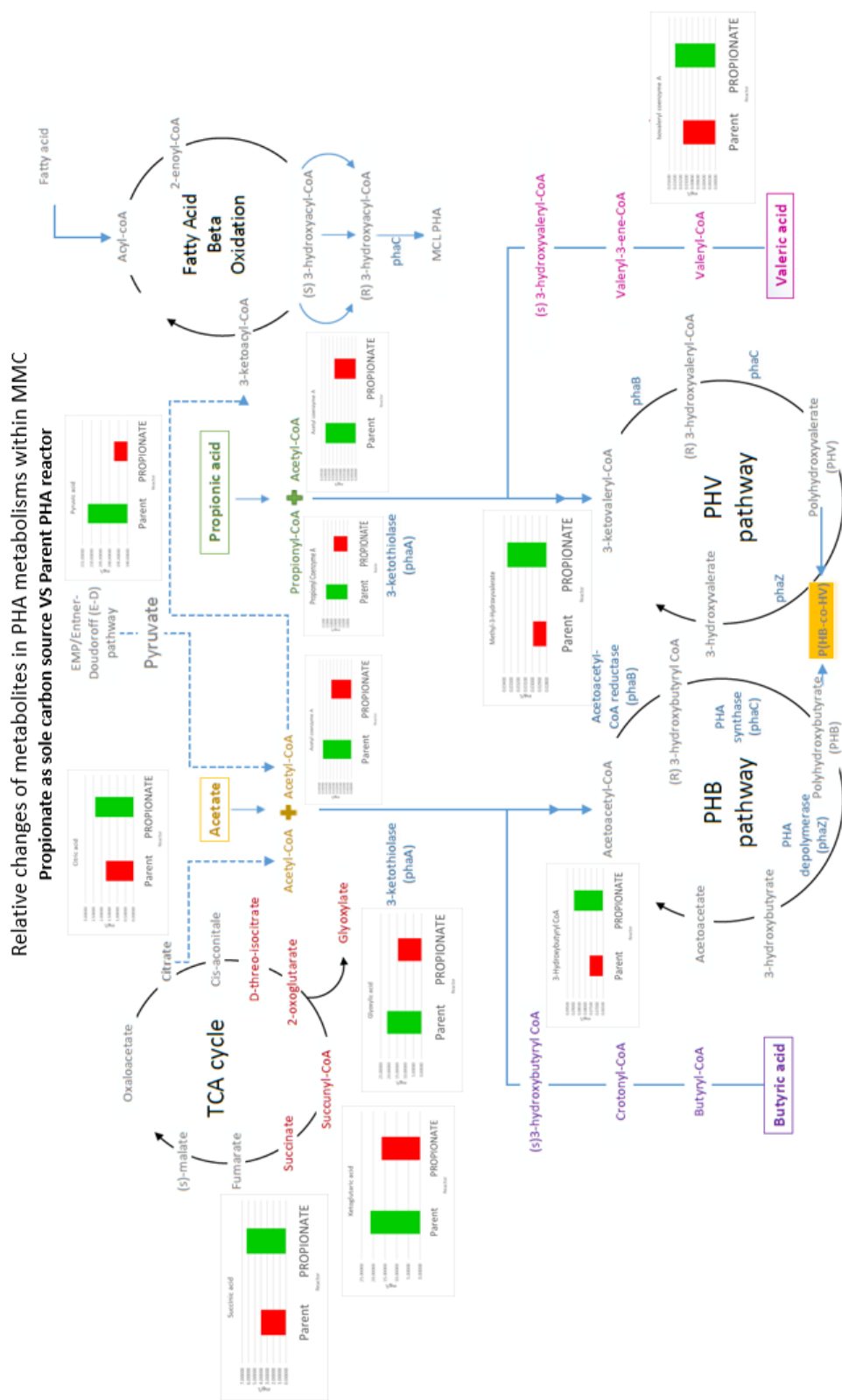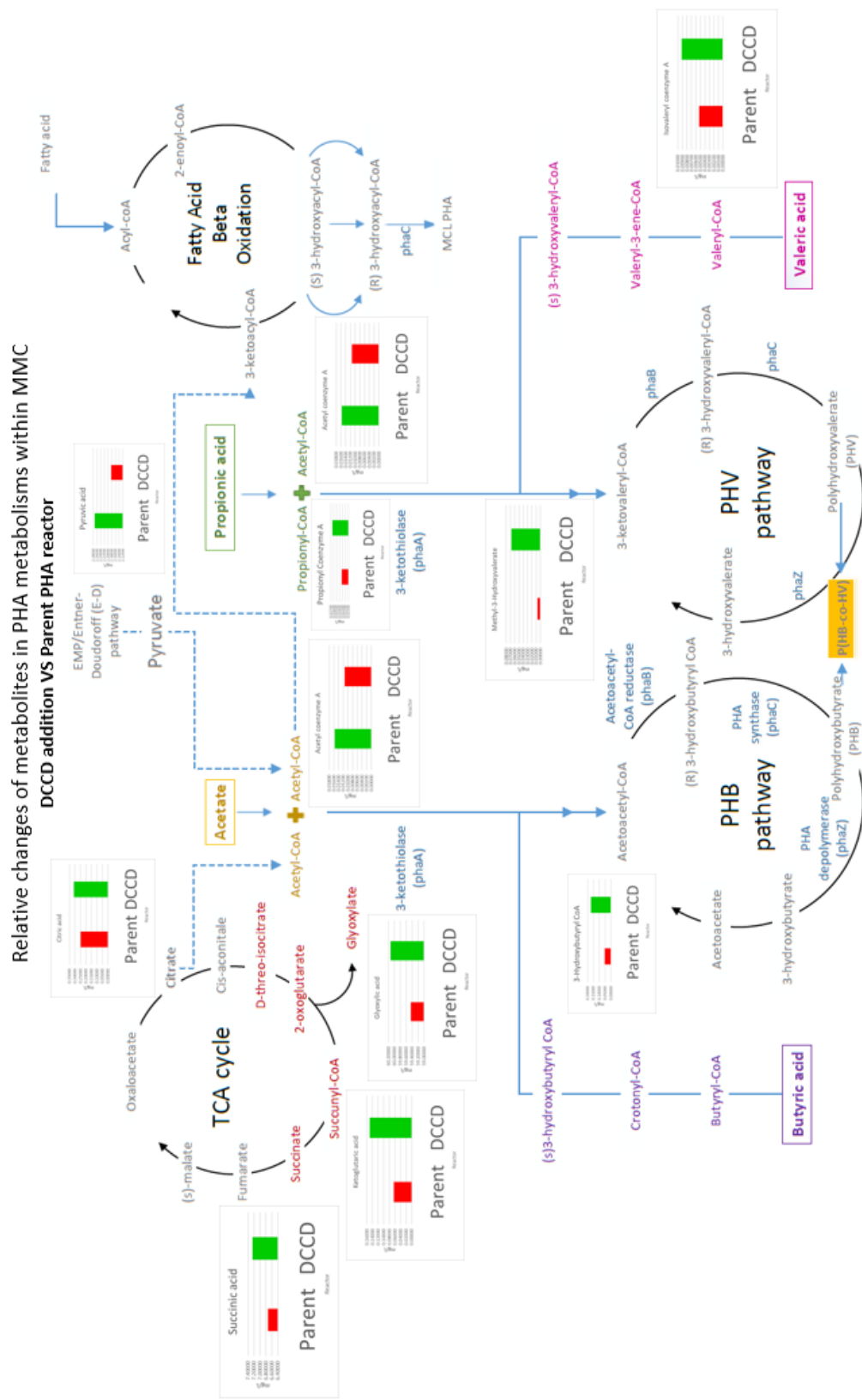
Figure 4.54: DCCD VS PHA reactor. Changes of metabolites in PHA metabolisms within MMC.
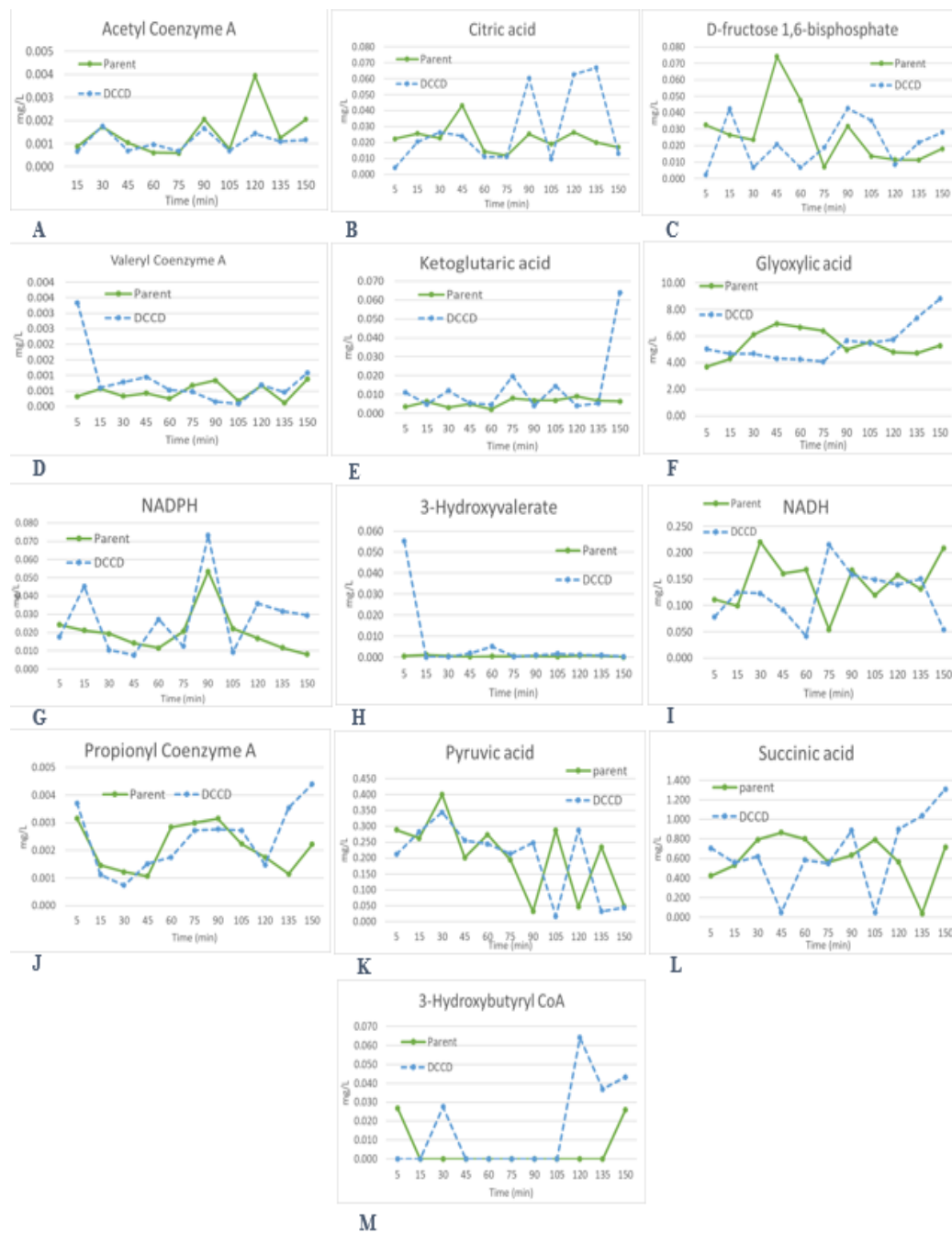
Figure 4.55: Levels of metabolites in each time point. DCCD VS PHA reactor.
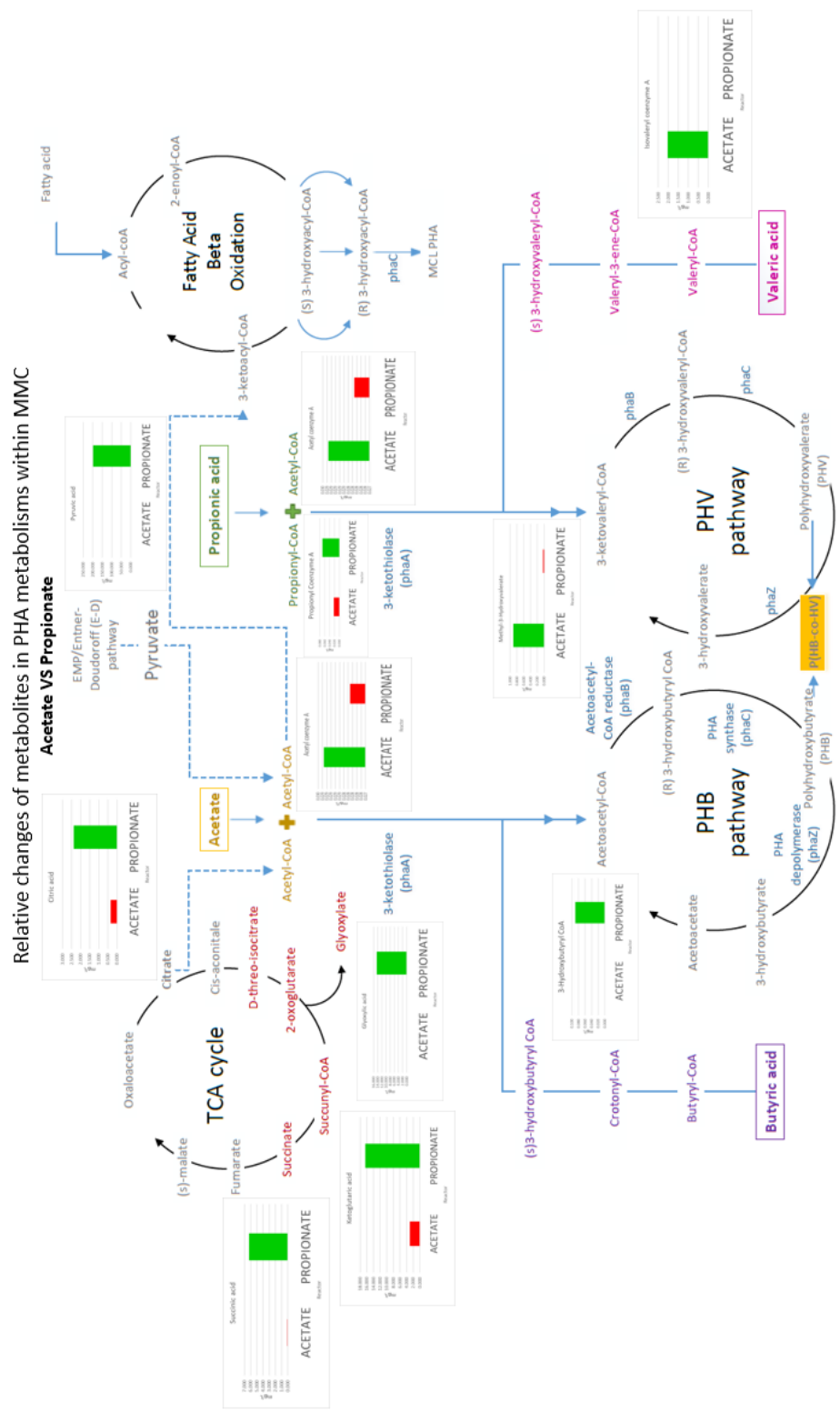
Figure 4.56: Acetate VS Propionate reactors. Changes of metabolites in PHA metabolisms within MMC.
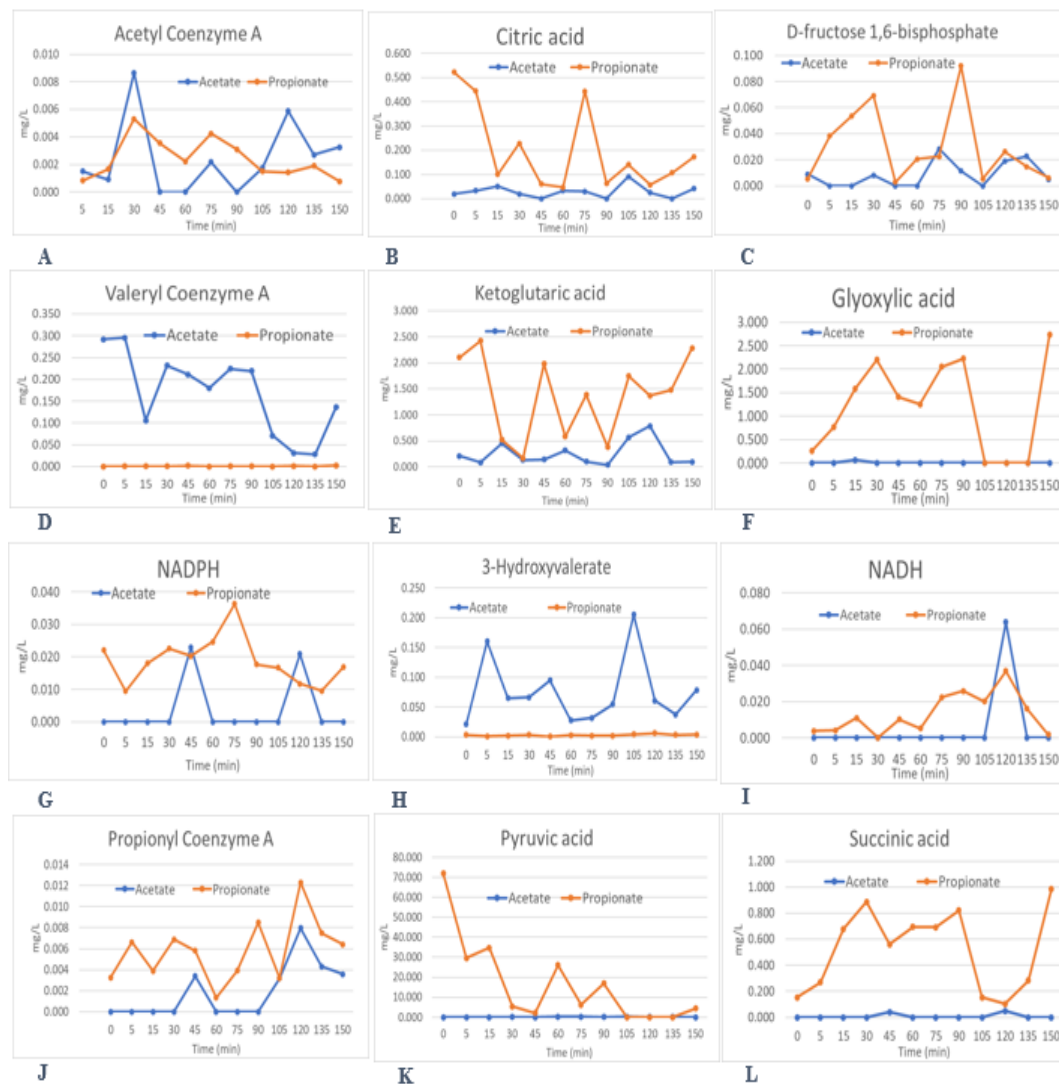
Figure 4.57: Levels of metabolites in each time point. Acetate VS Propionate reactors.

4.3.5   Feast-Famine metabolic response in PHA reactors

In this section, only PHA parent reactors were analysed with the purpose to compare the levels of key metabolites during the feast and famine metabolic response. All PHA parent reactors metabolomics results (mg/L) were plotted together to observe patterns and highlight the metabolic changes of both the feast and famine periods in a PHA system under real setting operations. Specific observations included:

- Acetyl-CoA levels appear to be high in the 'feast' period and decrease as the 'famine' period starts (Figure 4.58 A).
- Related, citrate levels between each time point did not change, excluding the one outlier. Ketoglutarate levels varied cyclically over time (Figure 4.58 B).
- Measurable metabolite concentrations associated with glycolysis – specifically D-fructose 1,6-bisphosphate and pyruvate –indicate activity of this pathway in regular parent reactors (Figures 4.58 C and 4.58 K).
- The glyoxylate pathway appeared to be eminently active in regular PHA parent reactors, with high concentrations of both, glyoxylate and succinate (Figures 4.58 F and 4.59 L).
- 3-Hydroxyvalerate was detected in all PHA parent reactors, indicating some level of PHA catabolism over the feast and famine periods (Figure 4.52H). In particular, the metabolite concentration increased substantially after 60 minutes and remained relatively high thereafter. (Figure 4.59 H).
- Propionyl-CoA concentrations appeared to be higher during the 'feast' period and seemed to decrease in the 'famine' phase (Figure 4.59 J).
- Significant NADH and NADPH concentrations were detected in all PHA reactors (Figure 4.59 G, I). In particular, NADH and NADPH concentrations increased substantially after 15 minutes. This could indicate less efficient oxidation and PHA synthesis.

Figure 4.58: Levels of metabolites in each time point. PHA parent reactors.
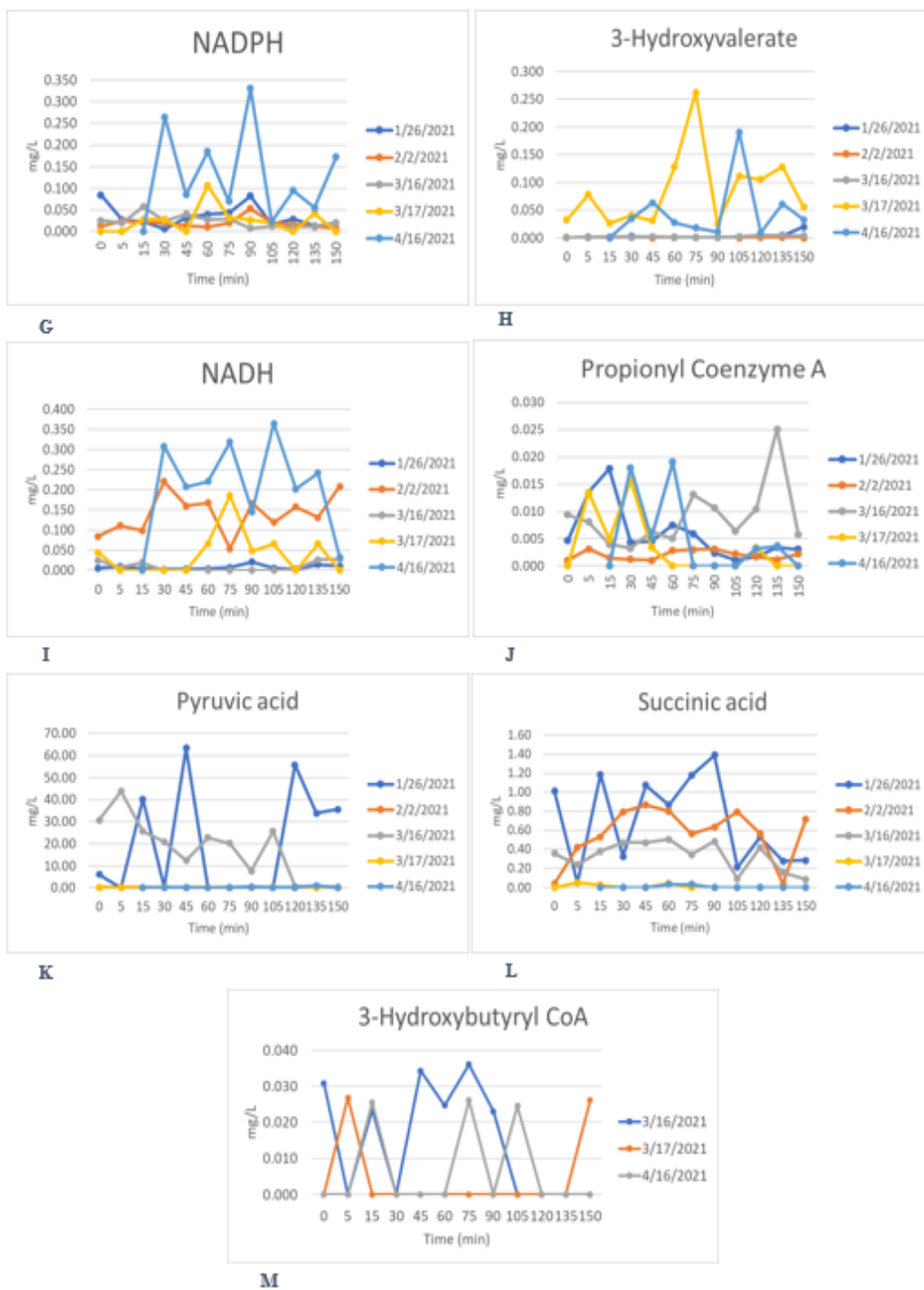
Figure 4.59: Levels of metabolites in each time point. PHA parent reactors.

Chapter 5:   Conclusions and Future Research

5.1   Conclusions

The research presented herein focused on developing an enhanced understanding of MMC and their metabolome dynamics when synthesizing PHA from fermented dairy manure under ADF conditions. The findings in this study aimed to better characterize the feast-famine response of MMC through a genomic and metabolomic approach. The presented results provide quality insights to understand what potentially induces feast, identified metabolites critical for PHA synthesis, and detected whether MMC enriched on fermented dairy manure under ADF operational conditions have enough abundance of key PHA genes to synthesize PHAs in a production level.

Results from this thesis lead to the following conclusions:

- Metabolomic findings confirmed the presence of glyoxylate in MMC synthesizing PHAs. Great amounts of glyoxylate were identified in all PHA systems (3.2 ± 2.0 mg/L, n= 36). This leads to the conclusion that the glyoxylate pathway is an active pathway. Similar to citrate in the TCA cycle, the glyoxylate pathway might need to be repressed, blocked or inhibit it in future experiments to see if its inactivation will result in the diversion of acetyl-CoA in PHA synthesis.

- NADH addition enhanced PHA production. As discussed, the purpose of NADH addition was to prove that NADH could potentially inhibit the TCA cycle and induce greater PHA synthesis. Metabolomic results revealed that NADH inhibited citrate in the TCA cycle. PHA analysis demonstrated that NADH also induced greater PHA synthesis.

- Results demonstrate a strong effect of DCCD and CCCP on the TCA cycle; these two chemicals have the potential to inhibit mechanisms associated with carboxylic acid uptake in MCC.

- Data indicates that MMC are capable of accumulating significant amounts of PHA even when carboxylic acid uptake is inhibited in MMC. This aspect of the research suggests that ATP could come from different sources, and that cells can still get

carbon to produce PHA even when VFA uptake is impaired. However, proving where the external source of carbon utilized by the MMC for PHA production comes from remains a challenge.

- The metabolic differences between MCC fed with acetate and propionate were eminently noticeable. However, in terms of PHA analysis, both reactors fed with acetate and propionate produced less PHAs that their respective parent reactors. MMC fed with both synthetic feeds also consume substantially higher amounts of carboxylic acids.

- Genomics results suggest that MMCs enriched in bench-scale systems and pilot-scales produce SCL PHA, with *phaC* class II genes detected. The detection of *phaC* class II genes in independent PHBV systems further suggests that this potential was not limited to the MMC enriched in one operational run, indicating unrealized MCL PHA production potential worthy of future exploration.

- Enrichment reactor "E.3.10" (3 days SRT and10 Cmmol/L-d OLR) had the highest abundance of the *phaC* genes in MMC. qPCR results revealed that E.2.10 reactor has a *phaC* class II gene presence of 13.6%, E.3.10 has a *phaC* class II gene presence of 17.3%, and finally, the E.4.10 reactor has a *phaC* class II gene presence of 14.9%.

- Despite the limitations encountered in metabolomics, the results obtained from the targeted analysis are valuable insights of a metabolic-level understanding of Feast PHA synthesis. Results showed that in MCC synthesizing PHAs from fermented dairy manure under ADF conditions, Acetyl-CoA and propionyl-CoA levels increase in the 'feast' period and decrease as the 'famine' period starts. D-fructose 1,6-bisphosphate which is a glycolysis metabolite, was detected in the five batch tests of the parent reactors. This is an important finding in the understanding of 'feast' and how MMC produce the ATP needed in this stage.

5.2   *Revisiting the Thesis Research Questions*

Results presented and discussed herein address the posed Research Questions as follows.

RQ1: How are MMC producing ATP during the feast stage? And why does a rapid uptake of VFAs always occur?

Hypothesis 1: Glycolysis provides ATP to activate VFA uptake and initiate Feast PHA synthesis.

Answer: The constant detection of D-fructose 1,6-bisphosphate in PHA systems allows the conclusion that glycolysis is active and thus could provide ATP to activate VFA uptake and initiate feast PHA synthesis.

RQ2: Why and how does PHA synthesis occur contrary to just cell growth?

Hypothesis 2: There are features that negatively affect the TCA cycle and re-direct acetyl-CoA to PHA synthesis: NADH can repress citrate synthase in the TCA cycle. This prevents acetyl-CoA from entering the TCA cycle, and instead acetyl-CoA is converted to Acetoacetyl-CoA by 3-ketothiolase (phaA). As a result, PHA synthesis will occurs and a declined flux of carbon through the TCA cycle will also occur.

Answer: Targeted metabolomics results demonstrated that NADH has the potential to repress citrate in the TCA cycle. Findings also showed that Acetyl-CoA levels increase when citrate is repressed. Generally, a higher PHA production was observed with NADH addition. However, how much NADH is needed to achieve a full inhibition remains to be investigated. These findings allow the conclusion that cell growth occurs when the majority of the Acetyl-CoA produced goes to the TCA cycle. This may raise concerns about Acetyl-CoA being mostly used in the TCA cycle to carry out cellular respiration instead of going to PHA synthesis, which can be addressed by adding NADH to the system.

RQ 3: Do MMC enriched on fermented dairy manure under ADF operational conditions have an enough abundance of key PHA genes to synthesize PHAs in a production level?

Hypothesis 3: Class II *phaC* genes detected in MMC are not actively transcribed. Optimization of *phaC* genes classes will demonstrate that MMC contains at least 2 of the 4 *phaC* gene classes (*phaC* classes I and II). MMC in bench and pilot-scale systems have the potential to synthesize both, short-chain-length PHAs and medium-chain-length PHAs.

Answer: qPCR studies confirm that MMC synthesizing PHAs from fermented dairy manure under ADF conditions contain *phaC* classes I and II. Specifically, and more interestingly, bench-scale systems MMC contain *phaC* class II, and pilot-scales systems MMC contain both, *phaC* classes I and II. These results cast a new light on the potential of MMC to synthesize both, short-chain-length PHAs and medium-chain-length PHAs. However, whether these *phaC* genes are actively transcribed, remains to be investigated through future transcriptomic studies.

5.3   *Future research*

This thesis has been mainly focused on developing a feasible metabolomics method to understand MMC and their metabolome dynamics when synthesizing PHA from fermented dairy manure under ADF conditions. After accomplishing this goal, and in addition to the inhibitors tests and genomics work, the results in this thesis provide a strong foundation for future work. Future research concerns deeper analysis of particular mechanisms, new proposals to try different inhibitors, and 'omics' technologies. The following ideas could be tested:

Genomics: Future studies could fruitfully explore the following PHA genes:
- Beta-ketothiolase (*phaA*)
- Acetoactyl-CoA reductase (*phaB*)
- Phasin (*phaP*)
- Regulator protein (*phaR*)
- PHA depolymerase (*phaZ*)

Each one of these PHA genes have an important function in PHA synthesis, and by understand them we could regulate the expression of some of them and avoid the suppression

of the *phaC* gene in our MMC. In addition, interesting research questions for future research can be derived from studying the PHA operon. Another recommendation is to continue studying the *phaC* gene from *Meganema*, a dominating PHA producing microbe in our MMC. These results will be leveraged to perform future transcriptomic investigations.

Transcriptomics: Future research should consider conducting preliminary transcriptomic analysis and identify functional PHA genes to target. Testing if genes such as *phaC*s are active in our PHA systems is suggested.

Metabolomics: Extending metabolites library to further study the feast and famine metabolic response is highly recommended. Future studies should aim to replicate metabolomics results in a larger scale, utilizing other inhibitors, and testing other comprehensive metabolites that should be detected in PHA metabolisms. Future research should test strategically unknown metabolites against library metabolites and monitor the concentration of metabolites in PHA systems. Looking for downregulation and upregulation of pathways is desirable for future work.

References:

1. Wiek, A., *Sustainability Science: Bridging the Gap between Science and Society*, in *K. Fukushi,   Masaru Yarime*, F. Farioli, Editor. 2012, Sustainability Science   7(Supplement 1):1-4: School of Sustainability, Arizona State University, Tempe, AZ 85287-5502, USA.

2. Hailin Zhang, J.S., *Animal Manure Production and Utilization in the US*. 2014.

3. (EPA), E.P.A., *Inventory of U.S. Greenhouse Gas Emissions and Sinks: 1990-2015.* 2017.

4. Lorimor, J., Powers, W., Sutton, A., Lafayette, W, *Manure Characteristics: Manure Management Systems Series, MWPS-18 Section 1, second edition.* 2004.

5. Moore, A., and Olsen, N., *Fertilizing potatoes in Idaho with dairy manure.* 2009: University of Idaho Extension.

6. Moore, A., and Ippolito, J.,, *Dairy Manure Field Applications- How much is too much?* 2009: University of Idaho Extension.

7. Chastain, J., and Henry, S., *Management of Lagoons and Storage Structures For Dairy Manure. Chapter 4.* 2007.

8. Li, W., Tse, H., & Fok, L., *Plastic waste in the marine environment: A review of sources, occurrence and effects.* 2016, Science of The Total Environment.

9. Europe, P., *Plastics – the Facts 2019: An analysis of European plastics production, demand and waste data*. 2019.

10. Coats, E.R., Gregg, M., & Crawford, R. L., *Effect of organic loading and retention time on dairy manure fermentation.* 2011, Bioresource Technology.

11. Chae, Y., & An, Y., *Current research trends on plastic pollution and ecological impacts on the soil ecosystem: A review.* 2018, Environmental Pollution, 240, 387-395.

12. Raza, Z., *Polyhydroxyalkanoates: Characteristics, production, recent developments and applications.*, S. Abid, and Banat, I., Editor. 2018, International Biodeterioration & Biodegradation.

13. Coats, E.R., *Polyhydroxyalkanoate synthesis by mixed microbial consortia cultured on fermented dairy manure: Effect of aeration on process rates/yields and the associated microbial ecology.*, B.S. Watson, & Brinkman, C. K., Editor. 2016, Water Research.

14. Bugnicourt, E., Cinelli, P., Lazzeri, A., & Alvarez, V., *Polyhydroxyalkanoate (PHA): Review of synthesis, characteristics, processing and potential applications in packaging.* 2014, Express Polymer Letters.

15. Coats, E.R., et al., *Production of natural fiber reinforced thermoplastic composites through the use of PHB-rich biomass.* Bioresour. Technol., 2008. **99**(7): p. 2680-2686.

16. Gerngross, T.U., *Can biotechnology move us toward a sustainable society?* Nat Biotechnol, 1999. **17**(6): p. 541-4.

17. Dias, J.M., Serafim, L. S., Lemos, P. C., Reis, M. A., & Oliveira, R., *Mathematical modelling of a mixed culture cultivation process for the production of polyhydroxybutyrate.* 2005, Biotechnology and Bioengineering.

18. Hanson, A.J., Guho, N. M., Paszczynski, A. J., & Coats, E. R., *Community proteomics provides functional insight into polyhydroxyalkanoate production by a mixed microbial culture cultivated on fermented dairy manure.* 2016, Applied Microbiology and Biotechnology.

19. Dias, J.M., et al., *Recent advances in polyhydroxyalkanoate production by mixed aerobic cultures: from the substrate to the final product.* Macromol Biosci, 2006. **6**(11): p. 885-906.

20. Khanna, S. and A.K. Srivastava, *Recent advances in microbial polyhydroxyalkanoates.* Process Biochemistry, 2005. **40**(2): p. 607-619.

21. Sharma, P.K., et al., *Synthesis and Physical Properties of Polyhydroxyalkanoate Polymers with Different Monomer Compositions by Recombinant Pseudomonas putida LS46 Expressing a Novel PHA SYNTHASE (PhaC116) Enzyme.* Applied Sciences, 2017. **7**(3).

22. Sprague, C., *Assessment of Operationally Effected Metabolic Conditions to Achieve Enhanced Polyhydroxyalkanoate Production on Fermented Dairy*

Manure. 2018: *Civil and*

Environmental Engineering, University of Idaho: Moscow, ID. p. p. 120.

23. Narancic, T., et al., *Recent Advances in Bioplastics: Application and Biodegradation.* Polymers, 2020. **12**(4).

24. Ong, S.Y., Chee, J.Y., Sudesh, K., Онг, С.Й., Чее, *Degradation of Polyhydroxyalkanoate (PHA): a Review*. 2017, *Journal of Siberian Federal University*

25. Kjeld W. Meereboer, M.M.a.A.K.M., *Review of recent advances in the biodegradability*

of polyhydroxyalkanoate (PHA) bioplastics and

their composites. 2020, Green Chemistry.

26. Madison, L.L. and G.W. Huisman, *Metabolic engineering of poly(3-hydroxyalkanoates): from DNA to plastic.* Microbiol Mol Biol Rev, 1999. **63**(1): p. 21-53.

27. Cui, Y.-W., et al., *Effects of carbon sources on the enrichment of halophilic polyhydroxyalkanoate-storing mixed microbial culture in an aerobic dynamic feeding process.* Scientific Reports, 2016. **6**(1): p. 30766.

28. Coats, E.R., et al., *Functional stability of a mixed microbial consortium producing PHA from waste carbon sources.* Appl. Biochem. Biotechnol., 2007. **136-140**: p. 909-926.

29. Coats, E.R., et al., *Synthesis of Polyhydroxyalkanoates in Municipal Wastewater Treatment.* Water Environ. Res., 2007. **79**(12): p. 2396-2403.

30. Coats, E.R., et al., *An integrated 2-stage anaerobic digestion and biofuel production process to reduce life cycle GHG emissions from U.S. dairies.* BioFPR, 2013. **7**(4): p. 459-473.

31. Coats, E.R., et al., *Toward polyhydroxyalkonate production concurrent with municipal wastewater treatment in a sequencing batch reactor system.* ASCE J. Environ. Engr., 2011. **137**(1): p. 46-54.

32. Guho, N.M., et al., *Pilot-scale production of poly-3-hydroxybutyrate-co-3-hydroxyvalerate from fermented dairy manure: Process performance, polymer*

characterization, and scale-up implications. Bioresource Technology Reports, 2020. **12**: p. 100588.

33.   Liu, H.-Y., et al., *Production of poly(hydroxyalkanoate) during treatment of tomato cannery wastewater.* Water Environ. Res., 2008. **80**(4): p. 367-372.

34.   Lemos, P.C., L.S. Serafim, and M.A.M. Reis, *Synthesis of polyhydroxyalkanoates from different short-chain fatty acids by mixed cultures submitted to aerobic dynamic feeding.* Journal of Biotechnology, 2006. **122**(2): p. 226-238.

35.   Dias, J.M.L., et al., *Metabolic modelling of polyhydroxyalkanoate copolymers production by mixed microbial cultures.* BMC Systems Biology, 2008. **2**(1): p. 59.

36.   Guho, N., *Polyhydroxyalkanoate production coupled with waste treatment using a three-stage sequencing batch reactor system fed dairy manure*, in *Civil Engineering*. 2010, University of Idaho. p. 89.

37.   Dionisi, D., et al., *Biodegradable polymers from organic acids by using activated sludge enriched by aerobic periodic feeding.* Biotechnology and Bioengineering, 2004. **85**(6): p. 569-579.

38.   Justyna Moˑzejko-Ciesielska∗, R.K., *Bacterial polyhydroxyalkanoates: Still fabulous?* 2016.

39.   Steinbüchel, A., Hein, S., *Biochemical and molecular basis of microbial synthesis of polyhydroxyalkanoates in microorganisms*. 2001.

40.   Ciesielski, S., Pokoj, T., Klimiuk, E., *Molecular insight into activated sludge produc ing polyhydroxyalkanoates under aerobic-anaerobic conditions.* 2008, Journal of Industrial Microbiology & Biotechnology.

41.   Sheu, D.S., Wang, Y.T., Lee, C.Y., *Rapid detection of polyhydroxyalkanoate accumulating bacteria isolated from the environment by colony PCR*. 2000, Microbiology 1124 146, 2019–2025.

42.   Stefan Neubauer, D.B.C., Hans Marx, Michael Sauer, Stephan Hann, Gunda Koellensperger, *LC-MS/MS-based analysis of coenzyme A and short-chain acyl-coenzyme A thioesters*. 2015, Analytical Bioanalytical Chemistry: Springer-Verlag Berlin Heidelberg 2015.

43.   Bartlett, L.G.R.a.M.G., *Chromatographic methods for the determination of acyl-CoAs*. 2018 Royal Society of Chemistry: Analytical methods.

44.   Oeding, V. and H.G. Schlegel, *Beta-ketothiolase from Hydrogenomonas eutropha H16 and its significance in the regulation of poly-beta-hydroxybutyrate metabolism.* Biochem J, 1973. **134**(1): p. 239-48.

45.   Luisa S Serafim   , P.C.L., Maria G E Albuquerque ,   Maria A M Reis, *Strategies for PHA production by mixed cultures and renewable waste materials*. 2008.

46.   Serafim, L.S., et al., *Strategies for PHA production by mixed cultures and renewable waste materials.* Appl Microbiol Biotechnol, 2008. **81**(4): p. 615-28.

47.   Alistair J. Anderson, E.A.D., *Occurrence, Metabolism, Metabolic Role, and Industrial Uses of Bacterial Polyhydroxyalkanoates*. 1990, American Society for Microbiology.

48.   Katie A. Third, M.N., Ralf Cord-Ruwisch, *The effect of dissolved oxygen on PHB accumulation in activated sludge   cultures*. 2003, Biotechnology and Bioengineering.

49.   Pijuan, M., et al., *Characterizing the biochemical activity of full-scale enhanced biological phosphorus removal systems: A comparison with metabolic models.* Biotechnol Bioeng, 2008. **99**(1): p. 170-9.

50.   Liu, W.-T., et al., *Role of glycogen in acetate uptake and polyhydroxyalkanoate synthesis in anaerobic-aerobic activated sludge with a minimized polyphosphate content.* Journal of Fermentation and Bioengineering, 1994. **77**(5): p. 535-540.

51.   Corey D DeHaven, A.M.E., Hongping Dai, Kay A Lawton, *Organization of GC/MS and LC/MS metabolomics data into chemical libraries*. 2010, Journal of Cheminformatics.

52.   Agin, A., et al., *Metabolomics – an overview. From basic principles to potential biomarkers (part 1).* Médecine Nucléaire, 2016. **40**(1): p. 4-10.

53.   Reo, N.V., *NMR-based metabolomics.* Drug Chem Toxicol, 2002. **25**(4): p. 375-82.

54.   Djukovic, G.A.N.G.a.D., *Overview of Mass Spectrometry-Based Metabolomics: Opportunities and Challenges*. Methods Molecular Biology.

55.   Bin Zhou , J.F.X., Leepika Tuli , and Habtom W. Ressom, *LC-MS-based metabolomics*. 2011, Mol Biosyst.

56.   Coskun, O., *Separation techniques: Chromatography.* North Clin Istanb, 2016. **3**(2): p. 156-160.

57.   Manuel Liebeke, K.D., Hanna Meyer,   Michael Lalk. 2011: Functional Genomics.

58.   Manuel Liebeke, K.D., Hanna Meyer,   Michael Lalk, *Metabolome Analysis of Gram-Positive Bacteria such as Staphylococcus aureus by GC-MS and LC-MS*. 2011: Functional Genomics.

59.   Sprague, C., *Assessment of Operationally Effected Metabolic Conditions to Achieve Enhanced Polyhydroxyalkanoate Production on Fermented Dairy Manure*. 2018, *Civil and Environmental Engineering,*   University of Idaho: Moscow, ID. p. 120.

60.   Stowe, E.J., *<p class="EndNoteBibliography" style="margin-top:0in;margin-right:0in;margin-bottom: 0in;margin-left:.5in;text-indent:-.5in">Dairy Waste Treatment Utilizing a Two-Phase Anaerobic Digestion System: Evaluation of Parallel Reactor Configuration and Mixing Intensity*. 2014, *Civil and Environmental Engineering,*   University of Idaho: Moscow, ID. p. 114.

61.   Stowe and E.R.C. E.J., and C.K. Brinkman, *Dairy Manure Resource Recovery utilizing Two-stage Anaerobic Digestion - Implications of Solids Fractionation*. 2015, B*ioresource Technology*

62.   Sprague, C.A., *Assessment of Operationally Effected Metabolic Conditions to Achieve Enhanced Polyhydroxyalkanoate Production on Fermented Dairy Manure*, in *Civil and Environmental Engineering*. 2018, University of Idaho: Moscow, ID. p. 120.

63.   Carleton and B.S., *Toward Maximal Polyhydroxyalkanoate Production from Dairy Manure: Controlling and Optimizing Biosynthesis with Implications for Design*. 2016, *Chemical Engineering* , University of Idaho.

64.   Alexandre and B. Crozes, *A Predictive Metabolic Model for Polyhydroxyalkanoate Production by a Mixed Microbial Consortium Cultured Under Aerobic Dynamic Feeding Conditions and fed Dairy Manure Fermenter Liquor*. 2019, University of Idaho: University of Idaho. p. P. 50-54.

65.   Association and A.P.-A.P.H., *Standard methods for the examination of water and wastewater.*   . 1998, USA:

APHA.

66.   Winkler, M., E.R. Coats, and C.K. Brinkman, *Advancing post-anoxic denitrification for biological nutrient removal.* Water Res, 2011. **45**(18): p. 6119-30.

67.   Ramakers, C., et al., *Assumption-free analysis of quantitative real-time polymerase chain reaction (PCR) data.* Neurosci Lett, 2003. **339**(1): p. 62-6.

68.   Ciesielski, S., Pokoj, T., Klimiuk, E., *Molecular insight into activated sludge produc ing polyhydroxyalkanoates under aerobic-anaerobic conditions.   .* 2008, Journal of Industrial Microbiology & Biotechnology

69.   Muyzer, G., E.C. de Waal, and A.G. Uitterlinden, *Profiling of complex microbial populations by denaturing gradient gel electrophoresis analysis of polymerase chain reaction-amplified genes coding for 16S rRNA.* Applied and Environmental Microbiology, 1993. **59**(3): p. 695.

70.   Stefan Neubauer, D.B.C., Hans Marx, Michael Sauer, Stephan Hann, Gunda Koellensperger, *LC-MS/MS-based analysis of coenzyme A and short-chain acyl-coenzyme A thioesters.* 2015, Analytical Bioanalytical Chemistry: Springer-Verlag Berlin Heidelberg 2015.

71.   Burow, L.C., Mabbett, A. N., Mcewan, A. G., and P.L. Bond, & Blackall, L. L., *Bioenergetic models for acetate and phosphate transport in bacteria important in enhanced biological phosphorus removal.* 2007, *Environmental Microbiology.*

72.   Sekyere, J.O., & Amoako, D. G., *Carbonyl Cyanide m-Chlorophenylhydrazine (CCCP) Reverses Resistance to Colistin, but Not to Carbapenems and Tigecycline in Multidrug-Resistant Enterobacteriaceae.* 2017, *Frontiers in Microbiology.*

73.   W. M. Hamman, M.S., *Relationship of potassium ion transport and ATP synthesis in pea cotyledon mitochondria.* 1977, *Can J Biochem.*

74.   Yu, J., *Production of PHA from starchy wastewater via organic acids.* Journal of Biotechnology, 2001. **86**(2): p. 105-112.

75.   Alexandre and B. Crozes, *A Predictive Metabolic Model for Polyhydroxyalkanoate Production by a Mixed*

Microbial Consortium Cultured Under Aerobic Dynamic Feeding Conditions and fed Dairy Manure Fermenter Liquor. 2019, University

of Idaho: University

of Idaho. p. P. 50-54.

76. Farell, E.M. and G. Alexandre, *Bovine serum albumin further enhances the effects of organic solvents on increased yield of polymerase chain reaction of GC-rich templates.* BMC Res Notes, 2012. **5**: p. 257.

77. Yang, M.K., Y.C. Lin, and C.H. Shen, *Identification of two gene loci involved in poly-beta-hydroxybutyrate production in Rhodobacter sphaeroides FJ1.* J Microbiol Immunol Infect, 2006. **39**(1): p. 18-27.

78. Coats, E.R., B. Watson, and C.K. Brinkman, *Polyhydroxyalkanoate Synthesis by Mixed Microbial Consortia cultured on Fermented Dairy Manure: Effect of Oxygen Mass Transfer on Process Rates/Yields and Microbial Ecology.* Water Res., 2016. **106**: p. 26-40.

79. Francisco Diez-Gonzalez, J.B.R., *Effects of carbonylcyanide-m-chlorophenylhydrazone (CCCP) and acetate on Escherichia coli O157:H7 and K-12: uncoupling versus anion accumulation*. 1997.

80. Mary Pinkerton, L.K.S., and, Phillip Dawkins, *THE MOLECULASRT RUCTURAEN D SOMET RANSPORPTR OPERTIESO F VALINOMYCIN*. 1969, Biochemical and Biophysical Research Communications.

81. Beechey, R.B., Roberton, A. M., Holloway, C. and K. T., I. G., *The Properties of Dicyclohexylcarbodiimide as an*

Inhibitor of Oxidative Phosphorylation*. 1967, *Biochemistry*.

82. Chen, J., et al., *Metabolic engineering of Escherichia coli for the synthesis of polyhydroxyalkanoates using acetate as a main carbon source.* Microbial Cell Factories, 2018. **17**(1): p. 102.

Other references:

United States Department of Agriculture

National Agricultural Statistics Service

Permission to use figures:

Permission to use figure: common PHA monomers   2

CS   Cody Sprague <CSprague@mountainwtr.com>
Wed 3/31/2021 1:49 PM
To: Alfaro Salmeron, Maribel (alfa8645@vandals.uidaho.edu)

3 Stage Reaction Diagram.pptx
47 KB

Hey Maribel,

You absolutely have my permission to use the figure you attached, I appreciate you reaching out. I have attached the Powerpoint file that I constructed the figure from (slide 5), along with the other figures that I created for my thesis that I also give you permission to use if you would like. Let me know if there is anything else I can do to help.

Good luck with your research!

Cody Sprague, E.I.T. | **Mountain Waterworks, Inc.**
PROJECT ENGINEER
Boise - Lewiston - McCall
P 208.780.3988
C 208.949.6112
E csprague@mountainwtr.com

Nicholas M. Guho
University of Idaho
Moscow, ID 83843
December 5, 2019

Re: Copyright permission

To whom it may concern:

I hereby grant permission to any graduate student at the University of Idaho to whom Dr. Erik R. Coats is an advisor to reprint any figure from my master's thesis "Polyhydroxyalkanoate Production Coupled with Waste Treatment Using a Three-Stage Sequencing Batch Reactor System Fed Dairy Manure" to which I hold the copyright in their own master's thesis or doctoral dissertation.

Sincerely,
Nicholas M. Guho
University of Idaho